



FEUP FACULDADE DE ENGENHARIA
UNIVERSIDADE DO PORTO

CoBlastTM industrial process validation

Ana Sofia Azevedo Oliveira

Supervisor: Eduardo Ascenso Pires, PhD

Co-Supervisor: Fernando Jorge Monteiro, PhD

Integrated Master in Bioengineering

Master in Biomedical Engineering

June, 2015

The present document is based on the work carried out during a curricular internship at the Portuguese company Ceramed S.A., under the local supervision of Doctor Eduardo Ascenso Pires, chief executive officer of Ceramed, and the scientific supervision of Professor Fernando Jorge Monteiro, professor of the Department of Metallurgical and Materials Engineering of Faculty of Engineering - University of Porto.

Abstract

Each year, a critical number of people is affected by healthcare-associated infections due to implantation of total hip and total knee prostheses and trauma implants. These last have an increased tendency for infection, mainly due to the fact that they are applied to repair complex injuries and open fractures. Infection together with the eventual loosening of an orthopaedic implant explains the limited lifespan of an orthopaedic device.

Research over the years focused on finding the best materials to develop a range of implant coatings with the ability to improve implant binding to the host bone tissue and avoid infection.

Hydroxyapatite based coatings are still one of the most frequently used implant coatings in the field of orthopaedic surgery and trauma, resulting in improved implant ingrowth and a longer lifespan of the prosthesis.

A great number of technologies are currently used to deposit implant coatings. While some of them require high temperatures that can alter coating crystallinity and compromise coating bioactivity, others act under room temperatures to apply coatings with limited thermal stability. Nevertheless coating delamination and cracking are still frequent.

Plasma-spray is the most used and accepted method for Hydroxyapatite coating application. This deposition process frequently affects coating crystallinity due to the high temperatures used in processing. Phase transformations tend to occur, what will enhance the resorption process of coating leading to implant instability.

Therefore, it is urgent for innovative and effective coating technologies, that do not require high temperatures, to reach the market of medical coatings, since those may help to accomplish a combined situation of a coating with both antimicrobial and osteoconductive properties.

It is crucial for the market of medical coatings to understand this urgency and to provide time, attention and investment to research and development of new technologies with industrial applicability. An insightful way of doing this is picking existing technologies with basic principles reported, observed and characteristic proof-of-concept demonstrated and seek their implementation in industrial production.

Ceramed S.A. is a Portuguese company with ten years of history, specialized in medical devices coatings, which counts on great number of partnerships focused on research and development of new concepts and technologies for the sector. This company comprehends the sector and market needs and is interested in making the industrial validation of an innovative technology for Hydroxyapatite coating application.

CoBlast is a cleaning, roughening, and coating technology that works under room temperature and pressure, with minimal substrate alteration developed by a co-founder of a company named *Enbio Limited*, which can offer the solution this field is waiting for.

This master thesis contributes to this by providing a Master Validation Plan for CoBlast process and performing the major Validation steps of this new coating technology.

Process validation is a key part of the Quality Management System for medical device manufacturers. It intends to establish by objective evidence that a process consistently produces a result or a product meeting its predetermined specifications.

On the course of this master thesis, the different phases of process validation were carried out. Installation Qualification was successfully accomplished, the objectives proposed for Operational Qualification have been met, and a study of Performance was developed. Further works should focus on going where this work had no time to go: process mass flow rate optimization.

Keywords: CoBlast, Medical device coating processes, Process Validation, Bioactive coatings, Hydroxiapatite.

Resumo

Todos os anos, um número significativo de pessoas é afetado por infeções relacionadas com a assistência médica de aplicação de próteses de substituição total de anca e joelho e implantes de traumatologia. Estes apresentam uma tendência superior para a infeção, devido ao facto de serem aplicados para reparar lesões complexas e fraturas expostas. A infeção somada à eventual rejeição do implante ortopédico explica o tempo de vida útil limitado deste tipo de dispositivos.

Ao longo do tempo, a investigação científica tem vindo a focar-se em encontrar os melhores materiais para desenvolver um leque de revestimentos para implantes com a capacidade de melhorar a fixação destes ao tecido ósseo do paciente e evitar infeções.

Os revestimentos baseados em Hidroxiapatite continuam a ser os mais frequentemente aplicados em implantes médicos na área da cirurgia ortopédica e de trauma, resultando numa melhor aceitação do implante e num aumento do seu tempo de vida útil.

Atualmente, um número considerável de tecnologias são usadas na aplicação de revestimentos em implantes. Enquanto algumas utilizam temperaturas altas que podem alterar a cristalinidade do revestimento e comprometer a sua bioatividade, outras atuam à temperatura ambiente de forma a aplicar revestimentos com baixa estabilidade térmica. Apesar disso, a delaminação e fratura do revestimento continuam a ser frequentes.

A deposição por plasma continua a ser a tecnologia mais bem aceite e utilizada para aplicação de revestimentos de Hidroxiapatite em dispositivos médicos. Este método afeta frequentemente a cristalinidade do revestimento devido às altas temperaturas envolvidas no processo, o que pode levar a uma rápida reabsorção do mesmo provocando instabilidade na zona do implante.

Por este motivo, é urgente que tecnologias inovadoras e eficientes que não necessitem de altas temperaturas cheguem ao mercado dos revestimentos de dispositivos médicos. Estas podem ajudar a atingir o objetivo de combinar num só revestimento tanto características antimicrobianas como osteocondutoras.

É crucial que este mercado entenda esta urgência e aja no sentido do investimento em investigação e desenvolvimento de novas tecnologias com aplicabilidade industrial. Uma forma perspicaz de o fazer, é trabalhar tecnologias promissoras com os seus princípios básicos já reportados e provas de conceito feitas e procurar a sua implementação na produção industrial.

A *Ceramed S.A.* é uma empresa Portuguesa com dez anos de existência, especializada na aplicação de revestimentos em dispositivos médicos, que conta com um número de parcerias focadas em investigação em desenvolvimento de novos conceitos e tecnologias no sector. A

Ceramed entende as necessidades do mercado e está empenhada em fazer a validação industrial de uma tecnologia inovadora para a aplicação de revestimentos de Hidroxiapatite em dispositivos médicos.

O CoBlast é uma tecnologia que limpa, cria rugosidade e reveste a uma temperatura e pressão ambiente, com mínima alteração do substrato, desenvolvida pelo cofundador da empresa *Enbio Limited*, que pode oferecer a solução que este sector espera.

Esta tese de mestrado contribui para isto ao fazer um Plano piloto de Validação para o processo de CoBlast e ao concluir os passos chaves dessa Validação de processo.

A Validação de Processos é uma parte chave dos Sistemas de Gestão da Qualidade em empresas de aplicação de revestimentos médicos. O seu intuito é provar com base em evidências objetivas que o processo é capaz de atingir um resultado ou produto de acordo com as suas especificações predeterminadas.

No decorrer desta dissertação de mestrado, as diferentes fases de Validação do Processo foram levadas a cabo. A Qualificação da Instalação foi bem sucedida, os objetivos propostos para a Qualificação Operacional foram cumpridos, e um estudo de Performance do processo foi feito.

Os trabalhos futuros deverão focar-se em fazer a otimização do fluxo de massa do processo.

Palavras-chave: CoBlast, Processos de aplicação de revestimentos em dispositivos médicos, Validação de processo, Revestimentos bioativos, Hidroxiapatite.

Acknowledgements

I would like to thank Dr. Eduardo Ascenso Pires for accepting and welcoming me at Ceramed and allowing me to take part in the company that he created, unique in Portugal. I am sincerely grateful for his supervision, support and knowledge, and foremost, for being an inspiring person, *a man who fights for what he believes in*.

I would like to express my sincere gratitude to Professor Fernando Jorge Monteiro. There are two moments that I am thankful for in the course of my master thesis planning: the day that I decided to contact Ceramed, and the day that I came to Professor Fernando Jorge Monteiro to ask him to be my supervisor in the Faculty of Engineering. Professor Fernando Jorge Monteiro was flawless in every aspect, an honest and forthright person that I am grateful to have met and have as my supervisor.

In full gratitude I would like to acknowledge all Ceramed, namely all the people that I had the pleasure to work with during this last four months. Because of you, getting up to work everyday was really easy. My special thanks to Ana Duarte, Director of Ceramed, Vânia Miranda, Regulatory Affairs Manager, André Baião, Responsible for Quality Control, Pedro Moura, Responsible for Plasma-Spray and Francisco Vale, Financial Director. From Ceramed affiliated companies, I would like to thank Hugo Araújo from Astrolabe and Luis Pinto and José Manuel Ventura from Altakitin.

I would like to thank Enbio Limited team for advising and helping me whenever I needed. Particularly, I would like to thank John O'Donoghue, Chief Executive Officer at Enbio and inventor of CoBlast technology, Barry Twomey, Vice President of Research and Development, John Collins, Conformity and Compliance Manager and Conor Dunne, PhD researcher at University College Dublin.

I must also acknowledge Faculty of Science and Technology, Universidade Nova de Lisboa (FCT/UNL), represented by Professor João Paulo Borges, for providing the resources and support to perform Scanning electron microscopy, X-ray diffraction and X-ray fluorescence on my-samples. My honest thanks to Professor João Paulo Borges and Professor João Pedro Veiga.

Without a doubt, I would like to thank my parents. Not only for the great life I have led thanks to them but also for the moment I am experiencing now, finishing my undergraduate studies. There are really no words for how much I am thankful to them. I would also like to thank to my brother, an influencer that I am pleased to have in my life.

A very special thanks goes out to my Lisbon house mates. I moved four months ago, and I shared a place with three awesome house mates: Vânia Pacheco, Gonçalo de Almeida and

Ana Carolina Leite. I want their names to be recorded here. With both little and big gestures they managed to make my day better when it wasn't being that bright, especially because of being far away from my loved ones. You rocked, guys.

I would like to thank my friends, both my childhood and my faculty friends that have always had a smile, two open arms, and a free spirit that keeps me young. I am sure they will celebrate with me this joyful moment.

Last but not least, I would like to thank all of the professors in FEUP that I had the pleasure to have as teachers, for all the lessons and enlightening that made me capable of doing this work today.

I would like to express my deepest gratitude to all my colleagues, my mates, my FEUP.

*“Every great advance in science has issued
from a new audacity of imagination.”*

John Dewey

Contents

Abstract.....	v
Resumo	vii
Acknowledgements	ix
Contents	xiii
List of Figures	xvii
List of tables.....	xix
List of Abbreviations	xxi
Chapter 1.....	1
Introduction.....	1
1.1 Motivation	1
1.1.1. Ceramed	2
1.1.2. Enbio Limited	2
1.2 Objective	2
1.3 Contributions	3
1.4 Document Structure	3
Chapter 2.....	5
Bioactive coating materials	5
2.1. Calcium orthophosphates.....	5
Chapter 3.....	9
Overview of medical device coating processes.....	9
3.1 Abrasive blasting	9
3.2 Thermal spraying techniques	9
2.2.1. Plasma spray	10
2.2.2. Flame spray	10
2.2.3. High velocity oxygen fuel (HVOF)	11
2.2.4. Electrical arch spray.....	11
3.3 Electrodeposition	11
3.4 Sputtering	12
3.5 Chemical vapour deposition (CVD).....	12
3.6 Physical vapour deposition (PVD)	13
3.7 Pulsed laser deposition (PLD)	13
3.8 Sol-gel immersion technique.....	14
3.9 Sintering	14
Chapter 4.....	15

CoBlast™	15
4.1 Invention	16
4.2 Deposition conditions and parameters	18
4.3 Reviewed Publications	20
Chapter 5.....	27
Process Validation	27
5.1 Purpose.....	27
5.1.1. Process Validation Decision	27
5.1.2. Statistical Principles	29
5.2 Phases of process validation.....	30
5.2.1 Installation Qualification (IQ).....	31
5.2.2 Operational Qualification (OQ).....	31
5.2.3 Performance Qualification (PQ).....	31
5.3 Monitor, Control and Revalidation	32
5.4 Regulatory specifications	32
Chapter 6.....	33
CoBlast Validation Plan.....	33
6.1 Raw materials and substrate	34
6.2 Equipment	35
6.2.1 Advanced Lathe	35
6.2.2 Powder feeder.....	37
6.2.3 Vacuum cleaner	38
6.2.4 Blender	38
6.3 Static Parameters & Parameters under Evaluation.....	40
6.4 Process requirements.....	42
6.5 Validation Protocol.....	43
6.5.1 Installation Qualification	44
6.5.2 Operational Qualification	44
6.5.3 Performance Qualification	48
Chapter 7.....	52
CoBlast Process Validation.....	52
7.1 Installation Qualification.....	52
7.1.1 CoBlast equipment IQ	52
7.1.2 Blending equipment IQ	57
7.1.3 Result and report of installation qualification.....	61
7.2 Operational Qualification	61
7.2.1 Blending OQ.....	61
7.2.2 Blasting OQ.....	65
7.3 Performance Qualification.....	81
7.3.1 Monitoring plan.....	85
7.4 Internal procedures	86
7.5. Economic Evaluation	87
References	90
Appendix A.....	96
Calculations	96
Raster Offset determination for each nozzle height.....	97
Appendix B.....	100
Equipment IQ checklists.....	100
CoBlast equipment IQ checklists	101
Blending equipment IQ checklists.....	106

Result of IQ checklist	109
Appendix C	110
Production Internal documentation	110
Work instructions	111
Appendix D	114
Raw material Certificates of Compliance	114
Ti-6Al-4V compliance certificate	115
HA compliance certificates	116
Al ₂ O ₃ compliance certificate	118
MCD 180 compliance certificate	119
Appendix E	120
CNC codes	120
SUB STEP A.....	120
SUB STEP B.....	121
SUB STEP C.....	124
ADHESION	126
SCREW	128
Appendix F	130
X-ray diffraction plots.....	130

List of Figures

Figure 3.1 - Schematic of a conventional DC arc spray torch with a nozzle	10
Figure 3.2 - Typical pulsed laser deposition (PLD) system	13
Figure 4.1 - CoBlast technology readiness level.....	15
Figure 4.2 - CoBlast application approach using fluid jet	17
Figure 4.3 - Schematic diagrams of three different nozzle configuration to deliver the dopants and abrasives of CoBlast to a surface	18
Figure 4.4 - Schematic of CoBlast deposition system with two nozzles.....	19
Figure 4.5 - Etched cross-sections of titanium substrates	25
Figure 5.1 - Process Validation decision tree. Adapted from GHTF (2004).....	28
Figure 5.2 - Illustration of a stable and unstable process	29
Figure 5.3 - Process capability study possible results illustration.....	30
Figure 5.4 - Control Chart	32
Figure 6.1 - Spinal fixation screw system	33
Figure 6.2 - Ti-6Al-4V substrates used for CoBlast validation tests.....	34
Figure 6.3 - Comco LA3250 Advanced Lathe exterior frame and inside chamber furnished with a single nozzle configuration.	35
Figure 6.4 - Comco LA3250 Advanced Lathe part tooling.....	36
Figure 6.5 - Comco LA3250 Advanced Lathe user interface	36
Figure 6.6 - Powder feeder Single-10C from Sulzer Metco	38
Figure 6.7 - Model of the inner structure of the machined PTFE V-blender made of two hollow cylindrical shells joined at an angle of 90°	39
Figure 6.8 - Schematic drawing of the set up put in place for powders blending OQ	46
Figure 6.9 - CoBlast Process Flow for test pieces	46

Figure 6.10 - Schematic drawing of the result of *TestSamples* CNC code..... 49

Figure 7.1 - V-blender horizontality testing made using a level tool 58

Figure 7.2 - HA, MCD and HA/MCD apparent density curves after 0 minutes of blending on a 1 liter V-blender. 62

Figure 7.3 - HA, Al₂O₃ and HA/Al₂O₃ apparent density curves after 0 minutes of blending on a 1 liter V-blender. 62

Figure 7.4 - HA, MCD and HA/MCD apparent density curves after 3 minutes of blending on a 1 liter V-blender 63

Figure 7.5 - HA, MCD and HA/MCD apparent density curves after 5 minutes of blending on a 1 liter V-blender 64

Figure 7.6 - HA, Al₂O₃ and HA/Al₂O₃ apparent density curves after 3 minutes of blending on a 1 liter V-blender 64

Figure 7.7 - HA, Al₂O₃ and HA/Al₂O₃ apparent density curves after 5 minutes of blending on a 1 liter V-blender 64

Figure 7.8 - SEM imaging of hydroxyapatite (HA) and blast media MCD (sHA) and Al₂O₃. 65

Figure 7.9 - Scanning Electron Microscopy images of Ti-6Al-4V as received, HA blasted samples and CoBlast samples prepared using HA as dopant media and Al₂O₃ or MCD as blasting media 67

Figure 7.10 - Cross-sections of the Ti-6Al-4V coupons blasted with HA, HA/MCD and HA/Al₂O₃ for three different nozzle heights 68

Figure 7.11 - Coating thickness evaluation results 69

Figure 7.12 - Coating roughness evaluation before acid etching 70

Figure 7.13 - Coating roughness evaluation after acid etching 71

Figure 7.14 - Normalized XRD patterns..... 72

Figure 7.15 - Shewhart X-bar and R control chart of roughness profile of samples blasted over time with HA/MCD. 83

Figure 7.16 - Shewhart X-bar and R control chart of roughness profile of samples blasted over time with HA/Al₂O₃..... 83

Figure 7.17 - Minitab® process capability report for roughness profile evaluation of HA/MCD blasted samples over time. 84

Figure 7.18 - Minitab® process capability report for roughness profile evaluation of HA/MCD blasted samples over time 84

List of tables

Table 2.1 - Existing calcium orthophosphates and their major properties	6
Table 6.1 - Programming quick reference for CoBlast using	37
Table 6.2 - Regulatory specifications for HA coatings.	42
Table 7.1 - Coatings thickness evaluation	69
Table 7.2 - Surface roughness before acid etching	70
Table 7.3 - Surface roughness after nitric acid at 65% etching	71
Table 7.4 - Ratio between the normalised intensity of 211 characteristic reflection of HA and 101 reflection of Ti corresponding to 31.5° and 40.2° (2 θ), respectively.....	73
Table 7.5 - D-spacing of the ten peaks used for HA coating crystallinity evaluation according to ISO 13779-3.	73
Table 7.6 - Integrated intensity of the peaks found in the XRD analysis of HA, Plasma, HA only, HA/MCD, HA/Al ₂ O ₃ samples from the ones referenced in ISO 13779-3 for HA coating crystallinity determination.	74
Table 7.7 - Crystallinity according to ISO13779-3.....	75
Table 7.8 - Crystallinity values obtained according to equation (7.1).	75
Table 7.9 - Highest peak of each phase to be identified if present in the samples analysed..	76
Table 7.10 - Limits on heavy metals' content as stated on ISO 13779-2 for HA coatings.....	78
Table 7.11 - Chemical elements detected using XRF analysis of samples coated using CoBlast with different nozzle heights	78
Table 7.12 - Adhesion tests performed according to ISO 13779-4 results	80
Table 7.13 - HA/MCD blasted surfaces over time roughness appraisal	81
Table 7.14 - HA/Al ₂ O ₃ blasted surfaces over time roughness appraisal	81
Table 7.15 - Economic factors taken into consideration in the economical evaluation made.....	87

List of Abbreviations

List of abbreviations

ACP	Amorphous Calcium Phosphates
ALP	Alkaline Phosphatase
Ang	Angiopoietin
APS	Air plasma spray
ASTM	American Society of Testing of Materials
BCA	Bicinchoninic Acid
bFGF	Basic Fibroblast Growth Factor
BG	Bioactive Glass
CATiM	Center for Technical Support to Metalworking Industry
CDHA	Calcium-Deficient Hydroxyapatite
CFR	Code of Federal Regulations
CO ₃ A	Carbonate Apatite
CNC	Computer Numerical Control
CVD	Chemical Vapour Deposition
DC	Direct Current
ECDC	European Centre for Disease Prevention and Control
ECM	Extracellular Matrix
EDX	Energy Dispersive X-ray spectroscopy
ESA	European Space Agency
EU	European Union
FA	Fluoro Apatite
FDA	Food and Drug Administration
FEUP	Faculdade de Engenharia da Universidade do Porto
GHTF	Global Harmonization Task Force
HA	Hydroxyapatite
HAI	Healthcare-Associated Infections
HAZ	Heat Affected Zone
HVOF	High-Velocity Oxygen Fuel
IAPMEI	Institute for Support to Small and Medium Enterprises and Investment
ICP-OES	Inductively Coupled Plasma Optical Emission Spectroscopy
iNOS	Inducible Nitric Oxide Synthase
IQ	Installation Qualification

ISO	International Organization for Standardization
LCL	Lower Control Limit
LSL	Lower Specification Limit
sHA	Sintered Apatite
MgA	Magnesium Apatite
MIB	Integrated Master on Bioengineering
MIT	Massachusetts Institute of Technology
NASA	National Aeronautics and Space Administration
OQ	Operational Qualification
PQ	Performance Qualification
PS	Plasma-spray
PTFE	Polytetrafluoroethylene
PVD	Physical Vapour Deposition
PXRD	Powder X-ray Diffraction
RPM	Revolutions Per Minute
SBF	Simulated Body Fluid
SEM	Scanning Electron Microscopy
SPC	Statistical Process Control
TCP	Tricalcium Phosphate
TRLs	Technology Readiness Levels
UCL	Upper Control Limit
USA	United States of America
USL	Upper Specification Limit
VAC	Volts in alternating current
VPS	Vacuum Plasma Spray
WHO	World Health Organization
XPS	X-ray Photoelectron Spectroscopy
XRD	X-ray Diffraction

List of symbols

θ	Angle
(-)	Anode
(+)	Cathode
ξ	Mean
ρ	Density
σ	Standard Deviation
V	Volume
Δ	Variation
m	Mass
h	Height

Chapter 1

Introduction

After the implantation of a medical device (e.g. orthopaedic device), a race for the surface takes place with bacterial colonization and tissue integration competing in order to conquer the surface of the implant (Gristina, 1987, Busscher et al., 2012). Bacterial biofilm may occur if the bacteria have the opportunity to adhere to the surface, divide and encapsulate themselves in a protective matrix that shields the bacteria from the effect of the systemically administered antibiotic. Subsequently, bacteria start to form colonies and the biofilm internal pressure may increase to a point where it bursts releasing the bacteria. This can cause infection of the surrounding tissue or expansion of the biofilm on a different location. When the infection persists local bone resorption takes place, leading to bone loss and implant loosening. On the other hand, eukaryotic cell adhesion (e.g. adhesion of osteoblasts) can lead to implant ingrowth followed by cell division and collagen matrix production. At last, subsequent calcification of the matrix allows bone apposition on the implant surface. Taking this into consideration, coatings that promote early tissue integration alone can be seen as a strategy to reduce infection.

1.1 Motivation

Each year, over six hundred million people are affected by healthcare-associated infections (HAI) worldwide with approximately 2% of the HAI being due to implantation of total hip and total knee prostheses, without taking trauma implants into account (WHO, 2012, ECDC, 2007). Trauma implants (e.g. plates, screws and stabilizing frames) have an even increased tendency for infection, mainly due to the fact that they are applied to repair complex injuries and open fractures. Infection together with the eventual loosening of an orthopaedic implant explains the limited lifespan of an orthopaedic device. HA-based coatings are still one of the most frequently used implant coatings in the field of orthopaedic surgery and trauma, resulting in improved implant ingrowth and a longer lifespan of the prosthesis (Capello et al., 2006).

Coatings may vary from releasing (e.g. RGD¹ or antibiotic-containing coatings) to non-releasing coatings (e.g. hydroxyapatite). Releasing coatings, are mostly applied to the surface

¹ Extracellular matrix domain of three aminoacids, arginine (R), glycine (G) and asparagine (D), that play an important role in cell adhesion, cell proliferation and differentiation.

by dip or spin coating, due to their limited thermal stability, while non-releasing are normally applied using high temperatures which may damage crystallinity and create unwanted or amorphous phases. Sol-gel technologies or electrophoretic deposition can be used to coat porous alloys (e.g. titanium), but still the production of crack free coatings remains challenging (Boccaccini et al., 2010).

Therefore, it is urgent for innovative and effective coating technologies, that do not require high temperatures, to reach the market of medical coatings, since those may help to accomplish a combined situation of a coating with both antimicrobial and osteoconductive properties. CoBlast is a cleaning, roughening, and coating technology that works under room temperature and pressure, with minimal substrate alteration developed by a co-founder of a company named *Enbio Limited*, which can offer the solution this field is waiting for.

1.1.1. Ceramed

Ceramed is a Portuguese company created in 2005 after four years of incubation with the support of the Center for Technical Support to Metalworking Industry (CATiM). The company is specialized in medical devices coatings and its services comprise plasma-spray coating with titanium and hydroxyapatite, surgical instruments coating with Physical Vapour Deposition, and titanium anodizing. Ceramed was the first European company to be ISO 13485:2003 certified, and is also ISO 9001:2008 certified for medical devices coating services (2015a).

Partnerships of this company include several Portuguese and Spanish institutes and universities, Massachusetts Institute of Technology (MIT) Portugal, Enbio Limited Ireland, Medovent Germany, Institute for Support to Small and Medium Enterprises and Investment (IAPMEI) Portugal, Flemish Institute for Technological Research (VITO Belgium) and Veterinary Hospital of São Bento Portugal (2015b).

Recently, Ceramed premises were moved to Loures, and equipment from Enbio for the production of CoBlast coatings was acquired. The company intends to optimize and validate the process in order to make the coatings deposited with this innovative room temperature technology a new service available to its clients.

1.1.2. Enbio Limited

Enbio Limited is a partnership established by Ceramed in 2007. This company was founded in 2006 to exploit the CoBlast concept (2015c). Currently, Enbio focuses the production, research and development on coatings for aviation and aerospace industries made using CoBlast. The company is achieving great successes in this field, having recently developed a partnership with the European Space Agency (ESA) to develop thermal control coatings for the Solar Orbiter mission in 2017 (2015f).

1.2 Objective

This work intends to provide a solid review on the existing medical implant coating techniques and the basic principles observed and reported in the development of an innovative coating technique called CoBlast.

Furthermore, the aim of this dissertation is to elaborate a Master Validation Plan for CoBlast technology and perform the validation of this innovative coating process and its further implementation as a new service to be provided by Ceramed within the scope of medical devices coating.

1.3 Contributions

A review on calcium orthophosphates used in medical device coatings, coating processes frequently adopted in medical device industry and CoBlast invention and principles.

A thorough explanation on how and why a Process Validation of a manufacturing process for medical devices should be carried out, and a compilation of the regulatory specifications needed to be taken into account to successfully validate a process to produce HA coatings.

A Validation Plan for CoBlast technology, the protocols and the results of all the tests performed at Ceramed. An economical appraisal of the process and future recommendations.

1.4 Document Structure

This dissertation is organized in seven major chapters: Introduction, Bioactive coating materials, Overview of medical device coating processes, CoBlastTM, Process Validation, CoBlast Validation Plan and CoBlast Process Validation.

The present chapter, Introduction, brings out the motivations, objectives and contributions of this dissertation.

Chapter 2 clarifies the importance of bioactive coatings in the medical field with a wide-ranging analysis of the use of calcium orthophosphates in orthopaedic prosthesis.

Chapter 3 provides an overview on the most frequently adopted medical device coating processes in medical industry in order to understand their properties, their weaknesses and strengths, and the global landscape where CoBlast will be inserted.

Chapter 4 presents the state-of-the-art of CoBlast technology since its invention until nowadays. It summarizes CoBlast processing principles and provides a small review of publications.

Chapter 5 reveals Process Validation within the Quality Management System requirements and its applicability to manufacturing processes for medical devices. A synopsis of statistical concepts, important considerations, and steps of process validation is made.

Chapter 6 focuses on the planning of CoBlast validation conducted at Ceramed and discloses the Validation Protocol implemented in the first validation of CoBlast. An overview on the equipment installed, raw materials used, parameters studied, requirements of the process and a clarification to the strategy adopted is made here.

Chapter 7 reveals the results obtained during the implementation of CoBlast validation protocol and infers about the state of validation of this process. This chapter is a validation report itself. Furthermore this chapter includes an economic analysis of the process in order to infer about the costs involved in a situation of production with the equipment and parameters in place.

Chapter 2

Bioactive coating materials

Most metals used in medical implants lack biologically active surface that promote osteointegration or wards off infection. Research over the years focused on finding the best materials to develop a range of coatings with the ability to improve implant binding to the host bone tissue.

Bioceramics, extracellular matrix proteins, biological peptides or growth factors have been used to enhance bioactivity and biocompatibility to the metallic surface of conventional orthopaedic prosthesis (Zhang et al., 2014). Coatings must be biocompatible in order not to trigger significant immune or foreign-body response, *osteoconductive* to promote osteoblasts adhesion, proliferation and growth on the surface of the implant to form a secure bone-implant bonding and *osteoinductive* to recruit various stem cells from surrounding tissue and circulation and induce differentiation into osteogenic cells (Albrektsson and Johansson, 2001). Furthermore the coating must have sufficient mechanical stability to withstand stresses associated with locomotion without detaching from the implant surface. Ultimately, addition of silver, nitric oxide, antibiotics, antiseptics and antimicrobial peptides, can improve anti-microbial properties minimizing the risk of prosthetic infection (Zhang et al., 2014).

2.1. Calcium orthophosphates

Calcium orthophosphates became known in history due to their great chemical similarity to the inorganic part of bones and teeth of mammals (Dorozhkin, 2013). All calcium orthophosphates (listed in Table 2.1) consist of three major chemical elements: calcium (oxidation state +2), phosphorus (oxidation state +5), and oxygen (oxidation state -2). The chemical composition may include hydroxyl ions as an acidic orthophosphate anion such as HPO_4^{2-} or H_2PO_4^- , and/or incorporated water as in dicalcium phosphate dihydrate ($\text{CaHPO}_4 \cdot 2\text{H}_2\text{O}$) (Dorozhkin, 2007). Most calcium orthophosphates are moderately soluble in water, but all dissolve in acids. Calcium to phosphate molar ratio (Ca/P) and solubility are important parameters to distinguish between the phases (i.e. phase purity and crystallinity have major influence on solubility) (Wang and Nancollas, 2008).

Hydroxyapatite (HA), one of the least soluble calcium orthophosphate, is a bioactive material that in a dense state dissolves slightly, but promotes the formation of a biological

apatite layer before interfacing directly with the tissue at the atomic level resulting in the formation of a direct chemical bond with bone. Less dense composites of tricalcium phosphate (TCP) and HA (i.e. β -TCP+HA and α -TCP+HA) or calcium-deficient hydroxyapatite (CDHA) and/or amorphous calcium phosphates (ACP) appear to be the good bioresorbable materials that dissolve and allow a newly formed tissue to grow into any surface irregularities but may not necessarily interface directly with the material (Dorozhkin, 2007).

Due to their poor mechanical properties (i.e. brittleness), bulk calcium orthophosphates bioceramics have limited load-bearing applications. The application of calcium orthophosphates coatings on metals, which support high loads but do not form mechanically stable links between the implant and bone tissues, allows the implant to participate in bone remodelling responses similar to natural bones. Phase purity and crystallinity of such coatings will have major influence on coating solubility, influencing coatings stability and bone response (Dorozhkin, 2012, 2009, 2011, 2013, Wang and Nancollas, 2008).

Table 2.1 - Existing calcium orthophosphates and their major properties. From Dorozhkin (2009) and Dorozhkin (2011) cited in Dorozhkin (2012).

Ca/P molar ratio	Compound	Formula	Solubility at 25°C $-\log(K_d)$	Solubility at 25°C (g/L)	pH stability range in aqueous solutions at 25°C
0.5	Monocalcium phosphate monohydrate (MCPM)	$\text{Ca}(\text{H}_2\text{PO}_4)_2 \cdot \text{H}_2\text{O}$	1.14	approximately 18	0.0 to 2.0
0.5	Monocalcium phosphate anhydrous (MCPA or MCP)	$\text{Ca}(\text{H}_2\text{PO}_4)_2$	1.14	approximately 17	a
1.0	Dicalcium phosphate dihydrate (DCPD), mineral brushite	$\text{CaHPO}_4 \cdot 2\text{H}_2\text{O}$	6.59	approximately 0.088	2.0 to 6.0
1.0	Dicalcium phosphate anhydrous (DCPA or DCP), mineral monetite	CaHPO_4	6.90	approximately 0.048	a
1.33	Octacalcium phosphate (OCP)	$\text{Ca}_8(\text{HPO}_4)_2(\text{PO}_4)_4 \cdot 5\text{H}_2\text{O}$	96.6	approximately 0.0081	5.5 to 7.0
1.5	α -Tricalcium phosphate (α -TCP)	$\alpha\text{-Ca}_3(\text{PO}_4)_2$	25.5	approximately 0.0025	b
1.5	β -Tricalcium phosphate (β -TCP)	$\beta\text{-Ca}_3(\text{PO}_4)_2$	28.9	approximately 0.0005	b
1.2 to 2.2	Amorphous calcium phosphates (ACP)	$\text{Ca}_x\text{H}_y(\text{PO}_4)_z \cdot n\text{H}_2\text{O}$, $n = 3$ to 4.5%; 15 to 20% H_2O	c	b	approximately 5 to 12 ^d
1.5 to 1.67	Calcium-deficient hydroxyapatite (CDHA or Ca-def HA) ^e	$\text{Ca}_{10-x}(\text{HPO}_4)_x(\text{PO}_4)_{6-x}(\text{OH})_{2-x}$ ($0 < x < 1$)	approximately 85	approximately 0.0094	6.5 to 9.5
1.67	Hydroxyapatite (HA, HAp or OHAp)	$\text{Ca}_{10}(\text{PO}_4)_6(\text{OH})_2$	116.8	approximately 0.0003	9.5 to 12
1.67	Fluorapatite (FA or FAp)	$\text{Ca}_{10}(\text{PO}_4)_6\text{F}_2$	120.0	approximately 0.0002	7 to 12
1.67	Oxyapatite (OA, OAp or OXA) ^f	$\text{Ca}_{10}(\text{PO}_4)_6\text{O}$	approximately 69	approximately 0.087	b
2.0	Tetracalcium phosphate (TTCP or TetCP), mineral hilgenstockite	$\text{Ca}_4(\text{PO}_4)_2\text{O}$	38 to 44	approximately 0.0007	b

^a Stable at temperatures above 100°C.

^b These compounds cannot be precipitated from aqueous solutions.

^c Cannot be measured precisely. However, the following values were found: 25.7 ± 0.1 (pH = 7.40), 29.9 ± 0.1 (pH = 6.00), 32.7 ± 0.1 (pH = 5.28). The comparative extent of dissolution in acidic buffer is $\text{ACP} \gg \alpha\text{-TCP} \gg \beta\text{-TCP} > \text{CDHA} \gg \text{HA} > \text{FA}$.

^d Always metastable.

^e Occasionally, it is called "precipitated HA".

^f Existence of OA remains questionable.

Plasma-spray is the most used and accepted method for HA coating application. Due to the high temperatures achieved during this deposition process, coating crystallinity decreases, and phase transformations may occur. Plasma-sprayed HA-coated implants are essentially composed of a mixture of crystalline, amorphous, and non-apatite phases such as $\text{Ca}_3(\text{PO}_4)_2$ (TCP), $\text{Ca}_4(\text{PO}_4)_2\text{O}$ (TTCP) or even CaO. The presence of TCP and TTCP phases may enhance the resorption process of HA coating leading to implant instability (Klein et al., 1994, Radin and Ducheyne, 1992). Therefore, it is important to explore other coating

techniques that do not require high temperatures for the application of HA bioactive coatings that promote osteogenesis and prevent infections.

Requirements and regulations for HA coatings are described in the Food and Drug Administration (FDA) guidelines as well as in the ISO standards and European Medical Regulations (Veselov et al., 2012).

Chapter 3

Overview of medical device coating processes

Surface modification of medical devices has been adopted over the years to retain key bulk properties of the device material while modifying the surface to improve biocompatibility. These surface engineering strategies tailor chemical and structural properties in a thin surface layer of the substrate in order to meet with design and functional requirements. This chapter gives an insight on the most commonly applied surface modification processes used in the medical field.

3.1 Abrasive blasting

Techniques such as grit blasting, shot blasting, sand blasting, shot peening and micro abrasion generally involve the mixing of an abrasive material with a fluid and delivery at high velocity to impinge the surface to be treated, and are here stated as abrasive blasting techniques. The delivery of the abrasive material can be classified as wet or dry depending on the fluid medium used to deliver the abrasive to the surface, gaseous or liquid.

Abrasive blasting techniques have many applications like metal cutting, cold working metallic surfaces and pre-treatment of surfaces to create surface roughness to improve further coating materials adhesion. In the biomedical sector, titanium implants are regularly grit blasted with alumina or silica to create a level of surface roughness that maximizes the adhesion of plasma sprayed HA coatings on the surface of the implants (Yang et al., 2009).

3.2 Thermal spraying techniques

Thermal spraying comprises a group of processes in which metallic and non-metallic materials are deposited in a molten or semi-molten state on a prepared substrate (Pawlowski, 2008). It uses a concentrated heat source to melt feedstock materials and process jets to propel the molten particles toward a prepared surface. The heat source can be generated chemically through combustion of fuels with oxygen or air, or electrical heating of industrial gases. Devices used to achieve this work are called guns or torches (Davis and Committee, 2004).

3.2.1. Plasma spray

In plasma-spray processing, powder materials are injected into a high temperature plasma² (i.e. radio frequency discharges) or plasma jets (i.e. direct current arc) being rapidly heated and accelerated before they flatten and solidify onto the substrate. Conventional direct current (DC) arc spray torch is represented in Figure 3.1. Temperatures over 8000K at atmospheric pressure are normally reached allowing the melting of any material. In order to avoid low deposition efficiency, the melting temperature must be at least 300K lower than the vaporisation or decomposition temperature (Fauchais, 2004).

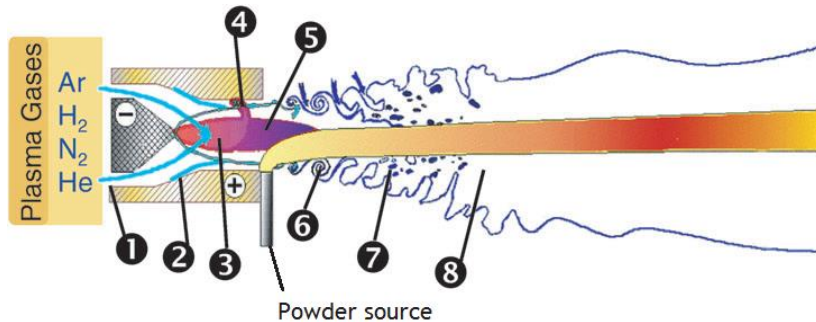


Figure 3.1 - Schematic of a conventional DC arc spray torch with a nozzle composed by a stick type thoriaated tungsten cathode (+) and a anode (-); 1 - Plasma forming gas injection, 2 - Cold boundary layer at the anode wall, 3 - Arc column, 4 - Connecting arc column, 5 - Plasma jet exiting the nozzle, 6 - Large scale eddies, 7 - Surrounding atmosphere bubbles entrained by engulfment process, 8 - Plasma plume. Adapted from Fauchais (2004).

Characteristic coatings of HA deposited using plasma spray are 20-300 μm thick and 3-6 μm rough (Sun et al., 2001). It was verified an increased cell proliferation on plasma-sprayed HA-coatings when compared with simply HA-grit-blasted surfaces (Borsari et al., 2005).

Oxide formations are frequent in air plasma spray (APS) processing. An option to avoid those is plasma-spray process conducted under controlled-environment spraying like low pressure or vacuum plasma spray (VPS). It is able to produce clean coatings with virtually no oxide inclusions (Davis and Committee, 2004).

3.2.2. Flame spray

Conventional flame spray requires combustion of a jet of fuel and oxygen in front of the torch, external to nozzle. Fuel and oxygen rates and ratio can be adjusted to induce the desired thermal output. Oxyacetylene torches are the most common, using acetylene as fuel in combustion with oxygen to generate high combustion temperatures. During processing the jet gas speed is below 100 m/s, and particles reach 80 m/s before impact. Open-flame (i.e. externally combusted) jet temperatures are generally above 2900K, and are controlled by mixing patterns of the combustion gases with the surrounding air as well as by the combustion

² Plasma is the term used to describe gas which has been raised to such a high temperature that it ionizes and becomes electrically conductive (Birka et al., 2012).

temperatures of the fuel/oxygen mixture. Powder is fed into these spray torches either by carrier gases or by gravity (Davis and Committee, 2004).

3.2.3. High velocity oxygen fuel (HVOF)

High velocity oxygen fuel (HVOF) requires extended internal-confined combustion and operates on a continuous, steady-state basis. High volume combustible gases are fed into a combustion chamber, like a long confining nozzle or barrel, through which the combustion gases exit the device with velocities ranging from 1525 to 1825 m/s, at the nozzle exit. High velocity combustion spray devices can be divided into two distinct classes according to their combustion chamber pressure: *high velocity* (i.e. pressure exceeding 241 kPa and heat inputs of 527 MJ) and *hypervelocity* (i.e. pressure ranging from 620 to 827 kPa and heat inputs of approximately 1GJ). These last use normally kerosene as fuel and air or oxygen to support combustion. The HVOF guns are air or water cooled where fuel/oxygen mixtures under pressure accelerate the gas stream down a confined cooled tube or nozzle. Powder materials are fed into the nozzle borne by a carrier gas, and become entrained into the confined high pressure flame/jet (Davis and Committee, 2004).

3.2.4. Electrical arch spray

Electrical arch spray, also called twin wire arc, arc spray or wire arc spray, uses a DC electric arc between two consumable electrode wires performing direct melting of particles. Molten particles are sprayed through the surface by a high-velocity air jet located behind the intersection of the wires, as the wires are fed into the arc and melted. The airflow ranges from 0.8 to 1.8 m³/min at up to 690 kPa, as the power supply design of the arc limits most systems to operating above 50A DC. Since the wires are melted directly by the arc in this technique, higher thermal efficiency is registered when compared with other thermal spray processes. However, the droplets are already molten when picked up and entrained in the jet, and, unlike other processes, the particles begin to cool immediately after leaving the arc zone. In order to minimize this effect combined with the effect of oxidation, short standoff distances and high atomizing air flows can be used (Davis and Committee, 2004).

3.3 Electrodeposition

Electrodeposition is a useful process for applying thin films to electrically conductive surfaces. In its simplest form, also known as electroplating, there is an electrodeposition bath containing metal ions, an electrode or substrate on which the deposition is desired, and a counter electrode. When a current flows through the electrolyte, the cations and anions move, according to their charges, toward the cathode and the anode, and may deposit on the electrodes after undergoing a charge transfer reaction. This process is directly related with Faraday's laws of electrolysis. Faraday's second law relates the mass (Δm) deposited over a unit area to the current density j flowing for a time t :

$$\Delta m = \text{const} \times jt \quad (3.1)$$

An important implication of Faraday's second law is that the ratio of the mass of the electrodeposit to its gram-equivalent weight is a constant equal to 96,500 coulombs. The amount of material electroplated depends directly upon the current on the substrate, and thus, a uniform current distribution is compulsory to generate a uniform film. Most materials that can be deposited through electrodeposition can roughly be delivered using other physical or chemical methods (e.g. thermal-spray, chemical vapour deposition, physical vapour deposition), nevertheless, electrodeposition can be more cost-effective in some applications (Pandey et al., 1996).

3.4 Sputtering

Sputtering is known as a deposition process capable of grow thin films of material on a substrate that uses irradiation of energetic species. The phenomenon occurs when a solid surface is bombarded with energetic ions and surface atoms of the solid are scattered backward due to collisions between the surface atoms and the energetic particles. Typical sputtering systems include DC diode, radiofrequency diode, magnetron diode and ion beam sputtering. The simplest model is the DC diode sputtering system composed by a pair of planar electrodes, a cathode and an anode, inside a sputtering chamber. The front surface of the cathode is conveniently covered with target materials to be deposited, as the substrates are placed on the anode. The sputtering chamber is filled with gas (e.g. Argon) at 1 to 5 Pa. Under the application of DC voltage between the electrodes, a glow discharge is maintained and Ar^+ ions formed in it are accelerated at the cathode fall and sputter the cathode target resulting in the deposition of thin films of the cathode target on the substrates (Wasa, 2012).

Conventional sputtering techniques have shown some advantages over the commercially available plasma spraying method, the most utilized technique to deposit HA. However, sputtered films are usually amorphous which can cause some serious adhesion problems when post-deposition heat treatment is needed (Hong et al., 2007).

3.5 Chemical vapour deposition (CVD)

Every chemical vapour deposition (CVD) process involves reactions that create a solid from gases in a synthesis process in which the chemical constituents react in the vapour phase near or on a heated surface. The material to be deposited is vaporized and is injected into the CVD chamber to make their way to the substrate. When the gaseous compounds react the solid deposit is formed as well as by-products gases which are removed by gas flow through the reaction chamber. In CVD the absolute temperature varies from 300K to 1200K, and pressure varies from few 0.1 Pa (i.e. low pressure chemical vapour deposition) to 100 kPa (i.e. atmospheric pressure chemical vapour deposition). The use of precursor chemicals almost always introduces impurities in the solid films (Dobkin and Zuraw, 2003).

3.6 Physical vapour deposition (PVD)

Physical vapour deposition (PVD) is a process in which a material to be deposited is vaporized from a solid or liquid source and transported in the form of a vapour through a vacuum or low pressure gaseous or plasma environment to the substrate, where it condenses (Mattox, 2010). The vacuum deposition comprises evaporating the source material in a vacuum chamber below 1×10^{-4} Pa. Kinetic energies of evaporating source material atoms are 1000-3000K and can be attained by resistive heating or electron beam deposition. PVD rate of condensation of vapour depends on the evaporation rate of the source material, source geometry and its position relative to the substrate, and condensation coefficient. The method allows the treatment of substrates with complex geometries and very small to very large size (Wasa, 2012).

3.7 Pulsed laser deposition (PLD)

A pulsed laser deposition (PLD) system is composed by three essential parts: substrate, solid target and laser source (Figure 3.2). The principles of action are similar to the ones explored in other processes herein explored, where the material of the target experiences evaporation and subsequent condensation on the substrate. The evaporation occurs as consequence of the incidence of laser pulses. There are many classes of high-power ultraviolet pulsed lasers, being Nd:YAG and KrF excimer (1 J/cm^2) the most successfully used in HA deposition (Kurella and Dahotre, 2005).

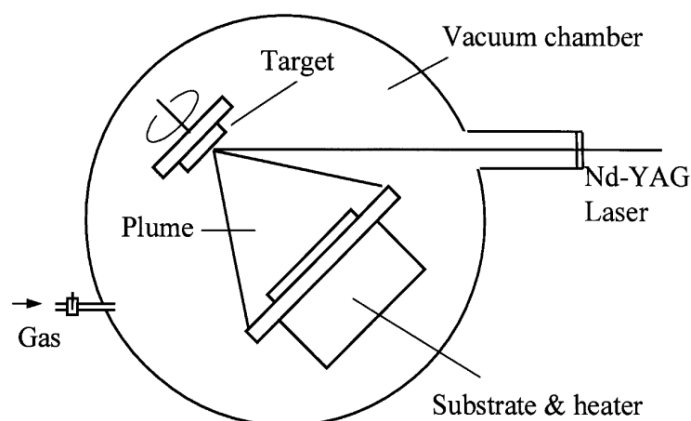


Figure 3.2 - Typical pulsed laser deposition (PLD) system. Laser pulses, irradiated through a quartz window, evaporate the target materials which condense on the substrate. From Zeng and Lacefield (2000).

3.8 Sol-gel immersion technique

Sol-gel processing requires colloidal suspensions (i.e. *sols*) conversion to viscous gels and drying. A wide range of inorganic and organic/inorganic composite materials can be prepared using this approach. Sol-gel thin layers can be applied to substrates using both spin coating and dip coating. In spin coating process the film is applied and dried in a few seconds, whereas in dip coating the film is applied at a rate of few centimeters per minute. Both techniques result in an inverse relation between the thickness of the film and its density: thin films are denser than thick films. These techniques allow the preparation of composite coatings which cannot be obtained by other methods, such as organic-inorganic hybrid materials (Wright and Sommerdijk, 2000).

3.9 Sintering

Sintering processing comprises the application of thermal energy to a powder compact, densifying it and increasing the average grain size (Kang, 2004). It aims to produce sintered parts with reproducible and designed microstructure through control of sintering variables (e.g. powder shape, size, composition, sintering temperature, time and pressure). Sintering is a process that leads to a reduction of the total interfacial energy of the powder compact. Ceramic coating sintering can result in considerable coating thermal conductivity and elastic-modulus increase, but can also lead to shrinkage-cracking, eventually causing spallation of the coating (Xu and Guo, 2011).

Chapter 4

CoBlastTM

CoBlastTM is a one-step metal transformation technology developed by John O’Donoghue, co-founder and current co-director of Enbio Limited. This technology is commercially applied to remove a metal’s oxide layer and replace it with a desired functional coating. (2015d) It uses conventional grit-blasting or micro-blasting equipment, and is performed at room temperature and pressure. These properties allow it to be applied to sensitive substrates without damage, preserving properties that are easily destroyed by heat treatment processes. Simultaneous roughening, chemical activation and coating adhesion achieved with this technique are great for substrates that normally suffer poor coating adhesion. Currently, CoBlast is a surface treatment with its basic technology research complete in respect to biocompatibility, lubrication and hydrophobicity in the medical field (Figure 4.1) (2015e).

	Thermo-optical control	Biocompatibility	Corrosion Resistance	Lubrication	Hydrophobicity
Space	TRL 6			TRL 3	
Aerospace			TRL 3	TRL 3	TRL 2
Oil and Gas			TRL 3		
Oceanic			TRL 3		TRL 2
Automotive			TRL 3	TRL 3	TRL 2
Industrial			TRL 3	TRL 3	TRL 2
Medical		TRL 4		TRL 3	TRL 2

Figure 4.1 - CoBlast technology readiness level concerning properties like thermo-optical control, biocompatibility, corrosion resistance, lubrication, hydrophobicity in the fields of space, aerospace, oil and gas, oceanic, industrial, and medical. From 2015c).

Technology readiness levels (TRLs) are used as the metric to assess the maturity of a technology. It consists in a scale developed firstly by National Aeronautics and Space Administration (NASA) in the 70s, that was lately approved by the Department of Defense

(DOD) of the United States of America (USA) and adopted world-wide (Mankins, 2009). TRL scale ranges from one to nine with definitions as followed (DOD and (DUSD(S&T)), 2003) :

- TRL 1: Basic principles observed and reported;
- TRL 2: Technology concept and/or application formulated;
- TRL 3: Analytical and experimental critical function and/or characteristic proof-of-concept;
- TRL 4: Component and/or breadboard validation in a laboratory environment;
- TRL 5: Component and/or breadboard validation in a relevant environment;
- TRL 6: System/subsystem model or prototype demonstration in a relevant environment;
- TRL 7: System prototype demonstration in an operational environment;
- TRL 8: Actual system completed and qualified through test and demonstration;
- TRL 9: Actual system proven through successful mission operations.

4.1 Invention

CoBlast is the trade name for a method of doping surfaces patented by O'donoghue and Haverty (2008), that comprises the removal of the oxide layer from a metal's surface and provision of dopant particles in fluid jet that impregnates the surface with the dopant.

Invention background lies in surface treatment techniques of bombardment of metal surfaces with abrasive materials, e.g. abrasive blasting techniques. Knowing that during the blasting some of the abrasive metal becomes impregnated in the surface of the metal, attempts of using abrasive blasting techniques as a means of putting a hydroxyapatite layer directly onto titanium surfaces were made (Ishikawa et al., 1997). Still, since the deposited layer could be removed under ultra-sonication with water after few minutes, it seems like no proper bond with the surface of the metal is achieved.

In this method, the metal oxide layer is removed by abrasively blasting the metal oxide surface with an abrasive material - e.g. silica, alumina, zirconia, barium titanate, calcium titanate, sodium titanate, titanium oxide, glass, biocompatible glass, diamond, silicon carbide, calcium phosphate, calcium carbonate, metallic powders, metallic wires, carbon fiber composites, polymers, polymeric composites, titanium, stainless steel, hardened steel, chromium alloys - by the same means used on the exploited abrasive blasting techniques described in section 3.1. This process focuses on the intentional addition of a material of choice to the surface - the *dopant* - that can be a polymer, metal, ceramic and combinations thereof. Respecting biomedical applications the dopant can be hydroxyapatite, modified calcium phosphates, therapeutic agents, silica, zirconia, biocompatible glass, carbon, chitosan/chitin, and others. These last can induce desirable chemical, physical and biological properties on the surface of biomedical implants. The addition of the dopant happens prior to reoxidation of the newly formed oxide layer. To prevent its early formation the removal of the oxide layer can be performed under an inert atmosphere. This procedure takes, thus, advantage of the inherent reactivity of metals to modify their surface. By having an abrasive impacting with sufficient energy (i.e. a material with sufficient particle size, density and hardness) to break the oxide layer and feeding the surface simultaneously with a dopant material, this last may be taken up while the oxide layer reforms around it. Thereof, the dopant material can become strongly bound within the oxide layer of the surface.

Different approaches can be adopted to achieve this. In one embodiment there is an almost synchronously delivery of a first set of particles containing a dopant and a second set

of particles with an abrasive from one fluid jet to a surface of an article to impregnate the surface of the article with the dopant (Figure 4.2). The energy dissipated at the impact site of the abrasive may be sufficient for the dopant to become ceramicised or otherwise bonded to the surface.

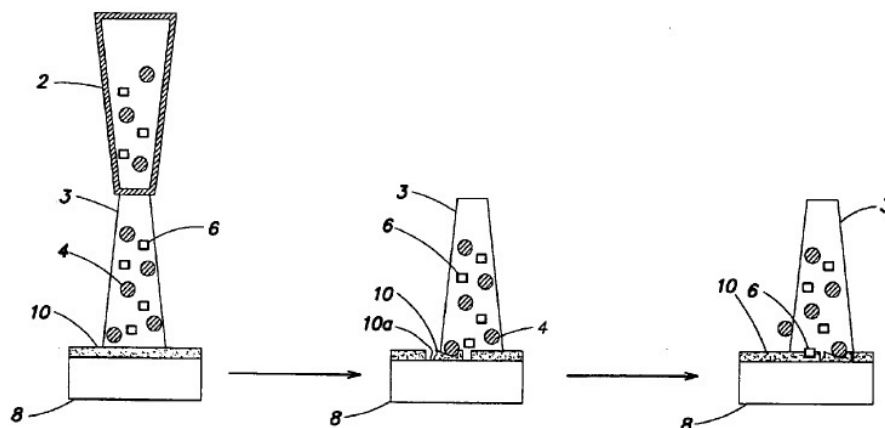


Figure 4.2 - CoBlast application approach using fluid jet (nozzle) (2) to bombard the surface (10) of the substrate (8) with abrasive (4) and dopant particles (6) almost simultaneous in the same stream (3). During the impact of the abrasive particles a new surface (10a) of the substrate is exposed. From O'donoghue and Haverty (2008).

Dopants and abrasives can be either contained in the same reservoir and delivered to the surface from the same jet (nozzle) or separated in different reservoirs and delivered by multiple jets. Three different nozzle configurations can be implemented to deliver dopant particles and abrasive particles to the surface (Figure 4.3). A single nozzle can be used as previously stated (Figure 4.3, A) or a combination of multiple nozzles (Figure 4.3, B and C) where two or more streams of particles are used where at least one stream abrasively blasts the oxide surface to expose the new metal surface and another stream bombards the new metal surface with dopant.

Concerning multiple jets, the particles of each jet can have the same (Figure 4.3, B) or different incident angles hitting the same spot on the surface simultaneously (Figure 4.3, C). To sum up, the final variables that must be considered in order to apply this technology are the abrasive particle, the abrasive particles size, the dopant, the dopant particles size, the stream carrier fluid (i.e. gaseous, liquid, basic etching liquid, acidic etching liquid), the number of nozzles used, incident angle(s) (ranging from 10 to 90°) power feeder pressure (ranging from 50 to 10000 kPa), deposition direction, speed of the movement of the nozzles over the surface, distance of the nozzles to the surface and raster offset. This topic is further explored in the following section 4.2.

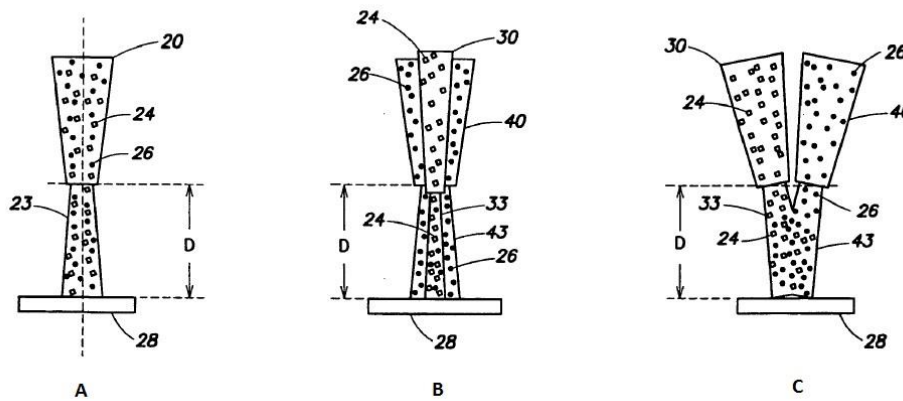


Figure 4.3 - Schematic diagrams of three different nozzle configuration to deliver the dopants and abrasives of CoBlast to a surface at a distance D : single nozzle (A), multiple nozzles with dopants and abrasives delivered from separate reservoirs where one nozzle is within another nozzle (B), and multiple separate nozzles with dopants and abrasives delivered from separate reservoirs (C). Elements: 20 - single nozzle; 23 - single stream; 24 - abrasive particles; 26 - dopant particles; 28 - substrate; 30 - one nozzle; 33 - stream of abrasive particles; 40 - another nozzle; 43 - stream of dopant particles. From O'donoghue and Haverty (2008).

The working ability of these systems is related with the use of converging-diverging nozzles, commonly known as De Laval nozzles. Converging-diverging characteristic design of the De Laval Nozzle allows the generation of supersonic gas exit flow velocity after a subsonic entry velocity. It was named after Karl Gustaf Patrik de Laval by the end of the 19th century and is often employed in propelling equipment like rockets and high-pressure jet engines.

4.2 Deposition conditions and parameters

CoBlast pre-deposition processing can include steps like mechanical polishing of substrates (e.g. using 1200 grit size silicon carbide paper) to provide uniform surface roughness (Barry and Dowling, 2012, Tan et al., 2012, Barry et al., 2013). Frequently, metal substrates are washed with 1M HCl (O'Hare et al., 2010, Keady and Murphy, 2013) and ultrasonically cleaned using isopropanol (O'Hare et al., 2010, Fleming et al., 2011, Keady and Murphy, 2013) to remove any contaminants. When metal polish is preformed, methanol and acetone ultrasonic wash is generally applied to remove loosely adherent particles (Barry and Dowling, 2012, Tan et al., 2012, Barry et al., 2013).

CoBlast processing is regularly applied using twin nozzles to deliver one stream of dopant and one stream of abrasive to a common area on the substrate surface (i.e. "blast-zone") (Keady and Murphy, 2013, Byrne et al., 2013, Barry et al., 2013), or using a single nozzle where dopant and abrasive are part of a mix media sprayed at the substrate in the same stream (O'donoghue and Haverty, 2008, Dunne et al., 2013). The angle of deposition can be adjusted, and it is common to be adopted an angle ranging from 75° to 82° when two nozzles are used with different nozzle angle for the abrasive and the dopant (Tan et al., 2011, Fleming et al., 2011) or the same angle for the abrasive and the dopant (Tan et al., 2012), or

90° when a single nozzle is used (Dunne et al., 2013, Dunne, Twomey, and Stanton, 2015, Dunne, Twomey, Kelly, et al., 2015).

Figure 4.4 presents in red the deposition parameters that according Tan et al. (2012) are essential to acquire HA coatings and in black the core components of a CoBlast processing system with two nozzles. Nozzles height (i.e. distance to the surface), nozzles speed over the surface, and feed pressure are often settled to a range between 8 and 23 mm, 12 and 15 mm/s (Fleming et al., 2011, Tan et al., 2012, Keady and Murphy, 2013), and approximately 414 to 620 kPa (Fleming et al., 2011, Tan et al., 2012) respectively.

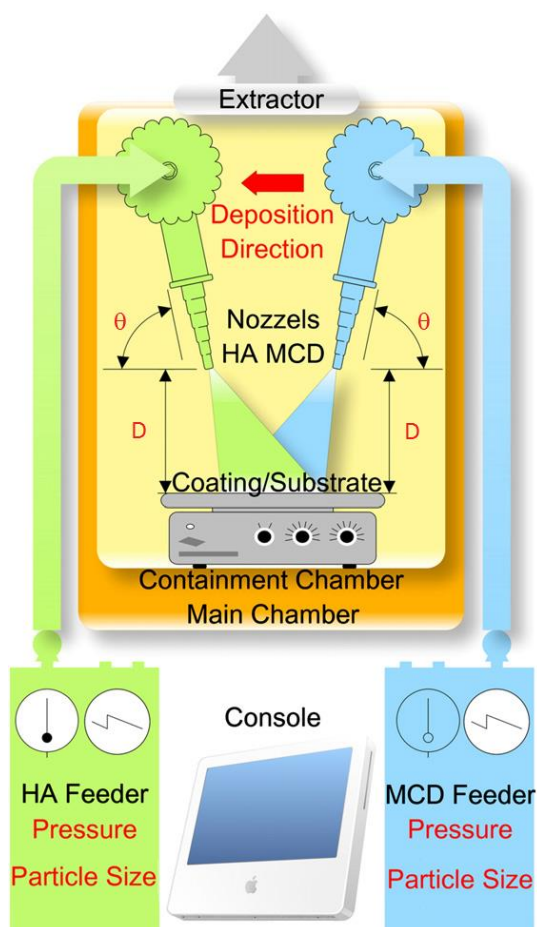


Figure 4.4 - Schematic of CoBlast deposition system with two nozzles. θ stands for the deposition angle and D for the distance to the substrate. MCD is a commercial granular apatitic abrasive made of sintered apatite (sHA). Black texts represent the core components of the system while red texts are the essential parameters to acquire the coatings. Adapted from Tan et al. (2012).

When a single nozzle is used, it is held at 90° to the surface (O'donoghue and Haverty, 2008). Its height is settled at 50 mm and pressure of the feeder ranges approximately from 500 to 550 kPa (O'donoghue and Haverty, 2008, Dunne et al., 2013).

The perfect combination of such parameters will be always dependent on the type of substrate, powder particles, and fluid carrier used. Nevertheless, the implementation of such standards is based on the experience of research teams that work directly and repeatedly

with CoBlast and, thus, has its intrinsic value. Unanimously, compressed air was used as fluid carrier by all of the groups mentioned herein.

Substrates are bombarded to ensure that the area of interest is covered. When more complex shapes pieces are processed by CoBlast, several strategies can be adopted. Keady and Murphy (2013) performed a three passes process applying 120° rotations to completely coat a wire. The same team coated stents by placing them in a mandril, rotating the mandril and coating the stent with a helical pattern.

Post-deposition processing may include air-cleaning of the samples using compressed air (O'Neill et al., 2009, O'Sullivan et al., 2010) sonication in isopropanol (Tan et al., 2011), storage in a desiccator and autoclave processing at 121°C for 20 minutes prior to packaging and use. Samples may also be simply ultrasonically washed in de-ionized water (O'Sullivan et al., 2011, Barry and Dowling, 2012), to remove any loose powder from the surface, followed by autoclave prior to use.

4.3 Reviewed Publications

O'Neill et al. (2009) reported on the capability of CoBlast process to deposit substituted apatites. Water contact angle of Ti-6Al-4V surface treated sheets with HA, Fluoro apatite (FA), Magnesium apatite (MgA) and Carbonate apatite (CO₃A) revealed significant surface modification for each material. XPS analysis showed that all surfaces exhibit minimal levels of titanium and high amounts of Ca, P, O and C after treatment consistent with complete treatment of the accessible surface. EDX revealed otherwise, finding significant levels of titanium in samples pointing to a limited depth of treatment. Adventitious carbon was also found in the XPS analysis. Coating thickness was estimated between 7 and 10 µm and SEM images unveiled roughening by the abrasive blasting and regions of titanium which appear to be folded in the outer HA layer in the metal-HA interface. Such apatite adhesion was attributed to the combination of kinetic energy resulting tribochemical bonding with mechanical interlocking due to substrate surface disruption. Standard tape adhesion test (ASTM D3359-02) lead to no evidence of coating delamination on each coated sample. The present study exposed also that substituted apatites had higher ion release likely attributed to the lower level of crystallinity determined by XRD. Finally, MTT assay showed comparable levels of MG-63 osteosarcoma-derived cell proliferation after 24h and significant enhanced cell proliferation on the carbonate samples after 72h. The authors conclude by saying that the combination of ion elution and XRD analysis suggests that the crystallinity of the dopant is conserved in the coating process as expected in a non-thermal processing method like CoBlast.

A year later, O'Hare et al. (2010) characterized the difference between surfaces produced by simple HA surface blasting and surfaces treated with CoBlast using alumina (Al) as abrasive and HA as dopant. *In vitro* response of osteoblast-like cells and bone growth in an *in vivo* animal model were observed. XPS surface analysis revealed the chemistry of the outermost surface region with significant levels of Ca, P and O on both samples (i.e. HA-microblast and CoBlast), and no significant level of titanium, suggesting effective deposition of HA into the surface and good surface coverage with both techniques. Differences between the two surfaces were found using EDX and Secondary Ion Mass Spectroscopy (SIMS): a smooth

interface occurs between HA and Titanium on HA-microblast surfaces and on the other hand a significantly roughened metal surface is created when CoBlast is used leading to the presence of Ti particles in the sampling depth of analysis (10 μm) of EDX. Transmission electron microscopy (TEM) detected no signal of alumina on the CoBlast samples, revealing no significant levels of contamination from Al abrasive particles after CoBlast processing. Scratch testing of HA-microblast samples suggested that the HA layer was only superficially adhered to the underlying metal. As opposite CoBlast coating proved to be very well adhered. CoBlast samples were rougher than HA-microblast. After HA removal by immersion in HCl and ultrasonic washing, roughness of pristine titanium was found in HA-microblast samples as CoBlast titanium surface retained the same surface roughness. This indicates that the topography of the metal surface was significantly modified by the CoBlast process. *In vitro* tests clearly demonstrated significantly greater MG-63 cell activity on CoBlast samples after 24h and 48h. After cell staining and observation under confocal laser scanning microscopy (CLSM) MG-63 cells were found to align with titanium polishing striations on both the control (i.e. polished titanium) and the HA-microblast surfaces. MG-63 cells were observed to be randomly distributed on the CoBlast surface suggesting that cells were proliferating on the bioactive HA surface. The analysis of this images on day 3 and 7 discovered a greater number of cells on CoBlast HA surface. *In vivo* results showed no adverse tissue response in any of the histopathology sections. The formation of new lamellar bone after 7 days on the CoBlast samples occurred all along the implant surface. In contrast, the untreated control surface samples had a woven morphology in the new bone around the implant. At this early time point, CoBlast surface seemed to have a greater amount of newly deposited bone. Both surfaces continued to be positive for new bone formation at 14 days. These data suggest that the CoBlast surface may provide for early stage osseointegration of metallic implants.

The potential of doped apatites as non-colonizing osteoconductive coatings deposited onto titanium surfaces using CoBlast was evaluated by O'Sullivan et al. (2010). Zinc substituted apatite (ZnA), silver substituted apatite (AgA) and strontium substituted apatite (SrA) were the dopants in study and HA was used to produce a positive control surface. Surface characterization revealed treated samples rich in Ca, P and O, and a dopant ion level of less than 5%. Silver samples had the lowest level of dopant ion incorporation and Zn produced the highest levels. Based on the low levels of Ti on the EDX analysis and gravimetric analysis of the coating mass, Sr doped surfaces seemed to have a higher depth of surface treatment. By using Inductively Coupled Plasma Optical Emission Spectroscopy (ICP-OES) SrA and ZnA were determined to contain the greatest amount of the respective dopant present in each coating and ion release into PBS buffer of each coating was accessed. The findings that over a 30-day period over 90% of the Sr and Zn still remained in the coatings whereas 90% of the Ag was released were linked directly to the antimicrobial properties of the treated surfaces: Ag apatite coating out-performed the other two surfaces in biofilm inhibition at days 7 and 14 (i.e. approximately 90% and 20% of biofilm inhibition respectively) and reached a antimicrobial performance against *Staphylococcus aureus* (*S.aureus*) of 57% when freshly prepared. MG-63 cell proliferation revealed that the surfaces were as osteoconductive as the well characterized HA surface and that no cytotoxicity was observed on any of the samples. The study also found that the deposition of substituted apatites significantly increased the surface roughness when compared to the HA control. Ion release rates of every sample was <1 ppm over the duration of the study which is less than all the

known exposure thresholds of these materials as stated in the article. Conclusions point to direct surface-bacteria interaction as the mechanism control of colonization process through effects exerted by the dopant ion over any surface topography or ion elution effects. Further optimization of the antimicrobial coating performance can be made by varying the loading of the dopant ion, tailoring the elution profile and controlling surface morphology.

In the same year, a different research team explored the possibility of using CoBlast process to apply bioactive glass (BG) onto Ti-6Al-4V alloy substrates (Tan et al., 2011). Different approaches were used and compared: BG as dopant and MCD-180 as abrasive, HA as dopant and BG as abrasive (HA/BG), HA as dopant and MCD-180 as abrasive (Osteozip). MCD is the trade name for a series of apatitic abrasives (sintered CaP, sHA) commercialized in different sizes by Himed, US. All the coatings were found to be hydrophilic (i.e. water contact angle $<90^\circ$), with BG being significantly the most hydrophilic and Osteozip least hydrophilic. Surface roughness does not differ significantly, but Osteozip was slightly rougher than HA/BG. Total amount of adsorbed protein was quantified by a bicinchoninic acid (BCA) protein assay and demonstrated significant differences with a sequence: BG>HA/BG>Osteozip. BG and HA/BG differences were attributed to their hydrophilicity differences, while HA/BG and Osteozip seemed to differ as a net result of roughness (i.e. higher surface roughness, larger surface area) and hydrophilicity. Cell attachment followed the same trend as protein adsorption after 25, 100 and 200 minutes, except that at 200 min a similar amount of cells were attached to BG and HA/BG. Differences in cell morphology were also reported, with cells on BG being the first to loosen their base by creating early lamellipodia at 25 min, and Osteozip cells possessing a spherical body at 100 min while BG cells had extensive lamellipodia and fairly flattened architecture. Cell attachment on BG-derived surfaces stabilized within 200 min and occurred faster than on the Osteozip surface. Besides, differences in the vinculin focal adhesion revealed that cell adhesion was better on BG-derived surfaces. ICP-OES ion release analysis over a 7 days period showed that Ca and P levels released by Osteozip samples were maintained around the baseline during this period, with a slight increase on day 1. This behaviour was attributed to the near 100% crystallinity of the HA surface deposited by CoBlast process, by the authors. Bioglass-derived surfaces have significant release of Ca and Si and a slight drop of P after 1 day of immersion. Regarding cell proliferation no significant difference was found in cell number between each surface after 24h, but from 3 days onwards, cell number on BG and HA/BG surfaces was significantly higher than Osteozip. After two weeks of differentiation, there was no significant difference in alkaline phosphatase (ALP) levels, while collagen production on BG was significantly lower than on HA/BG and Osteozip. Osteocalcin expression revealed that osteogenic differentiation was most advanced on the HA/BG surface. The authors inferred that BG surface is not as supportive as Osteozip in terms of osteogenic differentiation, though, HA/BG surpasses Osteozip in most aspects of osteoconductivity. In agreement with the collagen production results, cell detachment by AccutaseTM led to faster detachment of cells on BG than HA/BG and Osteozip surfaces. SEM images confirmed that BG cell layers contained less collagen content within the extracellular matrix (ECM). Basic fibroblast growth factor (bFGF)³ levels

³ bFGF is an autocrine growth factor that controls in vitro bone formation by stimulating bone cell replication and inhibiting differentiation related markers (Bodo et al., 2002, Bilezikian et al., 2008).

were higher at day 3 than at day 15 for all surface, and more abundant in BG than Osteozip, with HA/BG surfaces changing from paralleling to BG at day 3 to parallel to Osteozip at day 15. Higher bFGF is consistent with better proliferation, whereas lower bFGF is consistent with advanced osteogenic differentiation, which was in accordance with the results found. Angiopoietin (Ang) and inducible nitric oxide synthase (iNOS), proteins that can be linked to aseptic implant loosening, study, revealed that HA/BG has the best angiogenic potential among the three surfaces with Osteozip more likely to have better peri-prosthetic vascularization than BG, and BG-coated implants are more likely to loosen from the host. Nonetheless, the authors postulated that by working on maximizing the beneficial clinical features and minimizing adverse stimuli the reported Bioglass coatings are significant boosts to the current clinical standards.

The effect of the abrasive particle size on the surface properties for both microblast and CoBlast treatments was studied by O'Sullivan et al. (2011). MCD-106, MCD-180 and MCD-425 abrasive powder with different particle sizes (approx. 44, 124 and 355 μm respectively) were used as abrasive in microblast processing and as abrasive as well in CoBlast processing of samples. HA (approx. 40 μm) was used as dopant in CoBlast. EDX analysis of the powders revealed O, P and Ca in both MCD and HA as expected. Stoichiometric HA had a Ca/P ratio of 1.67. Increased Ca/P was found in MCD-106 and MCD-180, and was attributed to the presence of impurities such as tricalcium phosphate (TCP) as determined by powder x-ray diffraction (PXRD). PXRD results unveiled highly crystalline HA, and relative lower crystallinity of MCD apatites. MCD PXRD patterns demonstrated the more amorphous nature of this CaP material. EDX analysis of the coatings (i.e. microblast MCD-106, MCD-180, MCD-425, and CoBlast HA/MCD-106, HA/MCD-180, HA/MCD-425) showed that microblast samples had a thin coating of Ca/P successfully deposited but a higher amount of Ti indicating a lower degree of coating coverage than CoBlast samples. CoBlast samples displayed a Ca/P ratio of between 1.53 and 1.61, which was relatively close to the value for stoichiometric HA. It was verified that the smaller the particle size of the MCD abrasive used, the more HA was deposited. Coating thickness of all CoBlast samples was $< 10 \mu\text{m}$. Surface roughness measurements and SEM images denoted increased roughness in the resultant surfaces, for both microblast and CoBlast samples, as MCD abrasive size increased, resulting in a reduced coating thickness. A large standard error was observed for MCD-425 microblasted surfaces roughness pointed as a feature of the crude microblast process. XDR CoBlast pattern showed no evidence of TCP phase, indicating no compositional or crystallographic changes on HA powder during the blasting process and negligible uptake of the abrasive. FTIR analysis also suggested minimal uptake of the abrasive powders on CoBlast HA coatings during sample preparation. Regarding MG-63 cell proliferation, CoBlast surfaces exhibited excellent osteoblast attachment and proliferation compared with untreated Ti surfaces. MCD-106 and HA/MCD-106 surfaces were compared, showing significant higher cell proliferation on CoBlast coated substrate over uncoated titanium and microblast sample at day 5, without evidence of cytotoxicity on any of the samples evaluated. Cell morphology, after 24h, on microblast samples, was similar that observed on the untreated titanium surfaces: a small number attached with fibroblastic morphology, polarized in one direction with an average cell length 60-80 μm , with lamellipodia and filopodia extensions, and a larger number spherical indicating that not all the cells were involved in spreading and migration. MG-63 cells cultured on CoBlast surfaces had a polygonal shape rather than a polarized fibroblastic morphology indicating cell

spreading, with abundance of lamellipodia and filopodia. The research team concluded by saying that employing MCD abrasives offers an alternative to alumina as abrasive in CoBlast process.

Dunne et al. (2013) operated, for the first time, a single nozzle configuration to assess the influence of two blast media on the deposition of HA onto a titanium substrate. HA was sprayed, at the surface of commercially pure titanium (cp-titanium), conjugated with Al_2O_3 or sHA and compared with plasma-sprayed samples. HA powder with a particle size of 25-60 μm was used as the dopant or coating medium, while Al_2O_3 and sHA sintered apatite were used as the blast media with size particles of <150 μm and <180 μm respectively.

XRD analysis of as-received powder and deposited HA coatings revealed that there was a minimal change to the precursor HA during process. XRD analysis was also performed on the substrates after removal of HA coating and results achieved demonstrate that samples blasted with alumina and the plasma-coated samples both present peaks associated with alumina which is related to the Al_2O_3 particles embedded in the substrate during the surface treatment, or pre-treatment of plasma-sprayed samples. The intensity of the alumina peaks was higher for the plasma-coated sample when compared to the samples blasted with Al_2O_3 particles, which indicates a greater amount of alumina embedded in the plasma sample than the CoBlasted sample, result confirmed by EDX analysis. CoBlast samples exhibit peaks associated with titanium attributed to the very thin HA layer deposited (<10 μm) that covers the underlying titanium substrate. The reduction in grain size and/or an increase in strain of the treated substrates resulted in a broadening of the titanium peaks in the XRD analysis. For the plasma coating no titanium peaks were found due to the thicker coating of HA present (≈ 70 μm).

SEM imaging results of the surfaces before and after removal of HA coating demonstrate that plasma-coated samples produced a significantly higher surface roughness when compared with CoBlasted samples. This greater value for plasma samples is due to the difference in processing route once to provide sufficient surface area for attachment of the HA, the plasma-coated need to be submitted to a grit blasting process using an alumina grit with mean particle size >350 μm prior to coating. Roughness analysis showed that CoBlast processing increased titanium substrates Ra values by factors of 4.8 and 5.4 for the sHA and alumina blast media, respectively.

Coating adhesion determination was performed according to a modified version of the method presented in ASTM F1147 Bond strength was determined by measuring the force required to remove the stud from the surface. Additional, EDX analysis was performed on studs and titanium surfaces to examine the levels of coating removal using SEM and EDX analysis. Results showed that the coating adhesion increased from 50MPa for sHA-treated samples to 60MPa for the alumina treated samples. This increase in coating adhesion may be due to the increasing surface roughness produced by the alumina blast medium, which gives rise to a greater degree of mechanical interlock between the HA and the titanium substrate. On the other hand, an increase in roughness provides more surface area for tribo-chemical bond formation between the titanium surface and the HA. Tensile bond strength results achieved for CoBlasted treated samples were significantly greater than the plasma deposited in HA coating (5MPa). These differences in tensile bond strength results between both processes can be attributed to the method of adhesion.

Microstructural characterisation of the samples was performed using a Leica MEF4M (Wetzlar, Germany). Results showed that CoBlast and plasma process influence the substrate microstructure in different ways (Figure 4.5). CoBlast processing results in a severely deformed surface layer, a region characterised by gross deformation of the grains and the undeformed substrate consisting of equiaxed α -grains, three different regions previously identified for sandblasted cp-titanium. In the region characterized by gross deformation, the grains exhibited twinning, effect previously observed in shot peened cp-titanium by Thomas et al. (2012). The depth of this three layers change was identified as 25 μm and 35 μm for substrates blasted with sHA and Al_2O_3 as blasting media, respectively. The formation of the severely deformed surface layer is beneficial as the associated compressive strength in the surface layer improves fatigue performance, a key material property for medical device implants.

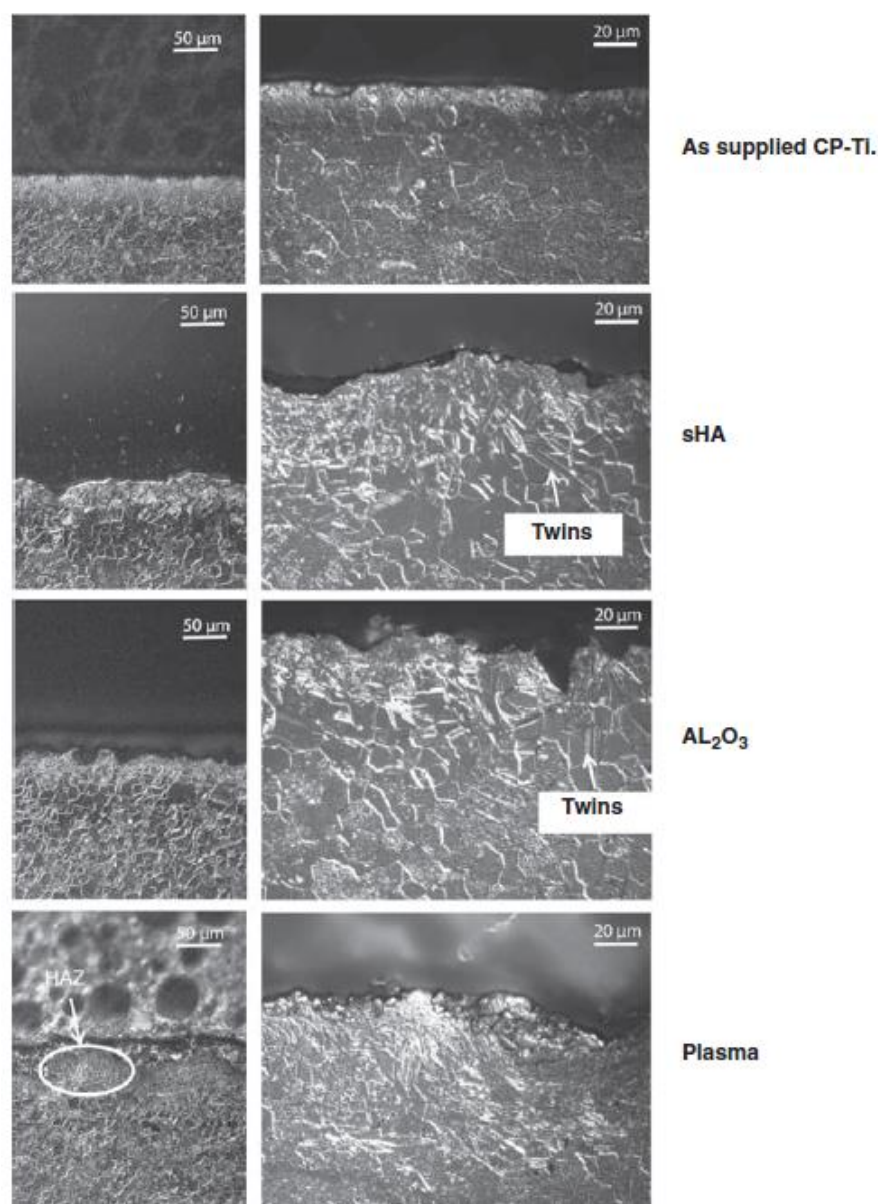


Figure 4.5 - Etched cross-sections of titanium substrates: as supplied cp Ti, CoBlast treated Ti with HA/sHA, CoBlast treated Ti with HA/ Al_2O_3 , and plasma-sprayed Ti. From Dunne et al. (2013).

In contrast, plasma processing resulted in the formation of a heat affected zone (HAZ) at the surface of the titanium substrate. Back transformed α -grains were identified within the HAZ. According to the authors, in previous studies where the formation of back transformed α -grains has been identified, α -case titanium has also been identified; α -case is a hard, brittle layer that forms when titanium is heat-treated in the atmosphere and the presence of brittle α -case titanium at the surface can result in delamination of the coating from the substrate.

As conclusion, the authors consider that the choice of blast medium is a key parameter in the CoBlast process. The choice of abrasive significantly influences the adhesive strength of the coating, surface roughness of both the substrate and coating and the microstructure of the substance. The authors consider that various blast media can be used in the CoBlast process to produce highly adhesive coatings with uniform crystallinity, although the study indicates that sHA is the most suitable candidate for use as a blast media in the coating of medical devices using CoBlast process.

Chapter 5

Process Validation

Process validation is a key part of the Quality Management System for medical device manufacturers. It is regulated by ISO 13485:2012 in European Union and defined by FDA Code of Federal Regulations (CFR) 21 in U.S. as *establishing by objective evidence that a process consistently produces a result or a product meeting its predetermined specifications*. Process validation is a vital process if the predetermined requirements of the product can only be verified by destructive testing (e.g. verifying sterilization requires the opening of all packages in order to ensure each one is sterile).

Nevertheless, although in some cases process validation is a regulatory requirement, companies may decide to validate or revalidate a process to improve overall quality, reduce costs, improve customers' satisfaction and reduce time to market for new products. In other words, process development and optimization may lead directly to the process validation, since the manufacturers will look for fulfilment of the requirements. Manufacturers should seek out technology-specific guidance on applying process validation to their particular situation, and some regulatory clauses place the responsibility on the manufacturer to specify those processes that require validation. Irrespective of the method used, a final report should be elaborated and records should be kept by the manufacturer (GHTF, 2004).

5.1 Purpose

One of the purposes of process validation is to guarantee traceability and reproducibility of the manufacturing results. It is important to identify the key process input variables and control them to ensure the outputs are in accordance with the requirements.

5.1.1. Process Validation Decision

According to ISO 13485:2012 section 7.52, the organization shall validate any processes for production provision where the resulting output cannot be verified by subsequent monitoring or measurement. This includes any processes where deficiencies become apparent only after the product is in use or the service has been delivered.

FDA 21 CFR 820.75 claims the same and adds that the process shall be validated with a high degree of assurance and approved according to established procedures, topic further discussed in sections 5.1.2 and 5.2, respectively.

The decision of when to validate or not validate a process is summarized in the decision tree of Figure 5.1. Briefly, after specifying process parameters and the outputs desired, the manufacturer should consider if the output can be verified by monitoring or measurement after manufacturing (Figure 5.1, A). If so, manufacturer should consider if the verification is sufficient to eliminate unacceptable risk and if it is cost effective (Figure 5.1, B). If considers so, the output should be verified and the process should be controlled (Figure 5.1, C).

On the other hand, if the output of the process is not able to be verified, then the decision should be to validate the process (Figure 5.1, D). Redesign the product or the process is also an option that can lead to improvement of the process and reduced variation (Figure 5.1, E), and ultimately lead to a point where simple verification is a possibility.

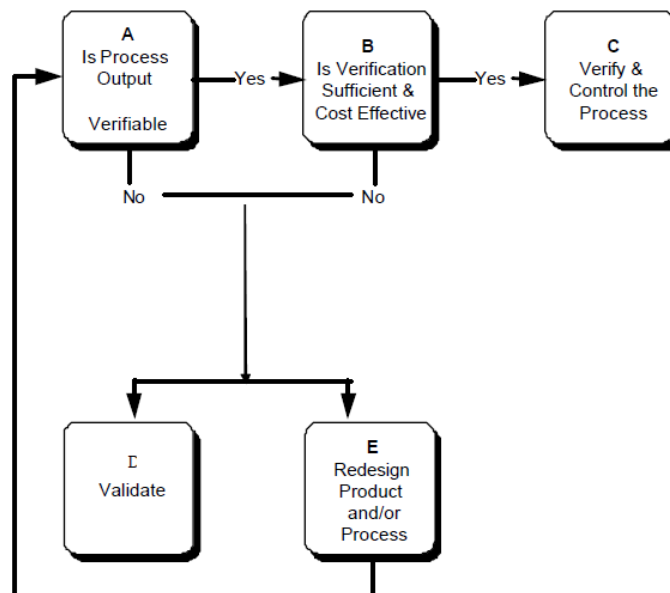


Figure 5.1 - Process Validation decision tree. Adapted from GHTF (2004).

Four conditions, thus, arise:

- Process validation is unavoidable and mandatory;
- Verification is sufficient and cost effective;
- Verification is sufficient but is not cost effective so validation is the best option;
- Process validation is currently unavoidable, but the manufacturer chooses to redesign the product or process to a point where verification is acceptable.

When the manufacturer considers verification sufficient and cost effective, he must consider what he is subscribing. A public FDA Warning Letter sent to Hammill Manufacturing Company in Ohio US – a manufacturer of orthopedic implants, spinal implants, surgical instruments, and implantable medical devices – clarifies the perspective of FDA about verification and process validation concerning medical equipment: *We have concluded that your response is inadequate because you are not testing every device to assure it meets*

specifications, and the results are not fully verified. All of these processes must be validated to ensure the specifications are consistently met or you must test all devices (2009). In short, FDA was telling Hammill Manufacturing to either perform 100% inspections on their products (i.e. every device) or validate all the processes involved in its manufacturing. Thus, an isolated acceptance sampling plan, where a sample of a product is used to make an accept or reject decision, is not considered verification of all products (i.e. confirmation by examination and provision of objective evidence that specified requirements have been fulfilled).

5.1.2. Statistical Principles

Process Validation relies on statistical principles that support the design of capable, stable and robust processes. A manufacturing process should be capable and stable to assure continued safe products that perform adequate, while robust design depends on selecting optimal targets for the inputs that make the outputs less sensitive (i.e. more robust) to the variation of the input. A process is considered stable when it produces a consistent level of performance where the variation and average of the response parameters measured over time are constant, leading to a reduced total variation. Contrariwise, an unstable process is constantly changing (i.e. average shifts, variation increases or variation decreases over time) increasing total variation (Figure 5.2).

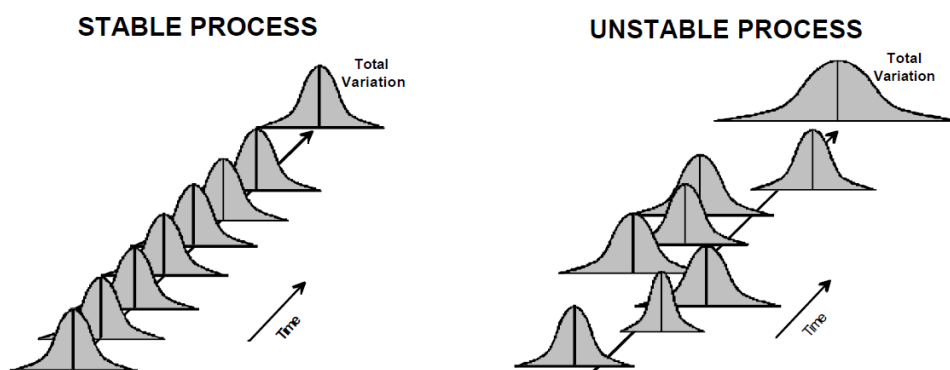


Figure 5.2 - Illustration of a stable and unstable process. Normal distributions are used to illustrate the averages and variations of a response parameter over time. From GHTF (2004).

Process capability is a concept largely implemented in statistical quality control. When a response parameter of a process is measured (i.e. value X), it must fit between lower and upper specification limits (i.e. LSL, USL respectively). Values of X outside these limits are considered nonconforming. Two indexes are frequently adopted to infer about process capability: C_p and C_{pk} . Process Capability index (C_p) indirectly measures the capability of a process to meet the requirement $LSL < X < USL$, with a response parameter with a standard deviation σ (Equation (5.1)).

$$C_p = \frac{USL - LSL}{6\sigma} \quad (5.1)$$

Large C_p values are desirable (i.e. large standard deviation is undesirable), and some recommend a $C_p \geq 1.33$ for an existing process and $C_p \geq 1.50$ for a new process (Kotz and Johnson, 1993). Large C_p values alone do not guarantee acceptability due to the absence of information about the process mean (ξ), therefore C_{pk} index was introduced to give the value of ξ some influence on the extrapolation of capability ((5.2)).

$$C_{pk} = \frac{\min(USL - \xi, \xi - LSL)}{3\sigma} \quad (5.2)$$

A process with a high degree of assurance of producing a conforming product will have a $C_{pk} \geq 1.33$ (Kotz and Johnson, 1993). Visually, a process capability study will involve collecting samples over a period of time and evaluate process capability and stability (Figure 5.3).

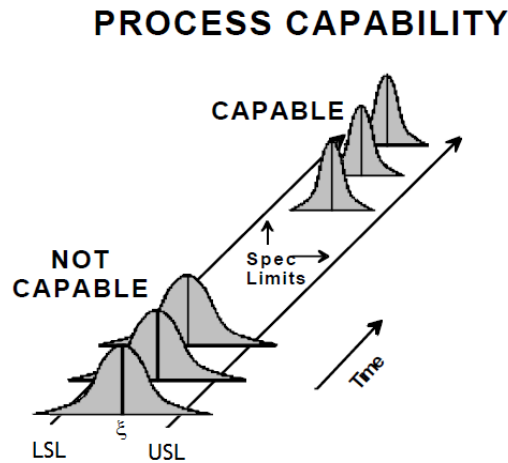


Figure 5.3 - Process capability study possible results illustration. ξ - Mean; LSL - Lower Specification Limit; USL - Upper Specification Limit. Adapted from GHTF (2004).

Regarding robust design theory, it attempts to reduce variation of the outputs caused by the variation of the inputs. The manufacturer must identify the key input variables, understand the effect of its variability on the outputs, understand how the inputs vary, and use all of these information to establish targets and tolerances (i.e. window) for the inputs. This approach establishes operating windows or control schemes that ensure that the output conforms to requirements. Taguchi and Clausing (1990) concluded that variation can be reduced by selection of the targets over the use of tighten tolerances. When nonlinear relationships exist between the input and the output, the manufacturer is able to select inputs targets that will make the outputs less sensitive to the inputs.

5.2 Phases of process validation

When the decision to validate is made, a plan of approach to be adopted and a definition of the process requirements should be made. Output parameters (e.g. product specifications) must be established as well as the methods and tools that will be employed in their

evaluation. All this information can be organized in a detailed validation protocol, essential to ensure that the process is adequately validated (GHFF, 2004). When more than one process is involved in the manufacturing of a final product, the company can conceive a master validation plan which identifies those processes to be validated, the schedule for validations, interrelationships between processes requiring validation, timing for revalidations and the protocol for each process validation. This protocol will embody the strategy to obtain, record and interpret data. These activities can be performed in three phases: Installation Qualification (IQ), Operational Qualification (OQ) and Performance Qualification (PQ) (FDA, 2011).

5.2.1 Installation Qualification (IQ)

The manufacturer is responsible for evaluating, challenging and testing the equipment in order to determine if it is appropriate for manufacturing a specific device.

At this stage the manufacturer shall obtain and document evidences that the equipment has been provided and installed in accordance with its specification and suits the required conditions (e.g. wiring, functionality, design features like materials cleanability, calibration, safety features, supplier documentation, spare parts list and environmental conditions).

5.2.2 Operational Qualification (OQ)

Operational qualification is a phase of process validation where the robustness of the process is determined. A worst case testing should be made to challenge process parameters, and prove that the resultant product meets all the defined requirements. Process control limits like time, temperature, pressure, linespeed and setup conditions must be tested, and a short term stability and capability of the process should be determined. At this stage, if applicable, software parameters and raw materials specifications must be checked also. An approach to process optimization is something that the manufacturer should apply at this stage.

5.2.3 Performance Qualification (PQ)

Performance Qualification is the process of obtaining and documenting evidence that the equipment, as installed and operated in accordance with operational procedures, consistently performs in accordance with predetermined criteria and thereby yields product meeting its specification. PQ intends to prove a long term stability of the process.

Process and product data should be analysed to determine the normal range of variation of the process output. PQ establishes process sensitivity to controllable cause like light, vibration, humidity, temperature, purity of process water (if applicable), and determines measures to eliminate them. OQ and PQ together must develop attributes for continuous monitoring and maintenance of the process.

A final report should be prepared summarizing all the protocols, requirements to be fulfilled (including reference to all regulatory specifications followed and standard tests performed) and results. It must be clearly conclusive about the validation status of the

process. Revalidation requirements must be defined. This records shall be maintained (FDA 21 CFR 820.75, ISO 13485:2012).

5.3 Monitor, Control and Revalidation

After validation a process must be monitored. During routine production, the attributes established by OQ and PQ must be checked and if any negative trend is found, the cause should be investigated and corrective actions must be taken. This is called maintaining a state of control. Control charts like the one presented in Figure 5.4 may be employed. Depending on the severity of the irregularities revalidation must be considered.

Revalidation is strongly advised when:

- Changes in the actual process are made, including procedures, equipment and production personnel that may affect quality or its validation status;
- Negative trends in quality indicators are found;
- Changes in the product design which affects the process are made;
- Processes are transferred from one facility to another;
- Change of the application of the process is introduced;

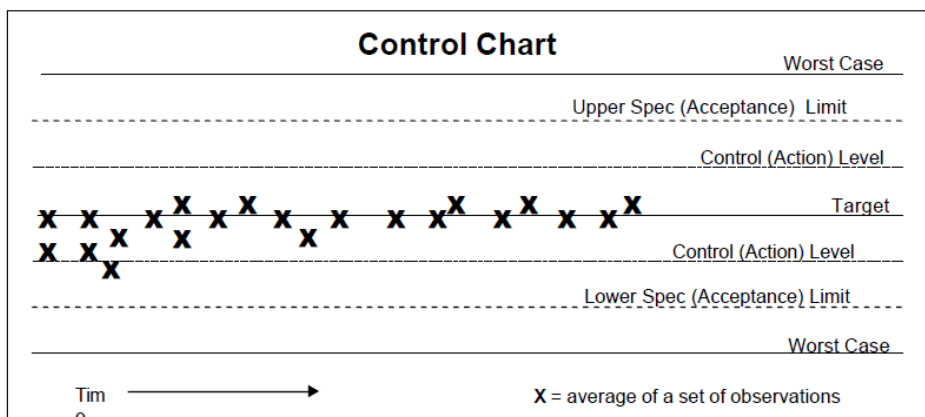


Figure 5.4 - Control Chart. From GHTF (2004).

5.4 Regulatory specifications

Regulatory specifications define the limits within which the process should occur. ISO and ASTM standards and FDA Guidelines clearly specify the requirements to be fulfilled by the manufacturer in respect to the validated process.

The manufacturer must ensure, by performing destructive testing in previously established periods of time, that the products are within standard specifications and therefore the process is controlled during routine production.

Process Validation according to ISO standards for HA coatings must be performed in order to ensure that the final product is within specification limits. Good Manufacturing Practices according to FDA Guidelines after process validation will allow manufacturer to have the process under control and easily identify any deviation that might occur.

Chapter 6

CoBlast Validation Plan

According to the revised literature, CoBlast HA coatings have high mechanical resistance, and coating crystalline content, and can provide high implant fatigue strength. It seems that highly resistant metallic implants can be created using CoBlast with a highly adherent coating at the implant surface leading to the possibility of an increased implant lifespan. These are important attributes, essential in several metallic implants sectors.

Choosing the best product to enter the market using CoBlast HA coatings, may be a crucial step for the success of this new coating technology in the medical field. Having this in mind, the list of products and clients of Ceramed was checked and the reported features of CoBlast HA coatings were carefully studied. Pedicle screws end up being chosen as the first product to be launched to the market with CoBlast HA coating (Figure 6.1).

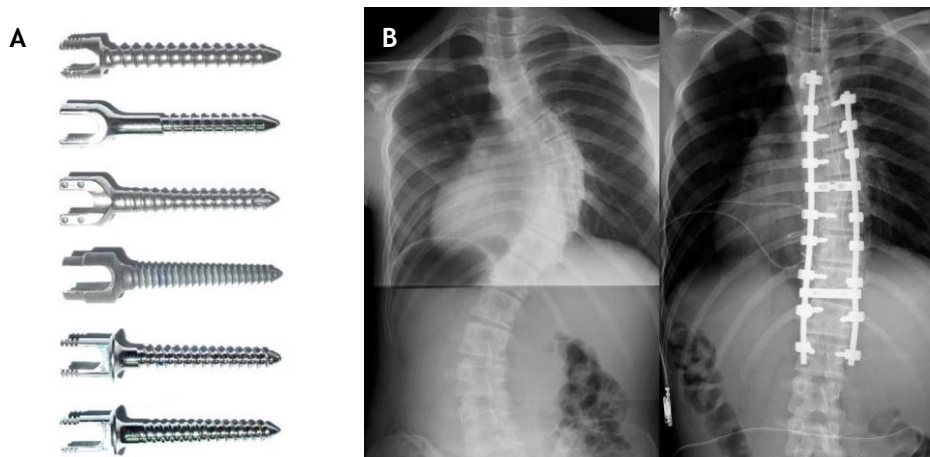


Figure 6.1 - Spinal fixation screw system (A). Pre-operative and post-operative x-rays of a patient with a transpedicular screw fixation applied to solve a scoliosis between T5 and T11 (B). From Maruyama and Takeshita (2008).

Pedicle screws are employed to rectify spinal deformities, trauma fractures, degenerative conditions of the lumbar spine and reconstruct the spine after a tumour resection by transpedicular screw fixation. Screw loosening is a very common complication at the post-operative period in this kind of surgeries, especially in osteoporotic patients (Upasani et al.,

2009, Hasegawa et al., 2005). The probability of need of removal from the body of this implant is low, and the need for highly fatigue resistant implant material is a reality due to the constant spinal loads.

When HA coating is applied over pedicle screws usually a coating layer of plasma-sprayed HA with a width of 60 μm is requested by Ceramed's clients. Plasma spray process is most often employed for commercial HA coatings on orthopaedic and dental implants and the same goes for pedicle screws.

Henceforth, the present process validation shall be conducted with the purpose of confirming the capability of CoBlast process to coat pedicle trauma screws, with HA, according to the FDA requirements and ISO standards. Furthermore, a comparison between CoBlast and Plasma-spray coated pedicle screws may be established in order to encourage clients to test CoBlast coatings.

6.1 Raw materials and substrate

Raw materials for this validation were chosen according to literature previously revised (section 4.3). Tests were conducted in order to evaluate the conditions to validate CoBlast for pedicle screws HA coating using two sets of coating/blast medium: HA/ Al_2O_3 and HA/MCD. Particle size was maintained in accordance with the studies so that they could support the technology in case of need for in vitro and in vivo evidences. Al_2O_3 with a FEPA grit 120 (medium particle size of approximately 100 μm) was ordered from Blasqem, Lda., MCD180 from Himed, USA, with a mean particle size of approximately 120 μm , was kindly offered by Enbio technical team, and a batch of HA with a size between 20-60 μm was kindly asked to Altakitin to exceptionally produce it. Since Altakitin is an affiliated company of Ceramed there is a natural interest that the HA used for CoBlast processing can be produced at Altakitin. For this reason this HA was produced, analysed, and used in this validation.

Since pedicle screws sent by Ceramed clients are mostly made of Ti-6Al-4V, the substrate for evaluation in this validation should be made of Ti-6Al-4V. In this particular case, flat coupons 25 x 25 x 1.6 mm of Ti-6Al-4V were used as substrate for coverage, chemical and crystallinity evaluation, and cylindrical specimens of the same material with dimensions 25 mm of diameter and 24.5 mm of height were used for adhesion tests (Figure 6.2).

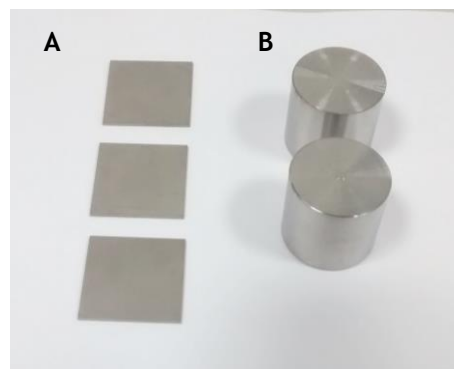


Figure 6.2 - Ti-6Al-4V substrates used for CoBlast validation tests: (A) flat coupons 25 x 25 x 1.6 mm and (B) cylindrical specimens with 25 mm of diameter and 24.5 mm of height.

Alongside with CoBlast samples, plasma-sprayed samples were prepared using the same type of substrates with plasma-sprayed coating corresponding to most common Ceramed's client requirements, so that a comparison between the results of the two company processes could be clearly presented to Ceramed's clients when asked. In order to do that, HA powder for plasma-spraying with a particle size of 60-160 μm (*forCOAT*, Altakitin) from the same batch of the HA used on CoBlast validation procedures was ordered.

6.2 Equipment

In order to implement CoBlast processing at Ceramed a set of equipment was acquired and gathered. This work started by a receiving the equipment at the new Ceramed facilities and perform a study of correct and safe installation of the equipment.

6.2.1 Advanced Lathe

Surface blasting is provided by an automated microblasting system from Comco Inc. - *Comco LA3250 Advanced Lathe* (Figure 6.3). This system supports up to four axes of motion, X, Y, Z and W for rotation, and comes with different part tooling allowing the blasting of multiple surface geometries (Figure 6.4).

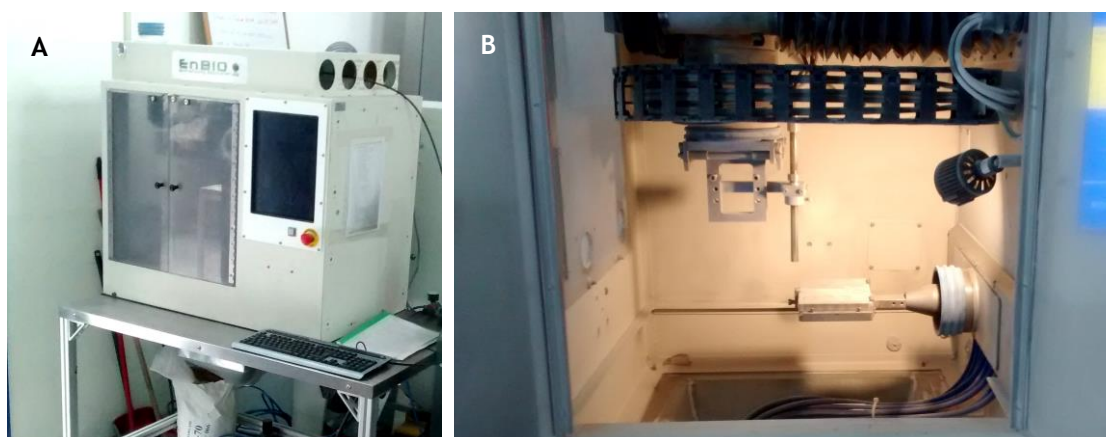


Figure 6.3 - Comco LA3250 Advanced Lathe exterior frame (A) and inside chamber (B) furnished with a single nozzle configuration.

The lathe works on electrical and pneumatic energy. The apparatus requires about 400 watts of electric power at 115 volts in alternating current (VAC), single phase, 50/60Hz. Since the voltage of the electrical grid is 220 VAC, it was concluded that an external transformer should be installed to allow connection to a 220-240 VAC supply.

Concerning air supply, this equipment demands compressed air for numerous purposes: bellows purge, spindle purge, blow off gun and electronics chamber purge. When all are active the maximum lathe air consumption is 198 liter/minute. The lathe's internal pressure regulator is set to 620 kPa, so the air supply must be between 620 - 965 kPa, regardless of consumption. All the system requires very clean and very dry air. The lathe was equipped

with the Comco AD5300 continuous duty membrane air drier to provide additional oil and moisture removal.



Figure 6.4 - Comco LA3250 Advanced Lathe part tooling. Two mandril pieces and a platform are provided to coat different piece geometries.

This lathe offers an intuitive user interface where the worker can choose the piece to coat and select when to start coating. A countdown starts on the screen indicating the time left for the coating procedure to end (Figure 6.5). All Part tooling have an identical base that makes mates with the lathe's spindle. An O-ring on the spindle seals it while vacuum is pulled through the center of the spindle stud to secure the tool. Each tool has a unique permanent pin and seven removable setscrews at the base, allowing the lathe software to identify which tool is being vacuumed in to the spindle.



Figure 6.5 - Comco LA3250 Advanced Lathe user interface. The user can select the piece to coat on the right side of the pane (A), after selecting the coating program if the part tooling is not correctly detected or is not the correct part tooling for the program about to start an alert in yellow is displayed (B) when the problem is solve the user can start the coating program and the countdown starts (C).

Different programs to coat different pieces can be developed by programming in industry-standard G-code. G-code is a widely used computer numerical control (CNC) programming language in which computerized machine tools can be programmed movement oriented. This lathe reads special G-Codes and M-codes. G-codes will make the machine do something with an axis or the coordinate system, while an M-code will control other miscellaneous items such

as blast control, subroutines and others. Table 6.1 holds a Programming quick reference for CoBlast using with the set equipment in place.

Table 6.1 - Programming quick reference for CoBlast using (adapted from Comco Inc. Operating and service instructions, 2008)

G00	Fast Move	R	Arc Radius (used with G02 or G03)
G01	Vector Move	S	Set Rotational Speed
G02	Clockwise Arc, Circle or Helix	F	Set Feed Rate
G03	Counter clockwise Arc, Circle or Helix	X	X-Axis Value
G04	Hold Position	Y	Y-Axis Value
G10	Define Position	Z	Z-Axis
G28	Home Axes	W	W-Axis
G90	Use Absolute Coordinates	P	Parameter Value (used with G02, G03, G04 and M98)
G91	Use Relative Coordinates	I	Circle Center Axis 1 (used with G02 or G03)
M03	Start Rotational Axis Clockwise	J	Circle Center Axis 2 (used with G02 or G03)
M04	Start Rotational Axis Counter clockwise	N	Line number
M05	Stop Rotational Axis	()	Comment
M30	End Program	^	Scaling (used with G00, G01, G02 and G03)
M98	Call Subroutine		

Multiple nozzle configurations can be adopted with this system. It was decided that the acquired lathe should be installed according to the latest studies on CoBlast: with a single nozzle configuration. Single nozzle set-up provides a simplified blasting procedure, with a reduction of the number of robots and a more effective control of the powder flow reaching a certain point of the surface.

6.2.2 Powder feeder

Powder feeder Single 10-C from Sulzer Metco was brought from CATiM with the equipment kept by Ceramed. This device was previously used by the company to feed powders for plasma-spraying and was installed at the new facilities as a feeder to preform CoBlast. It is able to supply a given amount of powder at a constant rate by using the principle of volumetric powder feeding. The powder insert contains a rotating disk with powder groove, a spreader and a suction head that together release a certain volume of powder per unit of time (Figure 6.6). The powder hopper has a capacity of 1100 cm³ of powder.

The system contains a pressure regulator up to 4 bar, and the revolution regulator of the rotating disk up to 10 revolutions per minute (rpm). The air consumption of the feeder is dependent of the revolutions per minute of the rotating disk and the air pressure used. The maximum air consumption is estimated in 10 l/min for a 4 bar pressure and 10 rpm. This equipment requires about 250W of electric power at 230 volts in alternating current (VAC), single phase, 50/60Hz.

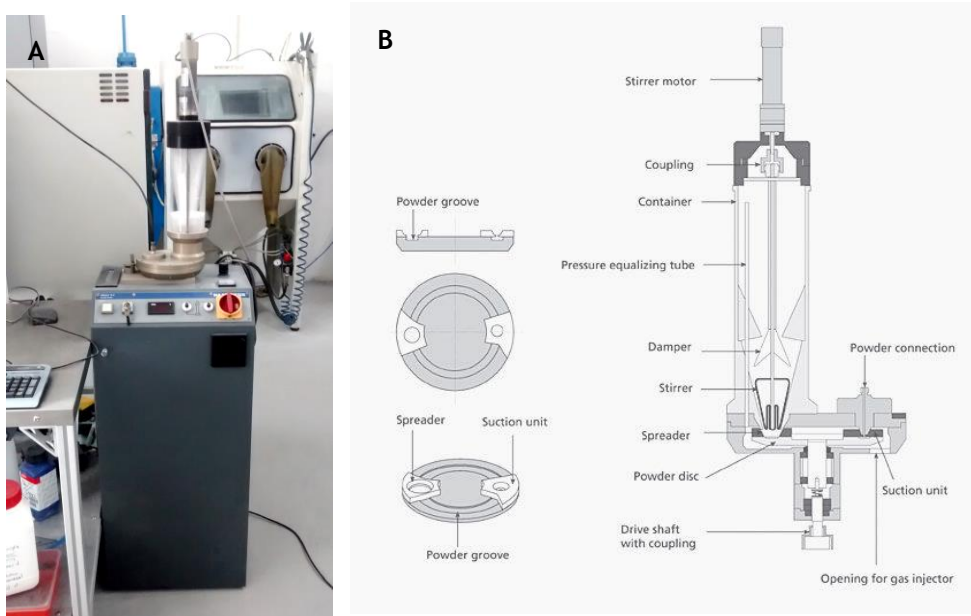


Figure 6.6 - Powder feeder Single-10C from Sulzer Metco with an 1100 cm³ powder insert (A). The powder insert (B) consists of a powder hopper with a stirrer motor, coupling, dampener and stirrer, and a powder feed drive that consists of a rotating powder disk with groove powder, a spreader and a suction unit.

The feeder system was studied in order to attain a mathematical relation between the input parameters (i.e. pressure and rpm) and the amount of powder fed (i.e. mass flow rate). Powder groove dimensions were measured and calculations were made to get its volume: $V_{\text{groove}} = 5.78 \text{ cm}^3$. In optimal conditions, one revolution of the plate will make the powder groove expel all the powder it can carry in its volume through the suction head exit. Thus, 5.78 cm³ will be the volume of expelled in one revolution. By knowing the density of bulk used, the mass flow rate can be determined according to equation 6.1.

$$\dot{m} = \text{rpm} \times V_{\text{groove}} \times \rho_{\text{bulk}} \quad (6.1)$$

This control will be important to deduce the amount of powder spent to coat each surface according to the time the lathe is spending in a certain coating program.

6.2.3 Vacuum cleaner

In order to collect spent powder and abrasive to and prevent it from reaching the operator, a dust collector must be connected to the lathe collar on its bottom designed for that purpose. A Sablex Universal Vacuum cleaner with an aspiration capacity of 600 m³/h was used to this end. Sablex universal vacuum cleaner requires about 550 watts of electric power at 230 VAC, three phase, 50/60Hz.

6.2.4 Blender

Powder mixing as a technique of dry particle blending, is a subject of research motivated by several industrial sectors like pharmaceuticals, food, ceramics, metals and polymers manufacturing. Mix uniformity can be affected by powder stream flow properties, poor

equipment design or inadequate operation, particle segregation or particle agglomeration driven by electrostatics, moisture and other factors. Some blenders have a limited mixing ability to improve upon component segregation typically caused by differences in particles characteristics like size, shape and density (Brone et al., 1998, Singhai et al., 2010).

When a microblasting system is installed with a single nozzle configuration, a mixture of powders (i.e. dopant and abrasive) is used for CoBlast processing. In order to mix the dopant, HA, with the abrasives, Al_2O_3 or MCD, a V-blender was chosen as suitable equipment.

V-blender, also known as a twin shell blender, has a remarkable blending performance with short blending times and efficient blending. This type of blender is used when precise blend formulations are required. An ingredient may be as low as 5% of the total blend size and still, its mechanism of diffusion, characterized by small scale random motion of solid particle, will produce uniform results. Blending made with this type of equipment can be influenced by the method by which materials are initially loaded into the blender (e.g. top to bottom, left to right), the filling level (i.e. volume of the material loaded into the blender, usually 50-60% of the total volume of the blender) and blending speed (Singhai et al., 2010). Blending rotation rate studies in a 1 liter 90° V-blender model using particles of dozens μm size show that, when the blender is filled properly, rotation rates between 8 and 24 rpm exert little influence on the mixing process: the key factor is the number of revolutions preformed (Brone et al., 1998). The same as saying that with a rotation rate near 24 rpm the appropriate number of revolutions to mix a set of powders will be accomplished faster.

A V-blender experimental prototype made of polytetrafluoroethylene (PTFE) machined according to the dimensions preconized elsewhere (Brone et al., 1998) with an inner volume of 1L was kindly sent by Enbio Technical team (Figure 6.7, A). After reception, the blender was assembled and installed in a structure with a three phase motor (IM B14A GL56-160, Guanglu, 230 VAC, 0.09 kW) and a gear reducer (RI 28, Line), bought from *Siepi - Sociedade Industrial de Equipamentos para indústria, LDA.*, to create a rotational movement of 20 rpm over the horizontal axis.

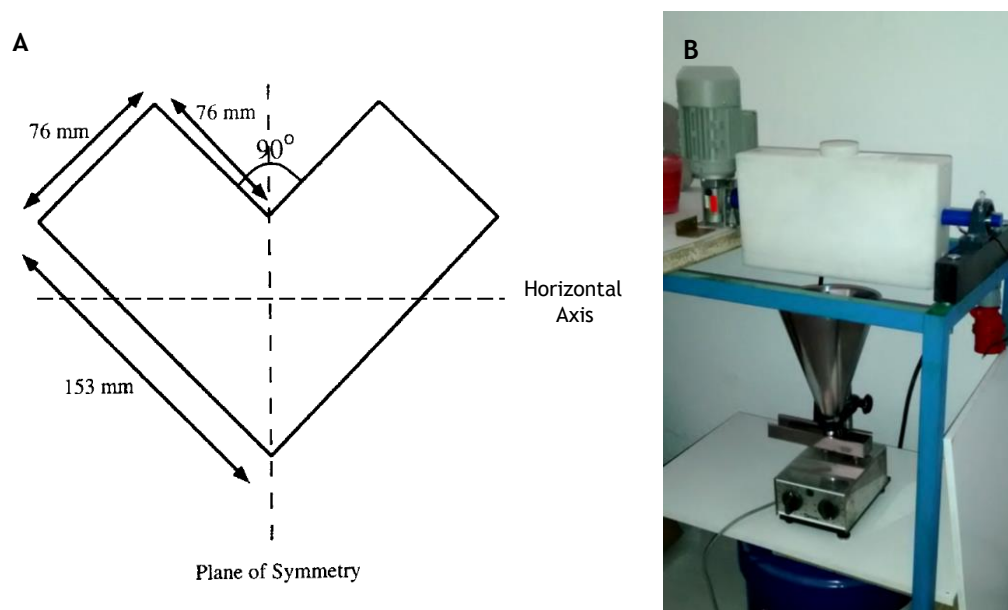


Figure 6.7 - Model of the inner structure of the machined PTFE V-blender made of two hollow cylindrical shells joined at an angle of 90° (A), adapted from (Brone et al., 1998). Final look of the apparatus for mixing powders (B).

Together with the V-blender, a Retsch Vibratory feeder for uniform, continuous feeding and conveyance of pourable bulk materials and fine powders was installed to collect the powders from the exit of the V-Blender. The apparatus for mixing of powders was then complete (Figure 6.7, B).

6.3 Static Parameters & Parameters under Evaluation

CoBlast is characterized by a set of parameters that can be changed in order to control the process: blast medium and coating medium (i.e. abrasive used to abrade the surface and dopant used to coat the surface), powders particle size, ratio dopant/abrasive, angle of the nozzle, speed of the nozzle, height of the nozzle, raster offset, blast pressure and the mass flow rate of powders. Since a single nozzle configuration was chosen at the installation of Comco Advanced Lathe, another parameter can influence CoBlast processing results: the time of powders blending.

Some of these parameters can be kept static based on previous works reported on the literature, company needs and equipment restrictions, and some of these can be studied in order to achieve better coating coverage, coating adhesion and crystallinity with less expenses (i.e. less energy involved in the process and less powder raw material spend). Regardless this work perspective based on process optimization, the focus of reaching first a situation of capability, and thus, stability of the process cannot be lost. Some parameters must remain static, and some must be studied towards this state of capability that will lead to a state of process validation, that over time can be optimized.

An approach for CoBlast validation of Ti-6Al-4V surfaces of pedicle screws with HA was thought carefully leading to the list of parameters that should be assumed as static and under evaluation on the first CoBlast validation for medical applications at Ceramed. This list is presented below:

Static Parameters

Coating medium: Altakitin HA with a particle size in the range of 20-60 μm must be used as coating medium.

Dopant/abrasive ratio: HA/ Al_2O_3 ratio and HA/MCD ratio must be maintained in accordance with the studies reviewed at 50%/50% (w/w) for both.

Blast pressure: Blast pressure should be held at 400 kPa since it is the upper limit admitted by the feeder and is a value with a good safety margin to the pressure value of the compressed air system of Ceramed.

Nozzle angle: Single nozzle configuration was adopted based on the recent studies made and, thus, the nozzle angle shall be kept in accordance to the revised literature for this type of configurations – 90° from the surface.

Nozzle speed: Nozzle speed shall be kept at 13 mm/min according to the latest studies using single nozzle (Dunne et al., 2013, Dunne, Twomey, and Stanton, 2015, Dunne, Twomey, Kelly, et al., 2015).

Mass flow rate: Coating and blast medium powder mixing mass flow rate was maintained at 50 g/min. A direct inquiry was addressed to the authors of the articles using CoBlast about this issue. This value was used so that in a first study the mass flow rate was a not a varying parameters that could cause significant differences in coating coverage at least.

Parameters under Evaluation

Blasting medium: The two blasting media used in the proof-of-concept studies for HA coatings with CoBlast shall be used separately to infer the possibility of validating the process for both. Thus, Al₂O₃ with a particle size <180 µm and MCD with a particle size of 180 µm should be studied separately.

Time of powders blending: The time of blending is a specific parameter that shall be studied for each combination of powders, since it may vary according to particles electrostatics size, weight and geometry.

Nozzle height: In order to accomplish a suitable value of particle impact energy at the surface of the material the hypothesis of lowering the nozzle height was planned. This was considered because of the adopted static value of 400 kPa as blast pressure is inferior to the one used in previous CoBlast studies as stated at section 4.2. Three different nozzles heights were studied – 50 mm, 40 mm and 30mm.

Raster Offset: Raster offset depends on the track width shaped by the type of particles in use and the blast pressure applied. A value of 3.3 mm was visually adjusted for the height of 50 mm which was in accordance with the latest study using CoBlast (Dunne, Twomey, and Stanton, 2015). Calculations were made to predict the raster offsets needed for other heights based on the geometry of De Laval Nozzle, and were assigned at 2.9 mm for a nozzle height of 40 mm and 2.6 mm for a nozzle height of 30 mm. Calculations that led to this values can be found in

Appendix A.

6.4 Process requirements

Regulatory specifications define the legal limits in which the process should occur. CoBlast process validation shall be conducted to produce HA coatings within the requirements for HA coatings, without the need of verification of each device coated by the quality control department of Ceramed. The actual regulatory specifications for HA coatings and HA powders as raw materials must be taken into consideration when the optimization and validation of CoBlast for HA coating occurs (Table 6.2).

Table 6.2 - Regulatory specifications for HA coatings.

	Characteristic	Specification	Standards	Illustration
Powder	Chemical Requirement (wt% máx.)	As	< 3	According to the specific requirements of the standards applied for HA used in medical applications, the raw material must be in conformity with the standards ASTM F1185-03 "Standard Specification for Composition of Ceramic Hydroxyapatite for Surgical Implants" and ISO 13779-1 - "Implants for Surgery - Hydroxyapatite - Part 1: Ceramic Hydroxyapatite"
		Cd	< 5	
		Hg	< 5	
Pb	< 30			
Total Heavy Metals	< 50			
	Ratio Ca/P	1,65 - 1,82	ISO 13779-1	According to the specific requirements of the standards applied for HA used in medical applications, the powder must be in conformity with the standards ASTM F1185-03 "Standard Specification for Composition of Ceramic Hydroxyapatite for Surgical Implants" and ISO 13779-1 - "Implants for Surgery - Hydroxyapatite - Part 1: Ceramic Hydroxyapatite"
	Crystalline Content	HA	> 95%	According to the specific requirements of the standards applied for HA used in medical applications, the powder must be in conformity with the standards ASTM F1185-03 "Standard Specification for Composition of Ceramic Hydroxyapatite for Surgical Implants" and ISO 13779-1 - "Implants for Surgery - Hydroxyapatite - Part 1: Ceramic Hydroxyapatite"
		Other Crystalline phases (α and β TCP; TCPM and CaO)	< 5%	
Coating	Chemical Requirement (wt% máx.)	As	< 3	According to the specific requirements of the standards applied for HA used in medical applications, the coating must be in conformity with the standard ISO 13779-2 - "Standard Specification for Implants for surgery- Hydroxyapatite - Part 2: Coatings of hydroxyapatite".
		Cd	< 5	
		Hg	< 5	
		Pb	< 30	
		Total Heavy Metals	< 50	

	Ratio Ca/P	1,67 - 1,76		
	Crystalline Content	HA	> 45%	
		Other Crystalline phases (α and β TCP; TCPM and CaO)	< 5%	
	Mechanical Resistance (MPa)	> 15	ISO 13779-2 ISO 13779-4	The test is performed according to ISO 137794 - "Implants for Surgery - Hydroxyapatite: Determination of coating adhesion strength" The aim of this test is to assess the tensile adhesive strength of coating layer to the substrate. Coated 25mm diameter specimens are linked to uncoated coupons with FM1000 or 3M-2214 structural adhesive. A tensile stress is applied to separate the coating and the substrate. The maximum tensile adhesive stress is recorded. Usually this test is performed on at least five coated coupons.

ISO 13779-2 standardizes the chemical content, ratio Ca/P and crystalline content of HA coatings. ISO 13379-3 establishes analytical methods such as XRD for crystalline content analysis and suggests ICP-MS for chemical analysis. Moreover, this standards outlines a sample preparation for analysis that comprises the detachment of coatings from the surface (e.g. by scraping it) with negligible contamination of the sample, asserting also that bulk samples shall be reduced to powder with less than 40 μm . With a thickness of < 10 μm , CoBlast coatings are virtually impossible to scrap in a viable amount for analysis with this techniques. Thus, the study here developed was conducted to meet the requirements of this standard, but the analytical methods used were adjusted to the type of coating produced, so that an *in loco* analysis of the samples and controls could be performed.

6.5 Validation Protocol

Building a strong and grounded validation protocol is one of the most important steps for process validation. Since, this is the first attempt to validate CoBlast for medical industry applications, this protocol must cover all the details that can influence the final results and study them thoroughly.

First analysis of CoBlast processing show that it can be put in place through two microblasting equipment configurations: single nozzle set up or double nozzle set up. Ceramed chose the single nozzle set up to be the one implemented in its facilities. This

configuration requires a process of mixture of powders to be carried out so they can be blasted at the same time. Therefore, the mixture of powders is also a process that needs proof of its stability and capability. CoBlast process validation will comprise the validation of two processes - coBlasting of the surfaces and powders blending.

An approach plan was made according to the process requirements stated in section 6.4. Limits for specific output parameters not set out in standards (e.g. roughness limits, thickness limits) shall be established as a result of OQ procedures to allow the creation of a monitoring plan for HA coating deposition on Ti-6Al-4V using CoBlast, and to infer about process capability on PQ procedures. Methods and tools that were employed in this evaluation were first organized in a protocol structured by Installation Qualification (IQ), Operational Qualification (OQ) and Performance Qualification (PQ) as required by FDA (2011).

6.5.1 Installation Qualification

IQ is performed after equipment's installation in order to evaluate machine's status, document the installation and confirm that the unit is set up according to the operating instructions and manual. The following checklists were created to guide these procedures on CoBlast process validation IQ:

- System identification checklist
- Components identification checklist
- Consumables identification checklist
- Documentation of conformity checklist
- System damages checklist
- System installation checklist
- User interface checklist
- Overall result of the IQ checklist

System verification must end with a final checklist of the overall results of IQ, a report of the differences or errors found, and a final deliberation about the state of IQ for this process. The first six check lists listed were prepared separately for each set of equipment: the equipment that acts directly on CoBlast of surfaces and the equipment that is used for powders blending. These documents can be found in Appendix B.

By the end of IQ, results shall be kept on file and the differences or variations that were verified during the procedures must be documented. A clear conclusion about the state of IQ must be made indicating one of three case scenarios possible:

- No differences or errors were found during IQ. IQ was successful, and according to the reported results the system is approved.
- Small differences or errors were found during IQ. Differences and errors are documented, and despite its occurrence the system is approved.
- Considerable differences or errors were found during IQ. According to the reported results the system is not approved. Necessary modifications or repairs will be made and IQ corresponding tests have to be repeated and documented.

6.5.2 Operational Qualification

By the time the equipment was acquired, tolerance testing of Comco Advanced Lathe was performed and approved by Enbio technical team. The tolerance test report was revised and filed in the internal documentation of Ceramed of CoBlast. Equipment operational tolerances were within the recommended values allowing this validation to start towards the identification of optimum operational parameters without interference of erratic Advanced Lathe equipment behaviour.

Blending equipment operational rotation rate shall be evaluated at this stage, on order to verify if the value of 20 rpm is in fact achieved for a 50%-60% blender filling conditions.

Furthermore, OQ procedures are planned to test additional operational parameters like time, temperature, pressure, linespeed and setup conditions. An effort to determine parameters' limits that will guarantee a short term stability and capability of the process shall be made at this stage. As explained later, crucial parameters that require evaluation at this stage are powders blending time and nozzle height with an individual raster offset. These parameters will be studied for two sets of coating/blasting medium: 50/50 (w/w) HA/Al₂O₃ and 50/50 (w/w) HA/MCD.

Before any test, raw materials specifications must be checked for compliance with the standards. Raw materials manufacturers' declarations of compliance shall be reunited, analysed and accepted by the team that is leading the validation process.

6.5.2.1 Blending OQ

Blending OQ procedures were planned based on the concept of powders apparent density (i.e. bulk density) defined by ISO 60 and ISO 697. The main purpose of blending operational qualification was to determine the blending time for which the final mix of HA with the abrasive (i.e., Al₂O₃ or MCD) was in fact 50%/50% (w/w) in all its extension.

Apparent density is the weight per unit volume of a material, including voids that exist in the tested material. One cup of 50 mL was used to measure apparent density for a controlled powders fall. Powders fall was controlled using the vibratory feeder from Retsch, with a vibration rate set to 50% of its capacity. A schematic drawing of the apparatus used is shown in Figure 6.8. The idea is that, when used with stable parameters, this vibratory feeder equipment can reproduce powders' "packaging". In order to confirm this thought, controls of simple powders HA, Al₂O₃, MCD were made.

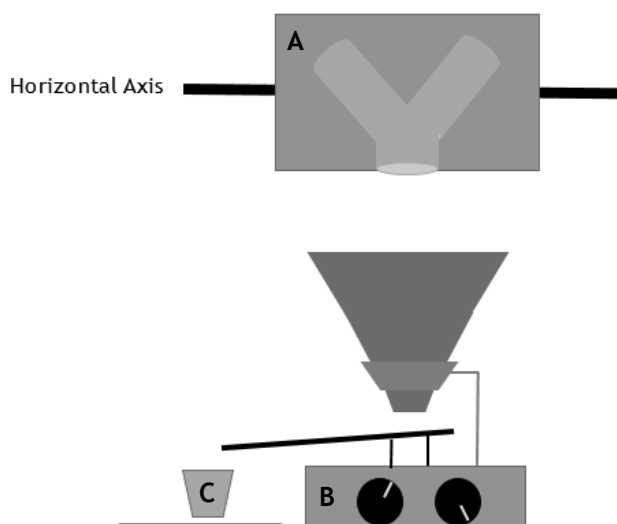


Figure 6.8 - Schematic drawing of the set up put in place for powders blending OQ. (A) is the V-blender, (B) is the vibratory feeder and (C) is the 50 ml cup.

As stated in section 6.2.4, several factors that can influence blending process in a V-blender. Therefore it important to reproduce all the steps exactly the same way in each test made. The following protocol was conceived:

1. Weight the 50 ml receiving cup;
2. Weight the necessary amount of each powder to fill 550 ml of the blender;
3. Pour the abrasive powder into the blender through the back exit of the v-blender;
4. Pour the HA powder into the blender through the back exit of the v-blender;
5. Close the blender and turn it on;
6. When the desired time of blending is over, turn off the v-blender;
7. Open the back exit of the v-blender and pour the bulk into the hopper of the vibratory feeder;
8. Turn on the vibratory feeder at 50% of its vibration capacity and collect the amount of powder necessary to overflows the 50 ml receiving cup;
9. Level the top of the receiving cup with a spatula such that it is completely full. Be careful not to compress or shake the powder;
10. Re-weight the receiving cup and its content;
11. Calculate the bulk density in g/ml by dividing the weight of the powder by the volume of the cup.

The number of cups weighted were the required to sample all the 550 ml of bulk present in the V-blender. The results obtained were presented as mean \pm standard deviation (SD) and statistical analysis was carried out by means of one-way ANOVA with Tukey post hoc tests using software GraphPad Prism 6.

6.5.2.2 Blasting OQ

After blending OQ procedures determination of the expected optimal operational parameters for powders blending conformity, blasting OQ took place. Samples routine preparation was designed to be as close as possible to the production procedures already implemented in Ceramed (Figure 6.9). HA/Abrasive was prepared using the V-Blender,

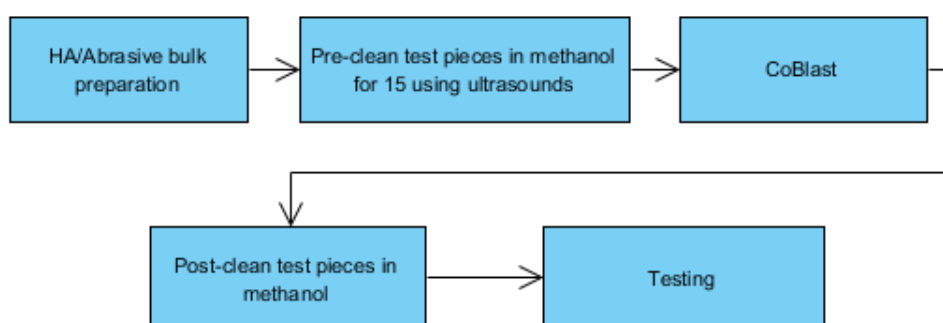


Figure 6.9 - CoBlast Process Flow for test pieces. Process flow is intended to replicate the regular process flow of an orthopaedic implant that will undergo coating deposition.

compressed air and chemically pure methanol (José Manuel Gomes dos Santos, LDA) were used to pre-clean and post-clean samples before and after coating deposition, and finally samples were tested.

CoBlast of samples was made using two different abrasive media (i.e. Al_2O_3 and MCD), and three different nozzle heights (i.e. 50 mm, 40 mm and 30 mm from the surface) with appropriate raster offset (i.e. 3.3 mm, 2.9 mm, and 2.6 mm respectively). For each situation the following resulting features were evaluated:

- Coating morphology using SEM technology and optical microscopy
- Coating thickness using optical microscopy
- Coating roughness using profilometry
- Coating crystallinity using XRD analysis
- Coating heavy metals content using X-ray fluorescence (XRF) technology
- Coating adhesion using Pull-off test

Scanning electron microscopy (SEM) observations were carried out using a Carl Zeiss AURIGA CrossBeam (FIB-SEM). Prepared samples have been previously coated with an Ir conductive film for avoiding charge effects. Normal mode, and backscattered mode were used to access coating morphology.

Coating thickness evaluation was made using cross sections of samples mounted in a polyester resin, then ground and polished. Mounted samples were examined using a Zeiss inverted optical microscope. Coating thickness was measured using AxioVision software. Results' statistical analysis was carried out using two-way ANOVA test ($p < 0.05$) with Tukey post hoc test.

Coating roughness values (i.e. R_a values) were obtained according to ISO 4287:1997 - *Geometrical Product Specifications (GPS) - Surface texture: Profile method - Terms, definitions and surface texture parameters*. R_a roughness was measured in two directions (e.g. x and y) using a Mitutoyo SJ-410 profilometer for both coated samples and acid etched samples in nitric acid 65% (AppliChem, Panreac), Six measurements were made for each conditions evaluated. Results values were presented as mean \pm SD, and statistical analysis was made using using Two way ANOVA test ($p < 0.05$) with Tukey post hoc test.

Coating crystallinity was evaluated according to ISO 13779-3 - *Implants for surgery - Hydroxyapatite - Part 3: Chemical analysis and characterization of crystallinity and phase purity*. An X-Ray Diffractometer Philips X'Pert PRO MRD equipped with a Cu tube was used over the angular range of 20 to 60° (2θ). All XRD scans were carried out with a resolution of 0.02° (2θ) and a sampling time of 50s per step. Origin 2015 software was used to integrate mean full peak values.

Samples heavy metals content was determined using XRF technology. Semi-quantitative elemental chemical analysis by fluorescence X-ray wavelength dispersion, was carried out using a sequential XRF spectrometer PANalytical WDS-4 kW AXIOS (PANalytical BV, Almelo, The Netherlands). The spectrometer uses a rhodium ampule for producing X-rays and the samples which were measured as helium flow. Spectra were deconvoluted by the least squares method and a semi-quantitative chemical analysis based on the approach of the basic parameters using the SuperQ IQ + program (PANalytical BV, Almelo, The Netherlands). Further correction was applied for medium so that titanium was not detected.

Adhesion procedures were handled according to ISO 13779-4. Ti-6Al-4V cylindrical specimens with dimensions 24.5 mm of height and 25 mm of diameter were coated. Polyamide epoxy FM1000 was the adhesive used to link a coated specimen with a non-coated one. The assembly was placed in an oven at 180° for two and half hours to cure FM1000. A tensile load at a constant rate of cross-head speed was applied using an Instron 4507 with a load cell of 100 kN. Adhesion cylindrical test specimens were coated using Adhesion CNC program (Appendix E).

6.5.3 Performance Qualification

IQ and OQ are successful act together demonstrating that the equipment is installed properly and that when operated in accordance with the defined operational procedures conform products can be obtained. PQ is preformed after to demonstrate a key feature of process validation: Process capability. It indents to prove a long term stability of the process, showing that it consistently performs in accordance with predetermined criteria and thereby yields product meeting its specifications.

6.5.3.1 Blending PQ

Samples for the first five analyses listed above on Blasting OQ were coated at the same time as samples for blending PQ were being prepared. PQ intends to demonstrate long term capability of the process: a good process performance. Since posteriorly to the blending procedure with optimized operational parameters, bulk undergoes handling to transfer it from the vibratory feeder mechanism to the powder feeder single 10-C of CoBlast equipment, segregation is likely to occur, and the 50/50 (w/w) bulk condition as bulk is being spread may not be verified over time. Therefore, the following CNC program was written so as this effect could be studied as soon as possible, since it could endanger the whole analysis.

TestSamples CNC code

[Filename]

name=TestSamples

[Requirements]

PartTooling=COUPON_TRAY

[Parameters]

units=mm

[ProgramData]

N10 F.125 (set the feedrate)

N20 G91

N25 G01 y55.0 F33.0 (use relative coordinates)

N30 G04 P.9 (hold position)

N40 G91

```

N50 M98 SUB_STEP A
N51 G91
N55 G00 y-8.5
N60 G91
N70 M98 SUB_STEP B
N80 G91
N90 G00 y-8.5
N100 G91
N70 M98 SUB_STEP C

```

```

N270 G04 P1

```

```

N300 G28 (finish homing, slowly)
N310 M30 (end of program)

```

Subroutines SUB_STEP A, SUB_STEP B and SUB_STEP C are responsible to coat each one of the three lines of 4 samples positioned on part tooling recognised by the system as COUPON_TRAY and can be found in Appendix E. The final looks of the blasting *TestSamples* CNC code result is represented in Figure 6.10.

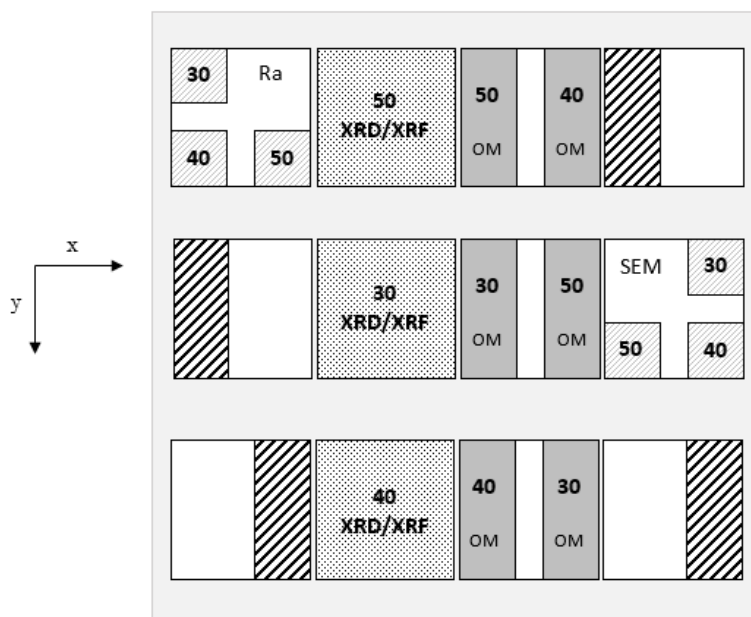


Figure 6.10 - Schematic drawing of the result of *TestSamples* CNC code. OM stands for Optical microscopy, XRD stands for x-ray diffraction, XRF stands for x-ray fluorescence, and SEM stands for scanning electron microscopy. Samples labelled with these abbreviations were used for those analysis. Samples represented with dashed lines only were used for blending PQ and were coated with a nozzle height of 40 mm.

Samples represented with dashed lines with nothing written over them were used for roughness measurements as a parameter that could indicate if the impact, and thus, particles size and distribution, was unvarying over time.

The risk is that powders handling during regular production, and the action of stirring them inside the feeder hopper can cause powders segregation and lead to non-uniform results across time. These non-conformities can be spotted by analysing surface roughness profile per example. If in a given time the amount of abrasive that is being expelled is reduced, the effect of surface roughness will be different. By positioning control samples across the robot coating route and performing enough coatings so that the feeder content can be all expelled, the preconized roughness analyses, before and after etching, should be enough to spot significant differences on HA/abrasive ratio that is being expelled.

6.5.3.2 Blasting PQ

Blasting PQ will focus on the results over time. PQ intends to prove a long term stability of the process. After defining the best operational parameters, samples must be prepared over time to study the influence of light, vibration, humidity, temperature, purity of the raw material, particle distribution of the previous (i.e. different batches with different particle distributions) and determine measures to eliminate them. This work needs to be done over time so that multiple factors that can influence the process can arise (e.g. differences in air humidity, on ambient temperature that can influence enormously the temperature of the compressed air, vibration of Ceramed's equipment and near companies over different week days). It is necessary to examine to what extent these factors can influence the results and define changes in operational parameters to operate CoBlast in all situations.

The extent of analysis and the time required to go through all conditions where outside varying factors that can affect the results of CoBlast arise is outside the enclosed time of this master thesis.

Even though, short term stability and capability of the process will be inferred with a OQ/PQ perspective after gathering the results of the analysis made.

At the end the CNC program that will be used to coat pedicle screws shall be developed and tested.

6.5.3.3 Process monitoring plan

When a process is validated there is no need for verification of 100% of the production results. Still, control of monitoring parameters with calibrated monitoring equipment shall be performed in order to identify possible states of processing non-conformity. Deciding representative parameters of the overall process that allow monitoring it and its state of validation is very important. Some of these features shall be measurable without destroying the actual product.

Coating thickness and coating roughness are good candidates for monitoring attributes. During OQ/PQ procedures the hypothesis of using these two parameters, on final product, as monitoring criteria was studied. Maintaining a state of control of the overall process (i.e. blending and blasting) might be complex, thus, a mid monitoring point between the two steps shall be thought.

Chapter 7

CoBlast Process Validation

CoBlast Process Validation was conducted to validate the deposition of HA coating over Ti-6Al-4V pedicle screws using CoBlast processing. Validation was executed according to the Validation Plan developed previously in Chapter 6.

Results disclosed in this chapter help to conclude about the type of analysis that can be made on HA coatings thin as 5-10 μm with remarkable adhesion properties in order to validate its process of deposition.

Moreover, the final goal of this validation is to ultimately contribute to launching to the market an innovative coating service with Ceramed brand on it.

7.1 Installation Qualification

All equipment was received at Ceramed's new facilities and installed according to suppliers and manufacturers' instructions.

Installation qualification for CoBlast comprises the qualification of the installation of two sets of equipment: equipment that performs CoBlast of surfaces and equipment that acts on the blending of the two powders (i.e. abrasive Al_2O_3 and dopant HA, or abrasive MCD and dopant HA).

7.1.1 CoBlast equipment IQ

CoBlast equipment was installed according to the instruction of the suppliers and manufacturers of the systems. IQ of this set of equipment was registered in the following checklists: System identification, Components identification, Consumables identification, Documentation of conformity, System damages, System installation and User interface.

System identification checklist

Purpose: List all system specifications and check them.

Equipment		Yes	No
Comco LA3250 Advanced Lathe			
Model	LA3250 - 29	✓	-
Serial No.	---	✓	-
Pressure min-max.	620 - 965 kPa (6.2 - 9.6 bar)	✓	-
Electrical connection	115 VAC, 50/60 Hz	✓	-
Transformer	220-240 VAC	✓	-
Power Input	400 W	✓	-
Air Input	198 l/min	✓	-
Software Version	Comco User Interface V 12.2	✓	-
	Comco Galil Service V 10.2	✓	-
	Comco Serial Service V 2.0	✓	-
	Comco Axis Control Utility V 7.0	✓	-
	Comco Bus Control Utility V 1.3	✓	-
Sulzer Metco Powder Feeder Single 10-C			
Model	Single 10-C	✓	-
Serial No.	---	✓	-
Pressure min-max.	0 - 400 kPa (0 - 4 bar)	✓	-
RPM min-max.	0 - 10 rpm	✓	-
Flow rate	0 - 10 l/min	✓	-
Electrical connection	230 VAC, 50 Hz	✓	-
Power Input	250 W	✓	-
Sablex Universal Vacuum Cleaner			
Model	Sablex Universal	✓	-
Serial No.	---	✓	-
Flow rate	600 m ³ /h	✓	-
Electrical connection	220 VAC, 50/60 Hz	✓	-
Power Input	550 W	✓	-

Declaration:

Systems are identified and specifications verified.		<u>Yes</u>	No
Remarks:	No additional remarks.		

Components identification checklist

Purpose: Identify and verify the availability of the equipment components.

Equipment	Available?	
	Yes	No
Comco LA3250 Advanced Lathe		
Air drier AD5300	✓	-
Mandril part tooling size 1	✓	-
Mandril part tooling size 1 (2)	✓	-
Mandril part tooling size 2	✓	-
Platform part tooling	✓	-
Sulzer Metco Powder Feeder Single 10-C		
Powder hopper of 1100 cm ³	✓	-

Declaration:

The components are identified and available.	<u>Yes</u>	No
Remarks:	No additional remarks.	

Consumables identification checklist

Purpose: Identify and verify the availability of the consumable components.

Equipment	Available?	
	Yes	No
Comco LA3250 Advanced Lathe		
Inside chamber halogen lamp	✓	-
Air filter	✓	-
Sulzer Metco Powder Feeder Single 10-C		
Spreader	✓	-
Suction unit	✓	-
Universal Vacuum Cleaner		
Air filter	✓	-

Declaration:

The consumables are identified and available.	<u>Yes</u>	No
Remarks:	No additional remarks.	

Documentation checklist

Purpose: To ensure that the necessary documentation for production with this equipment is correct and complete.

Equipment	Available?	
	Yes	No
Comco LA3250 Advanced Lathe		
Operating instructions	✓	-
Declaration of conformity by the manufacturer	✓	-
Sulzer Metco Powder Feeder Single 10-C		
Operating instructions	✓	-
Declaration of conformity by the manufacturer	✓	-
Universal Vacuum Cleaner		
Operating instructions	✓	-
Declaration of conformity by the manufacturer	✓	-

Declaration:

System documentation required is correct and available.	<u>Yes</u>	No
Remarks:	Declarations of conformity by the manufacturers were revised and filed with CoBlast Ceramed's internal documentation.	

System damages checklist

Purpose: To report any type of system damage.

Equipment	Damaged?	
	Yes	No
Comco LA3250 Advanced Lathe		
Is there any component or consumable damaged in this item?	-	✓
Sulzer Metco Powder Feeder Single 10-C		
Is there any component or consumable damaged in this item?	-	✓
Universal Vacuum Cleaner		
Is there any component or consumable damaged in this item?	-	✓

Declaration:

The equipment, components and consumables are free of visible damage?	<u>Yes</u>	No
Remarks:	No additional remarks.	

System installation checklist

Purpose: To determine if the system is placed properly with correct wiring and utilities available.

Equipment	Specification fulfilled?	
	Yes	No
Comco LA3250 Advanced Lathe		
Is the equipment properly connected to company's air system without any visible defect?	✓	-
Is the electrical connection made using a 220-240V transformer?	✓	-
Is the pressure regulator working properly from 0 to 1000 kPa?	✓	-
Sulzer Metco Powder Feeder Single 10-C		
Is the equipment properly connected to company's air system without any visible defect?	✓	-
Is the single phase electrical connection correctly made?	✓	-
Is the powder connection made between the powder exit and Comco LA 3250 Advanced Lathe single nozzle entry?	✓	-
Is the pressure regulator working properly from 0 to 400 kPa?	✓	-
Universal Vacuum Cleaner		
Is the three phase electrical connection correctly made?	✓	-
Is the air connection with the Comco LA 3250 Advanced Lathe collar made, and using an appropriate duct?	✓	-

Declaration:

Installation of CoBlast equipment is complete and correct.	<u>Yes</u>	No
Remarks:	No additional remarks.	

User Interface Menu Settings Checklist

Purpose: To ensure the user interface comes with the specified settings.

Equipment	Setting fulfilled?	
	Yes	No
Comco LA3250 Advanced Lathe		
Does the software language is English?	✓	–
Does the user interface exhibits a time countdown when a coating program is at work?	✓	–
Does the STOP button stops the program and returns the axis to home position?	✓	–
Does the START button re-starts the coating program?	✓	–

Declaration:

All user interface important features are implemented properly.	<u>Yes</u>	No
Remarks:	No additional remarks.	

7.1.2 Blending equipment IQ

In order to qualify the installation of the V-blender, additional careful procedures were adopted. The V-blender was machined by Enbio technical team and neither this construction nor the structure where it has been assembled were CE certified, or others. Tests like visual inspection, volume test of the hollow cylindrical shells of the V-blender horizontality of the axis of rotation confirmation were made. The results attained are presented below.

IQ of this set of equipment was finally registered in the following checklists: System identification, Components identification, Consumables identification, Documentation of conformity, System damages, System installation and User interface.

7.1.2.1 Visual inspection, angle between shells and volume verification

The V-blender was clean and without any scratches on its inner surface. In order to test its volume, compressed air at 600 kPa was used to assure cleanliness and void volume was filled with deionized water. The water was poured into a graduated measuring cylinder of 1 liter and the volume was verified. The volume of water was confirmed at 1 liter, and thus, the V-blender was classified as V-blender with a total volume (V_{Total}) of 1 liter.

7.1.2.2 Horizontality testing

Horizontality of the V-blender installation was successfully verified using a calibrated level tool (Figure 7.1).

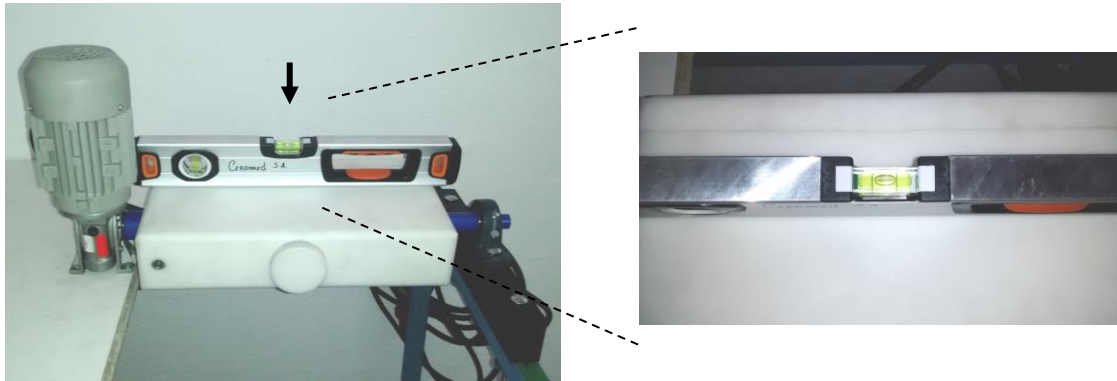


Figure 7.1 - V-blender horizontality testing made using a level tool. Horizontality of the installation was successfully confirmed.

System identification checklist

Purpose: List all system specifications and check them.

Equipment		Yes	No
V-Blender			
Model	90 ° V-blender	✓	-
Serial No.	---	-	✓
Speed	20 RPM	✓	-
Electrical connection	230 VAC, 50/60 Hz	✓	-
Power Input	90 W	✓	-
Retsch Vibratory Feeder			
Model	DR 15/40	✓	-
Serial No.	---	✓	-
Frequency	50 - 60 Hz	✓	-

Declaration:

Systems are identified and specifications verified.		<u>Yes</u>	No
Remarks:	Although the blender system has no serial number, the motor used to create rotation over its horizontal axis has it and the assembly was identified internally following Ceramed's internal procedures.		

Components identification checklist

Purpose: Identify and verify the availability of the equipment components.

Equipment	Available?	
	Yes	No
Retsch Vibratory Feeder		
Chute	✓	-
Hopper	✓	-

Declaration:

The components are identified and available.	<u>Yes</u>	No
Remarks:	No additional remarks.	

Documentation checklist

Purpose: To ensure that the necessary documentation for production with this equipment is correct and complete.

Equipment	Available?	
	Yes	No
V-Blender		
Operating instructions	-	✓
Retsch Vibratory Feeder		
Operating instructions	✓	-
Declaration of conformity by the manufacturer	-	✓

Declaration:

System documentation required is correct and available.	<u>Yes</u>	No
Remarks:	V-Blender has no operating instruction. An internal work instruction was to create the possibility for Ceramed's workers to use the V-Blender easily, according to Ceramed's internal procedures (Appendix C). Retsch Vibratory Feeder declaration of conformity by the manufacture was nowhere to be found.	

System damages checklist

Purpose: To report any type of system damage.

Equipment	Damaged?	
	Yes	No
V-Blender		
Is there any visible damage in this item?	-	✓
Retsch Vibratory Feeder		
Is there any component damaged in this item?	-	✓

Declaration:

The equipment and components are free of visible damage?	<u>Yes</u>	No
Remarks:	No additional remarks.	

System installation checklist

Purpose: To determine if the system is placed properly with correct wiring and utilities available.

Equipment	Specification fulfilled?	
	Yes	No
V-Blender		
Is the system placed on a horizontal and planar surface?	✓	-
Is the horizontal axis drilled in the correct central position?	✓	-
Is the three phase electrical connection correctly made?	✓	-
Does the blender cover insulates it efficiently?	✓	-
Retsch Vibratory Feeder		
Is the system placed on a horizontal and planar surface?	✓	-
Is the single phase electrical connection correctly made?	✓	-
Does the power button and switchers work properly?	✓	-

Declaration:

Installation of Blending equipment is complete and correct.	<u>Yes</u>	No
Remarks:	No additional remarks.	

7.1.3 Result and report of installation qualification

IQ results were assembled in an overall result of IQ checklist.

Overall result IQ check list

Purpose: List all the parameters evaluated in IQ. Confirm that all were executed and conclude about its success.

IQ result	Check carried out successfully?	
	Yes	No
System identification checklist	✓	-
Components identification checklist	✓	-
Documentation of conformity checklist	-	✓
Consumables identification checklist	✓	-
System damages checklist	✓	-
System installation checklist	✓	-
User interface checklist	✓	-

Small differences from what expected during IQ were found in what concerns Documentation of conformity of the equipment. The absence of conformity declaration by the manufacturer for the V-Blender and Vibratory Retsch Feeder may require detailed equipment study report to guarantee its conformity with Machines Directive 98/37/CE. Preliminary tests made with the equipment in place point to everything working as anticipated. Though, this study is considered something advisable in a near future. Meanwhile, differences are documented, and despite its occurrence the system is considered approved.

7.2 Operational Qualification

Before any test or sample preparation, raw materials specifications were checked for compliance with the standards. HA was in accordance with ISO 19779-1:2008 as required. Raw materials manufacturers' declarations of compliance were joined up, analysed and accepted for this process validation (Appendix D).

7.2.1 Blending OQ

RPM of the V-blender were verified by measuring the time it takes for the 55% filled V-blender to perform 10 revolutions. This time was 28.59 ± 0.09 s, which means that the 55% filled V-blender is operating with a rotation rate of approximately 19 rpm. This value is within the values of capable rotation rate for 1 liter V-Blender as exposed in section 6.2.4.

First control curves data was collected by performing a starting point analysis where as-supplied powders were tested under the same conditions as the future bulk form. All the procedure lines were followed using 600 mg of HA, MCD and Al₂O₃. After, a 300g of each

powder were tested as protocolled for a blending time of zero minutes. Blank curves were drawn (Figure 7.2, Figure 7.3).

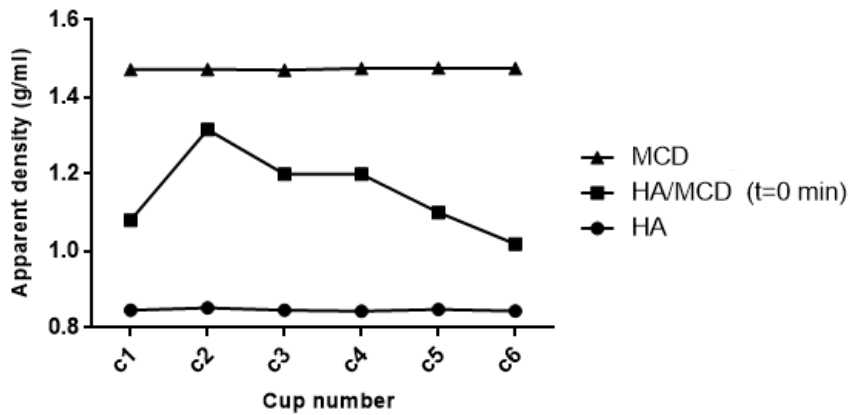


Figure 7.2 - HA, MCD and HA/MCD apparent density curves after 0 minutes of blending on a 1 liter V-blender.

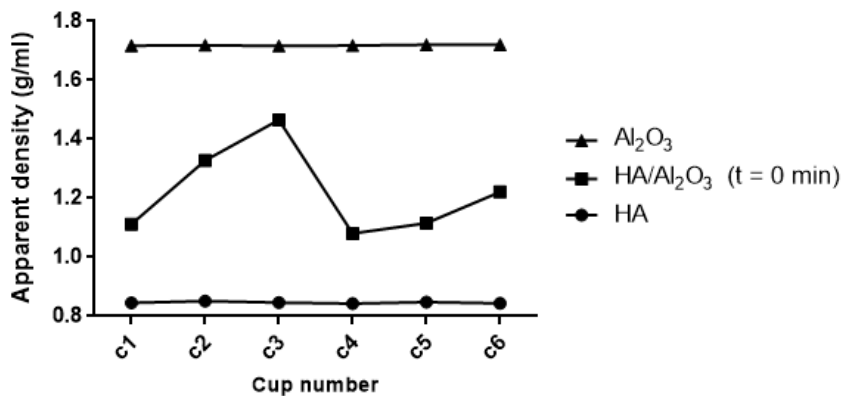


Figure 7.3 - HA, Al₂O₃ and HA/Al₂O₃ apparent density curves after 0 minutes of blending on a 1 liter V-blender.

The maximum value and the minimum value of the HA/MCD and HA/Al₂O₃ apparent density were considered limit values for the apparent density results of blending after 3 and 5 minutes. They were both 1.017 and 1.315 for minimum and maximum apparent density of HA/MCD and 1.080 and 1.466 for minimum and maximum of HA/Al₂O₃ apparent density.

After this first procedure value of apparent density of each one of the simple powders could be accurately calculated with negligible standard deviation:

$$\begin{aligned}\rho_{HA} &= 0.85 \text{ g/cm}^3 \\ \rho_{MCD} &= 1.47 \text{ g/cm}^3 \\ \rho_{Al_2O_3} &= 1.72 \text{ g/cm}^3\end{aligned}$$

Since powders blending shall be performed with the V-blender filled at 50-60% of its total volume, the mass of each powder required to fill the blender up to approximately 550 ml was calculated by performing the following deduction:

$$V_{total} = V_{HA} + V_{Ab} \quad (7.1)$$

$$V_{total} = \frac{m_{HA}}{\rho_{HA}} + \frac{m_{Ab}}{\rho_{Ab}} \quad , \quad m_{HA} = m_{Ab} = m \quad (7.2)$$

$$V_{total} = \frac{(\rho_{HA} + \rho_{Ab}) \times m}{\rho_{HA} \times \rho_{Ab}} \quad (7.3)$$

$$m = \frac{V_{total} \times \rho_{HA} \times \rho_{Ab}}{\rho_{HA} + \rho_{Ab}} \quad (7.4)$$

After calculating, a final mass of 300g of HA and 300g of abrasive were set as protocol values since they represent a 50/50 (w/w) HA/Abrasive value and the condition of 50-60% filling is fulfilled when these mass values are used for both HA/MCD and HA/Al₂O₃ bulk.

By placing first abrasives and after HA inside the V-blender and mixing for 3 and 5 minutes following results were obtained (Figure 7.4, Figure 7.5, Figure 7.6 and Figure 7.6)

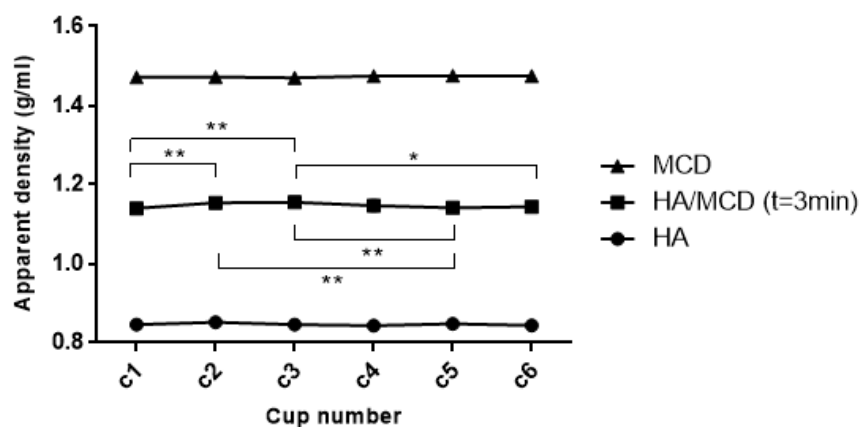


Figure 7.4 - HA, MCD and HA/MCD apparent density curves after 3 minutes of blending on a 1 liter V-blender. *, ** indicate a significant difference between the assigned conditions ($p < 0.05$, $p < 0.01$ respectively).

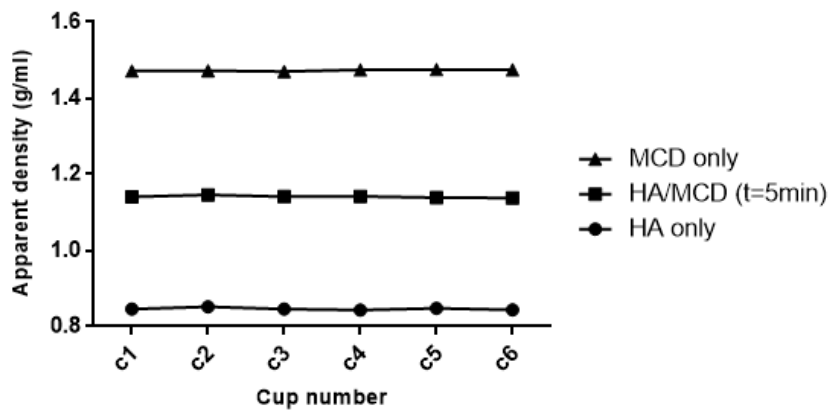


Figure 7.5 - HA, MCD only and HA/MCD apparent density curves after 5 minutes of blending on a 1 liter V-blender. No significant differences were found.

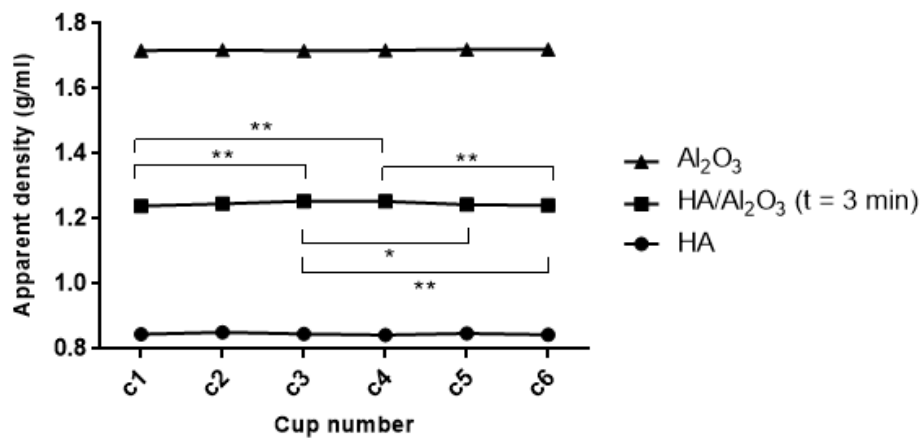


Figure 7.7 - HA, Al₂O₃ and HA/Al₂O₃ apparent density curves after 3 minutes of blending on a 1 liter V-blender. *, ** indicate a significant difference between the assigned conditions ($p < 0.05$, $p < 0.01$ respectively).

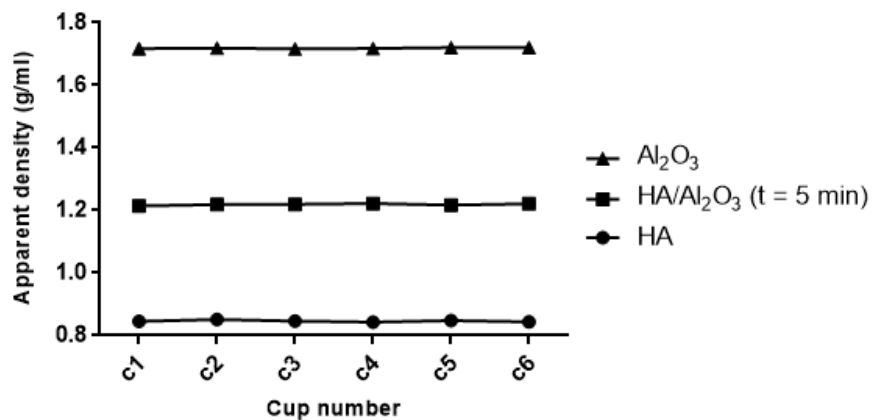


Figure 7.6 - HA, Al₂O₃ and HA/Al₂O₃ apparent density curves after 5 minutes of blending on a 1 liter V-blender. No significant differences were found.

Results show that for both bulks (e.g. HA/MCD and HA/Al₂O₃), blending powders for 5 minutes on a V-blender of 1 liter results in a bulk of 50/50 (w/w) in all its extension when poured over a vibratory chute (Figure 7.5 and Figure 7.7).

SEM imaging of the powders may help to explain the obtained results (Figure 7.8). Abrasive powders were cuboid shaped, very angular and far bigger than HA particles as expected. Among the abrasive particles, Al₂O₃ were clearly smoother than MCD. This might be attributed to the distinct route of manufacturing process of these two particles. HA particles were up to 4x times smaller than the abrasive particles and were perfectly round shaped.

HA/Abrasive bulk powders lack of segregation, even when poured over a vibratory chute, may be attributed to particles geometry. When in bulk, a perfect mix of HA/Abrasive particles may lead to a situation where HA particles become trapped within the interstices formed between the abrasive particles.

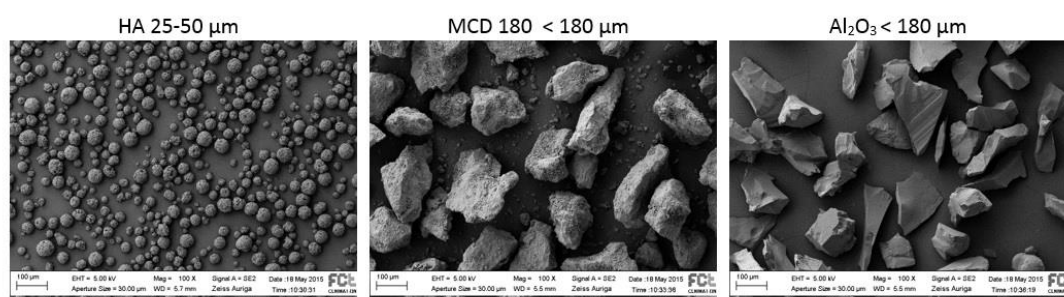


Figure 7.8 - SEM imaging of hydroxyapatite (HA) and blast media MCD (sHA) and Al₂O₃.

7.2.2 Blasting OQ

Blasting OQ was performed based on the tests made to assess the influence of the parameters under evaluation (e.g. two different blast media, 3 different nozzle heights with individual raster offset) on the following features:

1. Coating morphology evaluated using SEM and optical microscopy
2. Coating thickness evaluated using optical microscopy
3. Coating roughness evaluated using profilometry
4. Coating crystallinity evaluated using XRD analysis
5. Coating heavy metals content evaluated using XRF
6. Coating adhesion evaluated using Pull-off test

Test 1, 2, 3 and 4 can help to decide which operational parameters are better to achieve great HA coating surface coverage. Furthermore, XRD analysis is also useful to understand how coating crystallinity may vary with the operational parameters under evaluation and understand which one(s) better serve the limits defined by ISO 13779-2. Heavy metals content may also help to decide which operational parameters can and cannot be adopted. After all these prepositions are clear, coatings prepared with parameters that were not excluded by previous tests analysis shall be tested for coating adhesion compliance with ISO 13779-4.

7.2.2.1 Coating morphology

Coating morphology was assessed using SEM technology and optical microscopy (Figure 7.9, Figure 7.10). HA blasted surfaces presented a flakelike appearance, as if the HA particles had been crushed into the substrate surface. Visually no differences were found between the samples prepared with the three different blasting nozzle heights.

HA/MCD blasted surfaces appeared to be morphologically smoother than single HA surfaces but a small scale topographical variation was present. It seemed as if these were uniformly roughened highly regular surfaces. Apparently no big differences were present when the three nozzle heights conditions were compared, although for the height of 40 mm a smoother surface was detected.

HA/Al₂O₃ blasted surfaces seemed to be more irregular than HA/MCD blasted ones, especially for 40 mm nozzle height. This condition seemed to have led to a denser coating layer with apparent roughness peak to peak higher than the other two. On the contrary, for a nozzle height of 30 mm, SEM image revealed a smoother coating than the other two nozzle heights for the HA/Al₂O₃ condition.

One plasma-sprayed HA coated sample was also observed. This HA coating was porous with spherical shapes and bulge valleys. It was visibly cracked. These cracks can be attributed to thermal shock after the high temperature plasma coating application. These are common features of coatings that underwent rapid cooling.

Cross-sections observations revealed that when blasted with HA only a smooth interface between Ti-6Al-4V substrate and the coating arose (Figure 7.10). A thin layer of HA is noticeably deposited. When using a nozzle height of 30 mm, some coating narrowed sections are created.

HA/MCD blasted samples were well coated, without narrowed sections for all nozzle heights. Apparently thicker coatings are created when using MCD as blast media than for samples blasted with only HA. Furthermore, the underlying titanium has slightly jagged.

When HA/Al₂O₃ mixtures were used to blast substrate surfaces a very irregular layer of HA was deposited, and Ti-6Al-4V substrate surface is undoubtedly more jagged. Some coating narrowed sections were found with this blasting media for all three nozzle height conditions.

Apparently, there is no variation in coating coverage when the nozzle height used in blasting varies from 50 mm to 30 mm for the conditions HA/MCD and HA/Al₂O₃ blasted surfaces. However, when coatings using HA/MCD and HA/Al₂O₃ are compared, less pronounced jagged features are visible on the first ones. This can be attributed to the softer nature and less angular shape of MCD when compared to Al₂O₃.

Plasma-sprayed samples presented thicker coatings since they were prepared according to the requirements made for pedicle screws HA plasma-sprayed (e.g. 60 μm thick). The underlying titanium was undoubtedly more grooved than all other tested samples. This can be attributed to the grit-blasting pre-treatment with corundum abrasive (i.e. Al₂O₃) of approximately 400 μm and 900 μm applied to substrates that have undergone plasma-spray coating.

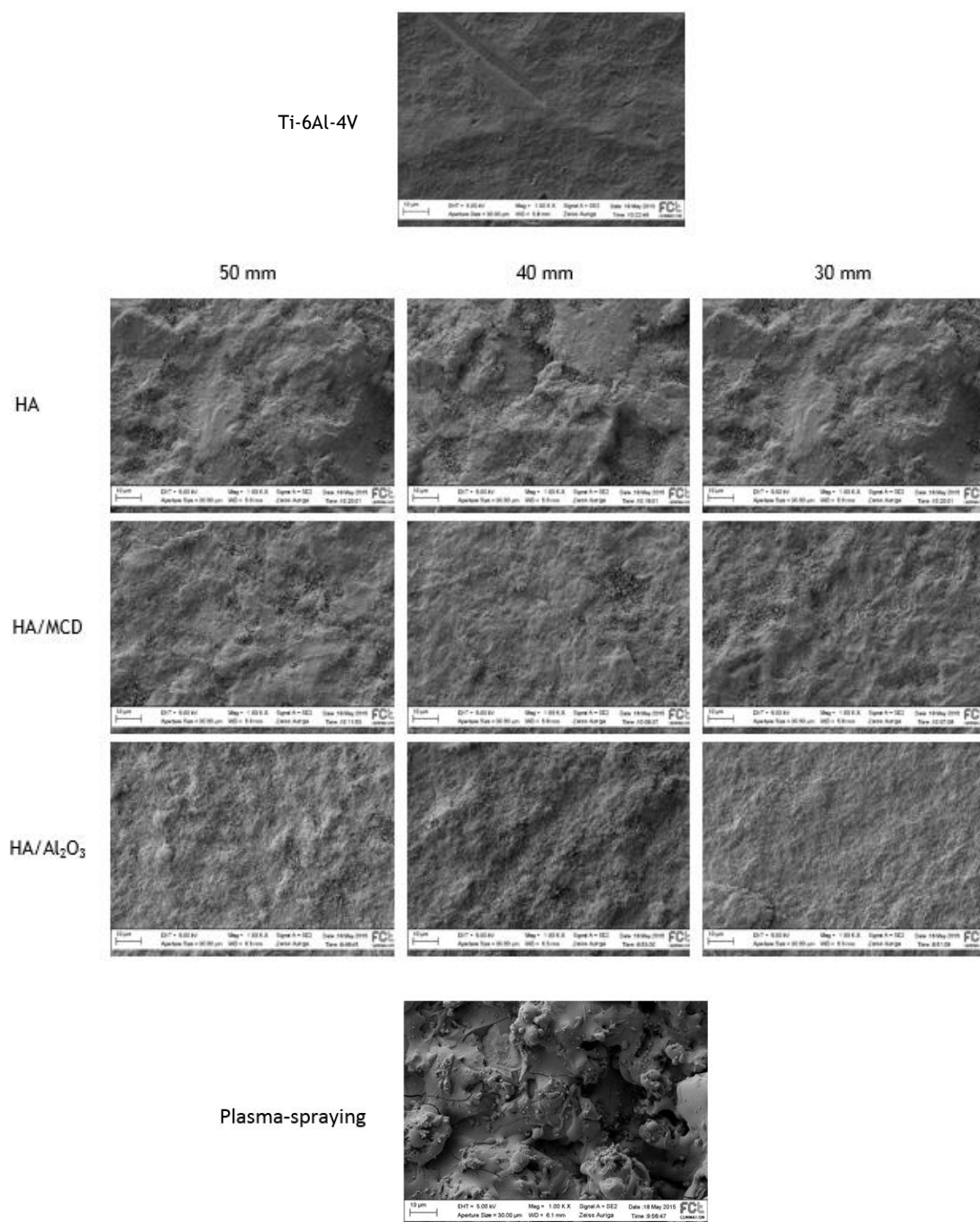


Figure 7.9 - Scanning Electron Microscopy images of Ti-6Al-4V as received, HA blasted samples and CoBlast samples prepared using HA as dopant media and Al₂O₃ or MCD as blasting media. Samples were blasted using 400 kPa of pressure and three different nozzle heights (50 mm, 40 mm and 30 mm).

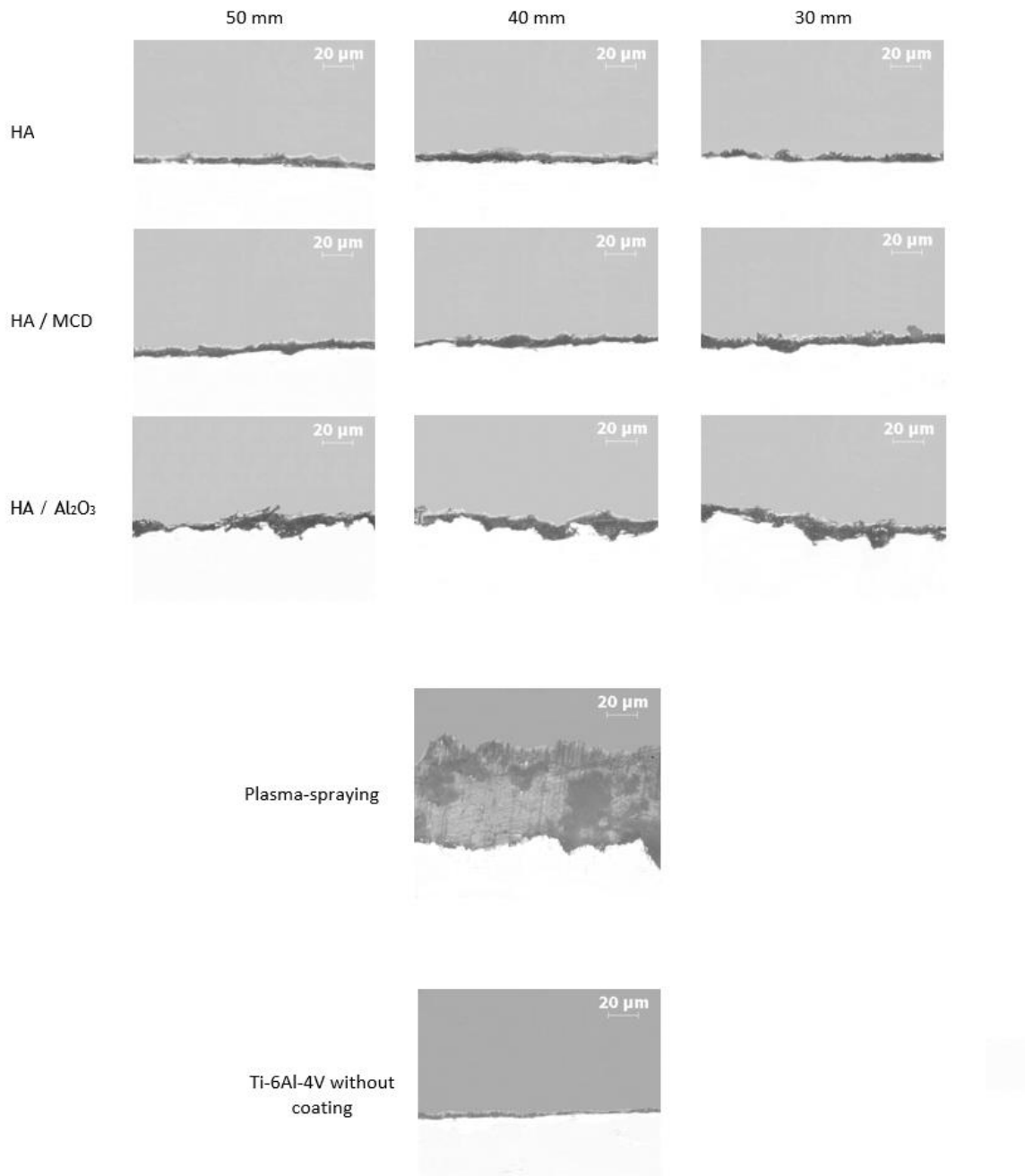


Figure 7.10 - Cross-sections of the Ti-6Al-4V coupons blasted with HA, HA/MCD and HA/Al₂O₃ for three different nozzle heights (50 mm, 40 mm and 30 mm). Plasma-sprayed HA coating with approximately 60 μm cross-section and Ti-6Al-4V substrate without coating were also observed.

7.2.2.2 Coating thickness

Coatings' thickness of HA coated samples was evaluated using optical microscopy and measured using AxioVision microscopy software (Table 7.1). Results show that there is no significant difference between coatings thickness when applied with the same blast media but with three different nozzle heights.

Table 7.1 - Coatings thickness evaluation (μm)

	50 mm	40 mm	30 mm
HA	3.98 ± 0.78	4.41 ± 0.45	4.32 ± 1.01
HA / MCD	6.50 ± 1.08	5.96 ± 1.21	5.72 ± 1.65
HA / Al ₂ O ₃	8.55 ± 4.74	9.43 ± 3.83	8.67 ± 3.47
Plasma	70.91 ± 9.84		

When different abrasive media are compared, coating thickness tends to increase from HA < HA/MCD < HA/Al₂O₃ regardless of the nozzle height used during blasting process. When this comparison is statistically analysed (Figure 7.11) no significant difference is found in coating thickness of surfaces blasted with HA and HA/MCD for all three different nozzle heights. Furthermore, when a nozzle height of 50 mm is employed, there is no difference between coatings' thickness of surfaces blasted with HA/MCD and HA/Al₂O₃. These results must be analysed carefully. Although in terms of coating thickness, HA/MCD and HA/Al₂O₃ deposited HA coatings, can have similar results, HA/Al₂O₃ thickness values are very uneven, resulting in a large standard deviation. These results may be attributed to the narrowed and jagged features together, observed on HA/Al₂O₃ blasted coatings cross-sections.

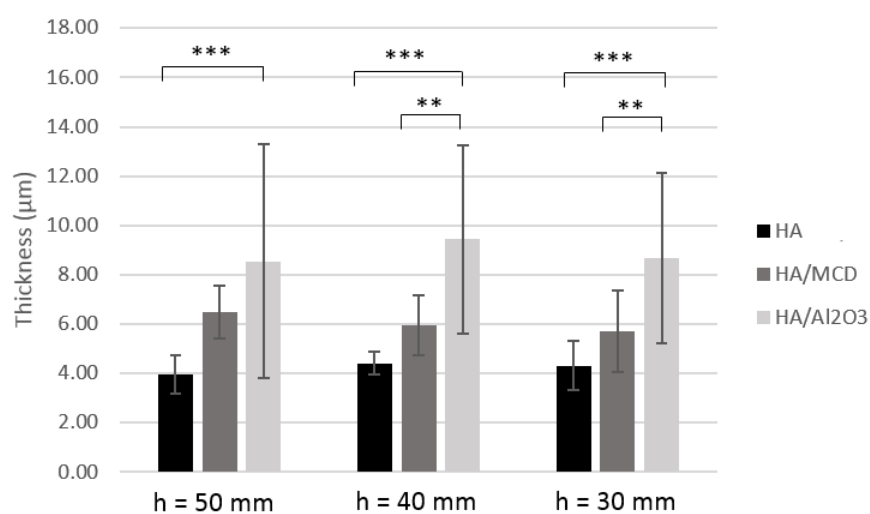


Figure 7.11 - Coating thickness evaluation results. **, *** indicate a significant difference between the assigned conditions ($p < 0.01$, $p < 0.001$ respectively).

7.2.2.3 Coating roughness

Coatings' roughness was registered using a Mitutoyo SJ-410 profilometer according to ISO 4287:1997. Roughness was measured before and after samples acid etching.

HA only blasted surfaces' roughness before acid etching was similar to HA/MCD surface roughness before acid etching for the three different nozzle heights used in blasting (Figure 7.12, Table 7.2). Both conditions resulted in coatings that were significantly different in roughness for a nozzle height of 50 mm when compared with a nozzle height of 30 mm.

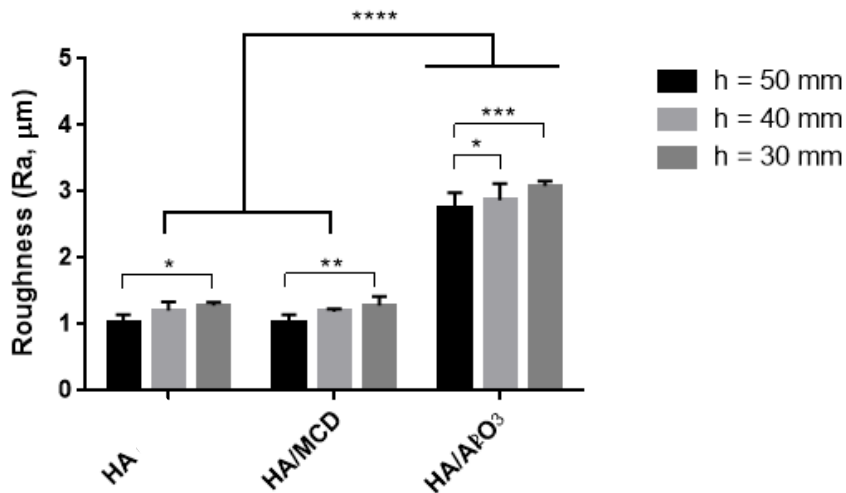


Figure 7.12 - Coating roughness evaluation before acid etching. *, **, ***, **** indicate a significant difference between the assigned conditions ($p < 0.05$, $p < 0.01$, $p < 0.001$, $p < 0.0001$ respectively).

HA/Al₂O₃ blasted surface presented differences in roughness when the nozzle height of 50 mm was compared with both 40 mm and 30 mm. When this blast medium is compared with the others, for all the three nozzles heights used in blasting, the roughness was significantly higher. This may, once again, be attributed to the increased hardness and angular shape of alumina when compared with MCD or the absence of blast medium.

Table 7.2 - Surface roughness (Ra, µm) before acid etching

	50 mm	40 mm	30 mm
Ti G5	0.58 ± 0.09		
HA	1.03 ± 0.10	1.21 ± 0.12	1.29 ± 0.04
HA / MCD	1.02 ± 0.11	1.19 ± 0.04	1.28 ± 0.13
HA / Al ₂ O ₃	2.75 ± 0.22	2.87 ± 0.23	3.09 ± 0.07
Plasma	7.85 ± 0.53		

After etching the coated substrates with nitric acid at 65%, no differences in surfaces roughness were found between the three nozzle heights used to blast the surfaces for HA, HA/MCD and HA/Al₂O₃ surface blasting conditions (Figure 7.13, Table 7.3). Results revealed that after coatings' dissolution, HA and HA/MCD blasting conditions were now significantly different in terms of surface roughness for all the three nozzle heights used in blasting. These results show that coating the surface with HA is quite different than coating with HA using MCD blast medium. After coatings' dissolution, HA/MCD blasted surfaces still have a roughness profile that could improve mechanical interlocking between bone and implant surface.

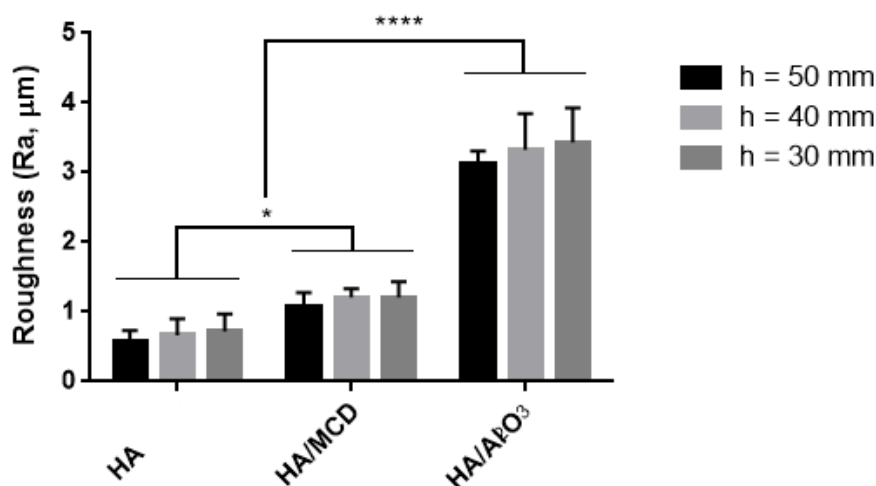


Figure 7.13 - Coating roughness evaluation after acid etching. *, **** indicate a significant differences between the assigned conditions ($p < 0.05$, $p < 0.0001$ respectively).

Once again HA/Al₂O₃ blast condition stands out. Blasting surfaces with HA/Al₂O₃ produces significantly higher surface roughness for all applied nozzle heights when compared with the other two coating/blast media even after acid etching.

Table 7.3 - Surface roughness (Ra, μm) after nitric acid at 65% etching

	50 mm	40 mm	30 mm
Ti G5	0.59 ± 0.14		
HA	0.59 ± 0.13	0.66 ± 0.22	0.72 ± 0.23
HA / MCD	1.08 ± 0.18	1.20 ± 0.11	1.21 ± 0.20
HA / Al ₂ O ₃	3.13 ± 0.16	3.33 ± 0.47	3.43 ± 0.45
Plasma	5.11 ± 1.06		

Furthermore, a tendency for surface roughness to increase after surfaces etching is noticed for both HA/MCD and HA/Al₂O₃ condition. Unlikely, when only HA is applied, after etching, the surface roughness significantly dropped ($p < 0.001$). The same happened for plasma-sprayed samples ($p < 0.05$). When surface roughness decreases, the amount of surface area available for osteoblast adhesion decreases. This may be deleterious for long term surface-bone interlocking.

7.2.2.4 Coating crystallinity

XRD analysis was carried on a compressed tablet of HA, blasted HA coatings using two different blasting media (i.e. MCD and Al₂O₃) and on a HA plasma-sprayed sample.

Before any coating crystallinity calculation, XRD patterns were normalized at relative intensity in order to determine the ratio of HA (211) to Ti (101) which can be faced as a HA coating coverage index (Figure 7.14,

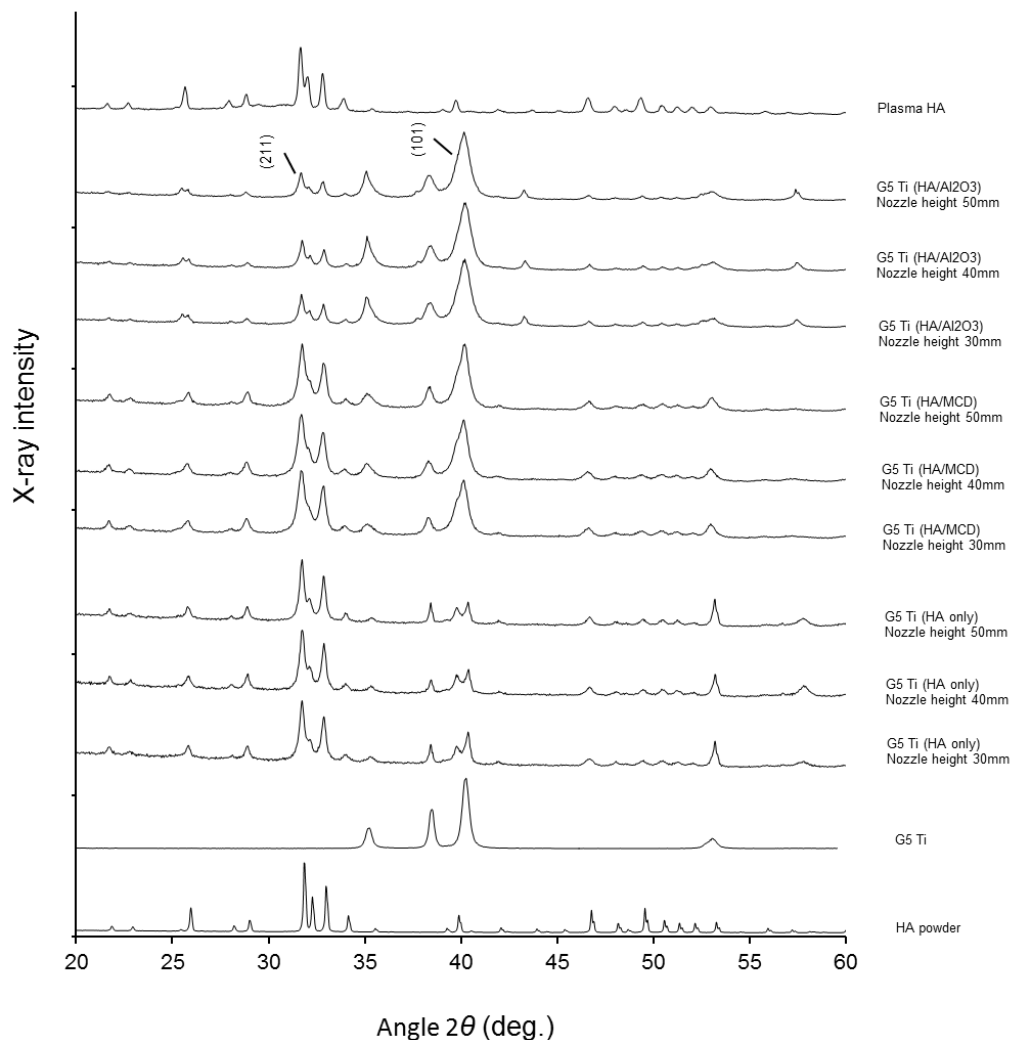


Table 7.4).

Figure 7.14 - Normalized XRD patterns of HA powder (e.g. raw material), G5 Ti substrate, HA only blasted G5 Ti, HA/MCD blasted G5 Ti, HA/Al₂O₃ blasted G5 Ti with 50 mm, 40 mm and 30 mm nozzle height blasting condition. An HA coated plasma sample was also analysed for comparison.

Table 7.4 - Ratio between the normalised intensity of 211 characteristic reflection of HA and 101 reflection of Ti corresponding to 31.5° and 40.2° (2θ), respectively.

Ratio HA (211) to Ti (101)	HA	HA/MCD	HA/Al ₂ O ₃
h=50mm	2.51	1.00	0.42
h=40mm	2.26	1.08	0.47
h=30mm	1.79	1.15	0.50

Coating degree of crystallinity has been accessed through two methods of XRD data treatment. Its calculation was performed following two accepted approaches:

1. Detection of the 10 peaks preconized by ISO 13779-3 for Hydroxyapatite, measurement of the integrated intensity of these ten line and comparison with a crystalline standard;
2. Detection of intensity of (300) diffraction peak (I_{300}) and intensity of the hollow between (112) and (300) diffraction peaks ($V_{112/300}$) of hydroxyapatite and evaluation of the percentage of crystalline phase (X_c) using the flowing equation (Landi et al., 2000)

$$X_c = 100 \times \frac{I_{300} - V_{112/300}}{I_{300}} \quad (7.1)$$

Blasted samples exhibit peaks associated with titanium which are present due to the thin nature of these coatings (i.e. < 10 μm) combined with the presence of the underlying Ti-6Al-4V substrate. The XRD signal obtained for these coatings contained an increased number of peaks present and variations in their intensity for different conditions studied. Origin software was used to integrate the 10 peaks preconized by ISO 13779-3 when found (Table 7.5). For conditions HA/MCD and HA/Al₂O₃ the 40.2° (2θ) titanium peak was so intense and broad that 39.8° (2θ) peak of HA was almost covered (Table 7.6).

Table 7.5 - D-spacing (m) of the ten peaks used for HA coating crystallinity evaluation according to ISO 13779-3.

D-spacing (m)	2θ
3.44 x 10 ⁻¹⁰	25.879242
3.17 x 10 ⁻¹⁰	28.126931
3.08 x 10 ⁻¹⁰	28.966514
2.81 x 10 ⁻¹⁰	31.820082
2.78 x 10 ⁻¹⁰	32.172726
2.72 x 10 ⁻¹⁰	32.902348
2.63 x 10 ⁻¹⁰	34.062034
2.26 x 10 ⁻¹⁰	39.856152
1.94 x 10 ⁻¹⁰	46.789193
1.84 x 10 ⁻¹⁰	49.497605

Table 7.6 - Integrated intensity of the peaks found in the XRD analysis of HA, Plasma, HA only, HA/MCD, HA/AL₂O₃ samples from the ones referenced in ISO 13779-3 for HA coating crystallinity determination.

HA powder - fully crystallized reference compound			Plasma sprayed sample		
Peak	Area	2θ	Peak	Area	2θ
1	2497.3654	25.9589	1	1090.2097	25.6581
2	569.0688	28.1982	2	723.3473	27.9308
3	940.9781	29.0338	3	994.4709	28.8332
4	4605.8262	31.8412	4	2017.3676	31.6741
5	2251.1249	32.2757	5	1091.2291	32.0418
6	3029.3519	32.9776	6	1519.1379	32.8105
7	1092.7331	34.1474	7	826.9738	33.9134
8	1072.9971	39.8961	8	537.4177	39.7290
9	1327.8774	46.7811	9	814.5239	46.6141
10	1460.0468	49.5552	10	756.8199	49.3547
Total	18847.3698			10371.4979	

HA (h = 50 mm)			HA (h = 40 mm)			HA (h = 30 mm)		
Peak	Area	2θ	Peak	Area	2θ	Peak	Area	2θ
1	985.1460	25.7918	1	1037.7363	25.8586	1	621.4587	25.8252
2	415.6093	28.0645	2	462.6682	28.0645	2	215.5921	28.1313
3	777.2244	28.9001	3	699.6339	28.9335	3	555.3656	28.9001
4	1428.6129	31.7410	4	1432.9745	31.7410	4	1603.8306	31.7410
5	447.9789	32.1086	5	465.1581	32.1086	5	467.1635	32.1421
6	1065.8112	32.8439	6	1092.1315	32.8773	6	746.1080	32.8773
7	358.4734	33.9803	7	379.2789	33.9803	7	362.3672	34.0471
8	550.9204	39.7958	8	604.9479	39.7624	8	428.5104	39.7624
9	278.4766	46.6809	9	317.6979	46.6809	9	236.1135	46.6809
10	282.1698	49.4549	10	305.8162	49.4549	10	191.4109	49.4883
Total	6590.4230		Total	6798.0438		Total	5427.9203	

HA/MCD (h = 50 mm)			HA/MCD (h = 40 mm)			HA/MCD (h = 30 mm)		
Peak	Area	2θ	Peak	Area	2θ	Peak	Area	2θ
1	1196.8444	25.8587	1	1170.2901	25.7918	1	1199.0001	25.8252
2	502.2739	28.0645	2	479.3795	27.9977	2	504.0286	28.0979
3	994.0698	28.9335	3	993.8693	28.8667	3	1039.3239	28.8666
4	2333.4613	31.7410	4	2513.7591	31.7076	4	2622.0148	31.6741
5	445.1046	32.1755	5	437.11665	32.1088	5	455.4489	32.1086
6	1433.2921	32.8439	6	1471.6277	32.8439	6	1587.3031	32.8439
7	676.3050	34.0138	7	701.7563	33.9469	7	704.6641	33.9469
9	405.8666	46.6474	9	410.8799	46.5806	9	448.5973	46.6141
10	366.7287	49.4883	10	370.5724	49.3881	10	411.9996	49.3881
Total	8353.94647		Total	8549.2511		Total	8972.3804	

HA/Al ₂ O ₃ (h = 50 mm)			HA/Al ₂ O ₃ (h = 40 mm)			HA/Al ₂ O ₃ (h = 30 mm)		
Peak	Area	2 θ	Peak	Area	2 θ	Peak	Area	2 θ
1	678.7950	25.4910	1	704.1293	25.5578	1	700.2356	25.4910
2	415.1748	28.0311	2	413.7376	28.0645	2	413.5705	27.9977
3	581.0508	28.7998	3	585.5963	28.9001	3	599.4332	28.8666
4	1295.7751	31.6741	4	1265.3438	31.7410	4	1368.5693	31.7076
5	235.6790	32.1086	5	278.9445	32.1420	5	276.4712	32.1420
6	730.1320	32.8439	6	775.0352	32.8773	6	808.5079	32.8439
7	678.9956	34.8827	7	628.3269	34.8827	7	654.5469	34.8827
9	259.2753	46.6140	9	277.8916	46.6809	9	288.3362	46.6474
10	244.4190	49.4215	10	257.6711	49.4549	10	275.4686	49.4549
Total	5119.2966		Total	5186.6765		Total	5385.1395	

After integration of the present peaks, the calculated peaks areas were used to determine coating crystallinity in relation to the adopted standard crystalline standard (i.e. HA powder tablet), (Table 7.7).

Table 7.7 - Crystallinity (%) according to ISO13779-3. Values were calculated by summing the areas of the found peaks for each sample and dividing this value for the sum of the same peaks area of the crystalline reference.

Crystallinity (%)	HA	HA/MCD	HA/Al ₂ O ₃	HA powder	Plasma
h=50mm	34%	47%	29%	(Reference as if 100%)	55%
h=40mm	36%	48%	29%		
h=30mm	29%	50%	30%		

Intensity of I_{300} and intensity of the hollow between $V_{112/300}$, were easily detected for all XRD patterns. Crystallinity values obtained with this method are presented in Table 7.8.

Table 7.8 - Crystallinity values obtained according to equation (7.1).

Crystallinity (%)	HA	HA/MCD	HA/Al ₂ O ₃	HA powder	Plasma
h=50mm	69%	59%	58%	94%	76%
h=40mm	67%	58%	63%		
h=30mm	65%	61%	62%		

Identification of the crystallized phases was conducted by means of the largest peak for each expected phase. Five phases are identified in the standard ISO 13779-3 and the relevant d-spacing for the highest peak of each phase referenced (Table 7.9)

Table 7.9 - Highest peak of each phase to be identified if present in the samples analysed.

Compound	XRD Pattern	D-spacing	2 θ	Intensity
TTCP	JCPDS 25-1137	2.995	29.806	100
α -TCP	JCPDS 09-0348	2.905	30.752	100
β -TCP	JCPDS 09-0169	2.880	31.026	100
HA	JCPDS 09-0432	2.814	31.772	100
CaO	JCPDS 04-0169	2.405	37.346	100

To identify the presence of a phase the relevant d-spacing must be shown to be present. Straight lines were drawn for each d-spacing present on Table 7.9 on the XRD charts to detect the presence of each phase (Appendix F). From these, only the HA peak was present in all blasting conditions. When plasma sample XRD pattern was carefully observed, TTCP, α -TCP, β -TCP and CaO weak signals could be spot, in addition to the HA 31.77 (2 θ) intense peak.

MCD blasting media contains < 35% of α -TCP, β -TCP and TTCP. Since it is possible that some of this abrasive become impregnated into the surface during blasting, an effort was made to find other characteristic peaks of these phases on the HA/MCD coatings XRD signals. Any other characteristic peaks of these phases was found. HA/MCD coatings patterns were overlapped with the HA powder pattern. Apart from the Ti G5 (i.e. Ti-6Al-4V) peaks, all other peaks matched HA peaks (Appendix F). Even so, the intensity of the hollow between (112) and (300) diffraction peaks was higher than the one detected for the HA raw material powder. β -TCP has a characteristic peaks in this region, more precisely at 32.45 (2 θ). This increased intensity on the valley region can be due to the presence of this β -TCP peak. Nevertheless no other β -TCP peak was found. Consequently, it is likely that negligible or none MCD impregnation happened.

When HA/Al₂O₃ XRD signals were overlapped with HA powder XRD signal, Ti G5 peaks were highlighted. When a thorough analysis was done, peaks characteristic of Al₂O₃ were identified. This blasting media was clearly part of the coating obtained with HA/Al₂O₃ blasting for all nozzle height conditions. A stronger signal evident in the 57.49 (2 θ) region for a nozzle height of 50 mm may indicate that this Al₂O₃ inclusion was higher for this condition.

Moreover, when HA blasted surfaces XRD patterns were analysed HA and Ti G5 peaks were recognised. In addition, 57.49 (2 θ) peak was also present. This peak, characteristic from Al₂O₃, may indicate that Al₂O₃ was present in these surfaces. This is possible, since the equipment used to blast surfaces with HA was the same used to blast surfaces with HA/Al₂O₃. Although an effort was made to clean properly the equipment, Al₂O₃ become easily impregnated in the powder feeder components. Sometimes it necessary to brush firmly the spreader and suction unit to remove visible Al₂O₃ particles.

XRD results show that HA/MCD blasting condition resulted in better surface coverage than HA/Al₂O₃. This is in accordance with the previous results obtained with optical microscopy, where HA/Al₂O₃ blasted surfaces presented severe coating narrowed sections. Furthermore the ratio HA/Ti for HA blasted surfaces, was higher than HA/MCD blasted surfaces. Blasting the surface with HA alone may lead to Ti-6Al-4V greater surface coverage, but this

deposition, as seen in section 4.3, results in a weak interaction between the coating and the surface causing is an easy washable film.

Crystallinity results obtained for the XRD patterns of the samples analysed, following two different approaches, were different. When equation ((7.1) is used, all crystalline values found are above the specified limit of $> 45\%$. On the other hand, when the integration of peaks intensity proposed in ISO 13779-3 was used, only HA/MCD coatings and Plasma coatings fulfil the required specification.

In fact, using a HA tablet with an augmented thickness and no underlying titanium as crystalline reference for coatings of $<10\ \mu\text{m}$ thick with underlying titanium may not be the best approach to attain a feasible comparison between the XRD patterns of a CoBlast coating and a HA raw material powder. Appending to the different compaction level and thickness of both HA films, the noise and interference signal introduced by the presence of Ti-6Al-4V can help weaken and distort the HA signal.

Aside from energy resulting from mechanical impact of particles, no other apparent explanation could justify a decreasing on HA crystallinity when applied via CoBlast. Further tests shall be made to investigate this possibility.

Due to the thin coating layer deposited by CoBlast process ($<10\ \mu\text{m}$), samples exhibit peaks associated with titanium which are present due to the underlying Ti-6Al-4V substrate. Plasma coating does not exhibit the titanium peaks due the thicker coating of HA ($\approx 70\ \mu\text{m}$).

Although only HA peaks were detected in plasma XRD plot, when overlapped with HA powder raw material curve, an amorphous halo in the 27° and 32° (2θ) region can be detected on plasma-sprayed samples. The high cooling rate of the melted HA particles when deposited onto the metal substrate by plasma-spray, is once again detected. The presence of amorphous HA is undesirable since the amorphous HA dissolves faster *in vivo* when compared to crystalline HA phases. This can result in delamination of the coating (Ogiso et al., 1998).

7.2.2.5 Heavy metals coating content

Chemical analysis was carried out by XRF to spot the presence of heavy metals in the samples. ISO 13779-2 requires that samples content on heavy metals is less than a certain amount of mg/kg of Arsenic, Cadmium, Mercury and Lead and total heavy metals (Table 7.10).

Table 7.10 - Limits on heavy metals' content as stated on ISO 13779-2 for HA coatings

Element	mg/kg
As	< 3
Cd	< 5
Hg	< 5
Pb	< 30
Total Heavy Metals	< 50

Among the detected signals, Ti which was the strongest signal detected was promptly corrected and removed during XRF analysis. After its removal, % (w/w) of each element detected were normalized for a range of 0-100%. XRF results can be seen on Table 7.11.

Table 7.11 - Chemical elements detected using XRF analysis of samples coated using CoBlast with different nozzle heights. Strong grey highlighted elements appeared only on that condition of nozzle height. Light grey values were used to denote elements that do not appear in one of the neighbour nozzles heights. A plasma spray sample was analysed also. The indexes in brackets are the % (w/w) of that element in the sample.

50 mm	40 mm	30 mm
HA		
Mg (0.29)	Mg (0.33)	Mg (0.49)
Al (5.25)	Al (6.58)	Al (5.79)
Si (0.11)	Si (0.09)	P (31.8)
P (29.7)	P (31.5)	Ca (60.2)
Ca (60.5)	S (0.07)	Cr (0.94)
Cr (0.75)	Ca (59.3)	Fe (0.40)
Fe (0.64)	Cr (1.17)	Zr (0.08)
Ni (0.07)	Fe (0.59)	Mo (0.03)
Zr (2.19)	Zr (0.08)	Sn (0.32)
Nb (0.01)	Mo (0.04)	
Mo (0.04)	Sn (0.26)	
Sn (0.39)		

HA/MCD		
Mg (0.24)	Mg (0.36)	Mg (0.31)
Al (2.28)	Al (2.13)	Al (1.60)
Si (0.18)	Si (0.15)	Si (1.51)
P (29.4)	P (29.3)	P (28.9)
Ca (66.7)	S (0.04)	Ca (68.0)
Cr (0.58)	Ca (66.7)	Cr (0.59)
Fe (0.30)	Cr (0.49)	Fe (0.22)
Ni (0.05)	Fe (0.45)	Zr (0.05)
Zr (0.05)	Cu (0.07)	Nb (0.01)
Mo (0.03)	Zr (0.05)	Mo (0.02)
Sn (0.20)	Mo (0.02)	Sn (0.21)
	Sn (0.20)	

HA/Al ₂ O ₃		
Mg (0.16)	Mg (0.08)	Mg (0.16)
Al (21.2)	Al (21.1)	Al (20.6)
Si (0.09)	Si (0.16)	Si (0.09)
P (25.3)	P (25.8)	P (25.5)
Ca (51.9)	S (0.04)	Ca (52.5)
Cr (0.67)	Ca (51.6)	Cr (0.70)
Fe (0.31)	Cr (0.64)	Fe (0.32)
Ni (0.05)	Fe (0.24)	Ni (0.06)
Zr (0.06)	Cu (0.04)	Zr (0.06)
Nb (0.01)	Zr (0.05)	Mo (0.03)
Mo (0.03)	Nb (0.01)	Sn (0.09)
Sn (0.20)	Mo (0.03)	
	Sn (0.20)	

Plasma
Mg (0.13)
Si (0.04)
P (19.7)
S (0.02)
Ca (79.9)
Zr (0.02)
Mo (0.01)
Sn (0.09)

None of the analysed samples showed traces of heavy metals. The uncertainty associated with analytical XRF results makes the analysis of the % (w/w) values obtained a limited practise (Rousseau, 2001). Regardless the limited analysis of the % (w/w) of each element, the detection of the elements present is accurate. If any heavy metal element would be present in these samples it would be easily detected with this technique. As so, to assume

that no heavy metallic element was present in the analysed samples is a trustworthy assumption.

7.2.2.6 Coating adhesion

Coating adhesion testing was performed in accordance to ISO 13779-4. Five coated specimens were tested for both HA/MCD and HA/Al₂O₃ blasted samples with a nozzle height of 40 mm. Five specimens coated with a 60 µm HA plasma-sprayed layer were also tested. Specimens only glued with adhesive FM1000 only were used as control for the maximum stress that the adhesive can withstand when prepared according to this standard. Acquired results are presented in Table 7.12.

Table 7.12 - Adhesion tests performed according to ISO 13779-4 results. Results are expressed in MPa.

Sample number	HA/MCD	HA/Al ₂ O ₃	Plasma
Adhesive only	51.44	59.43	64.71
1	>51.44	>59.43	14.11
2	>51.44	>59.43	16.85
3	>51.44	>59.43	18.98
4	>51.44	>59.43	14.22
5	>51.44	>59.43	15.89
Average	>51.44	>59.43	16.01±1.65

Regarding the tensile bond strength of the HA layers, this experiment demonstrates that the coating adhesion of MCD treated samples is higher than 51.44 MPa and higher than 59.43 MPa for the Al₂O₃ treated samples. All samples tested ended up breaking with remaining adhesive on the coating side, which means that the tensile bond strength of the HA layers deposited with CoBlast is higher than the tensile bond strength of the glue. Even so, when specimens containing only adhesive were prepared they were firstly grit blasted with the blast media only for each condition. The increase in coating adhesion from >51.44 to >59.43 may be due to the increasing surface roughness produced by the alumina blast medium, which gives rise to a greater degree of mechanical interlock between the adhesive and titanium substrate.

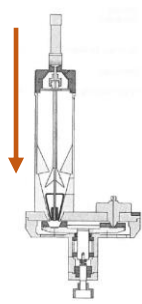
Although it was impossible to accurately measure the tensile bond strength of the HA layers CoBlast deposited, it is possible to say that the adhesion of these layers was more than the 15 MPa required by the standard 13779-2.

Trying two films of adhesive FM1000 as suggested on ASTM 1147 for highly porous coating, may be something to test in the future. Another suggestion may be trying another epoxy glue, with higher tensile bond strength.

7.3 Performance Qualification

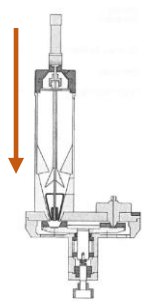
Short term process capability was accessed through roughness analysis. Samples coated over time with a nozzle height of 40 mm were used. Samples were coated until a full powder feeder hopper was totally spent. Roughness measurements results can be found on the following tables (Table 7.13, Table 7.14).

Table 7.13 - HA/MCD blasted surfaces over time roughness appraisal.



Sample	HA/MCD					
	Ra along x			Ra along y		
N1	1.378	1.112	1.032	1.286	1.118	1.167
N2	0.942	1.046	1.342	0.961	1.014	1.011
N3	1.153	0.980	1.241	1.359	1.344	1.108
N4	1.046	0.923	0.980	1.198	1.326	1.139
N5	1.405	0.970	1.130	1.047	1.249	1.066
N6	0.996	1.060	1.022	1.187	1.126	0.987
N7	1.057	1.122	1.288	1.264	1.157	1.268
N8	0.874	1.416	1.145	1.116	1.201	1.277

Table 7.14 - HA/Al₂O₃ blasted surfaces over time roughness appraisal.



Sample	HA/Al ₂ O ₃					
	Ra along x			Ra along y		
N1	2.937	3.161	3.215	3.049	2.867	3.025
N2	2.491	2.423	3.033	2.511	2.420	2.405
N3	2.370	2.927	2.257	2.724	2.616	2.432
N4	2.960	2.500	2.966	2.829	2.847	3.050
N5	2.874	2.671	3.001	3.361	2.580	3.421
N6	3.499	2.948	3.175	3.142	3.552	3.140
N7	3.375	2.283	3.104	3.310	2.886	2.887
N8	2.518	3.318	2.852	2.982	3.128	2.831

Coating roughness was measured along the direction of coating (i.e. along x axis) and against it (i.e. along y). Statistical analysis using two-way ANOVA revealed that there were no significant differences between surface roughness profile when measured along x and y axis. No roughness differences were found between the two coating directions for both HA/MCD and HA/Al₂O₃ blasted surfaces.

When samples roughness was compared from N1 to N8, no significant differences were found between HA/MCD blasted surfaces roughness profile, while for HA/Al₂O₃ blasted surfaces, N2 and N3 roughness profiles were significantly different from N6 ($p < 0.01$).

Although these roughness profiles are statistically different from each other, this difference can be an acceptable one. There is virtually no system capable of producing exactly the same output each time regardless of the input parameters chosen. Furthermore, there is always an error associated with the measurement of the evaluated features. This limits of tolerable differences are predicted by Statistical Process Control (SPC).

All processes have an acceptable limit of variation that is limited by a lower control limit (LCP) and an upper control limit (UCL). These limits can be calculated by using a Shewhart X-bar and R control chart for samples size with less than 10 measurements. If after building this chart, the process is visibly stable and consider to be in statistical control, only common causes of variation remain. This is evidenced on a control chart by the absence of data points beyond the control limits, and non-random patterns of variation.

Control limits (i.e. LCL and UCL) should not be mistaken with Specification limits (i.e. LSL and USL). Specification limits are indicated by ISO and FDA standards for HA medical coating, or by clients in the case of a feature that is not limited by any normative standardization or regulatory force, or even by the manufacturer.

Perhaps, a CoBlast coatings' client may request a coating thickness of $8 \pm 2 \mu\text{m}$, and a roughness profile of no less than $1 \mu\text{m}$ and no more than $10 \mu\text{m}$. These are two features that are not limited by HA coatings standards. In this case, thickness LSL is equal to $6 \mu\text{m}$ and USL is equal to $10 \mu\text{m}$, while roughness profile LSL is $1 \mu\text{m}$ and USL is $10 \mu\text{m}$. Also, when ISO 13779-2 requires a tensile bond strength of no less or equal than 15 MPa for HA coatings, the manufacturer shall yield this value as a coating tensile bond LSL.

Control limits, on other the hand, are determined using moderate complexity statistical tools, chosen according to the sample size, through analysis of a process products feature (e.g. thickness, roughness, crystalline content, heavy metals coating content, adhesion, and others). Sampled feature values end up being aligned in a control chart limited by calculated control limits, indicating which products are conform or non-conform (e.g. in or out of the control limits range). If all measured values are within the controls limits range and no random point is spotted, then the process is considered stable.

Process capability can only be studied afterwards, when the process is considered in statistical control (i.e. is stable), and is calculated using Specification Limits as stated in section 5.1.2.

In this study, software Minitab® 17 was used to calculate control limits, build the control charts, and determine process stability based on the roughness profile of samples of this routine production. The obtained control charts can be seen in Figure 7.15 and Figure 7.16.

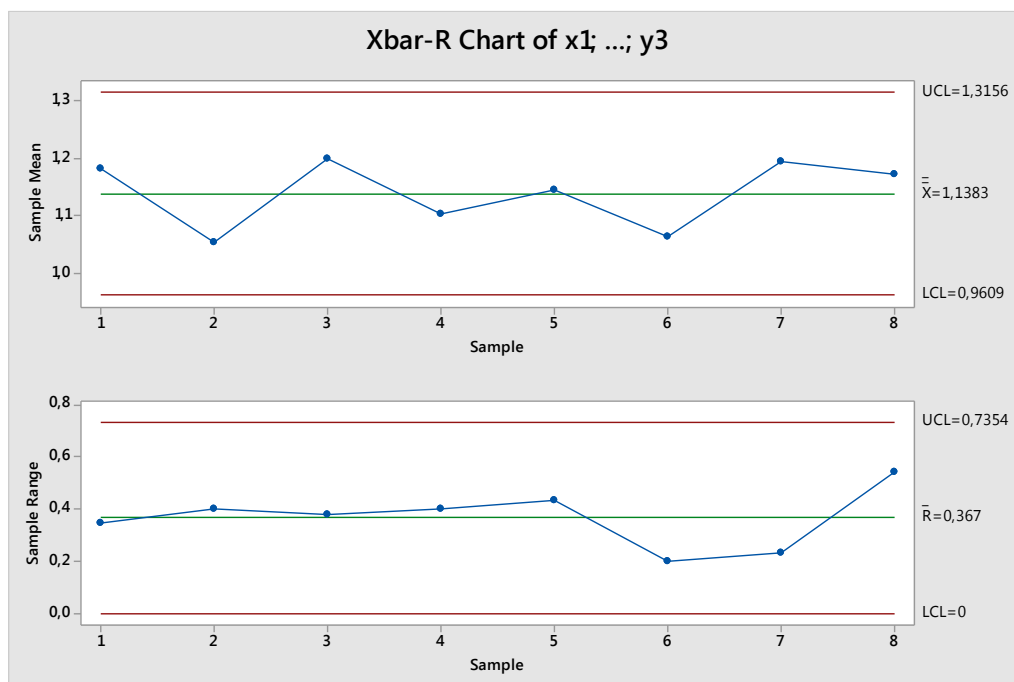


Figure 7.15 - Shewhart X-bar and R control chart of roughness profile of samples blasted over time with HA/MCD.

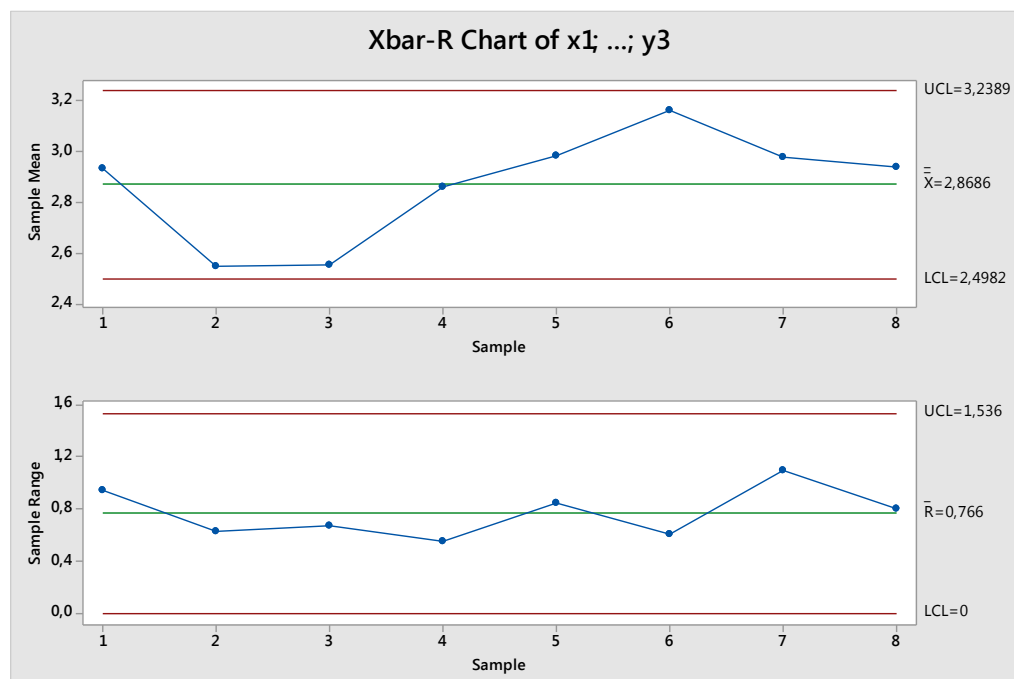


Figure 7.16 - Shewhart X-bar and R control chart of roughness profile of samples blasted over time with HA/Al₂O₃.

Since the process is in statistical control for both X-bar and R control charts for HA/MCD and HA/AL2O3, process capability can be studied for both blasting conditions. Specification limits for roughness profile are not normative. This capability study was made using a roughness LSL and USL of 1 μm and 10 μm respectively (Figure 7.17, Figure 7.18).

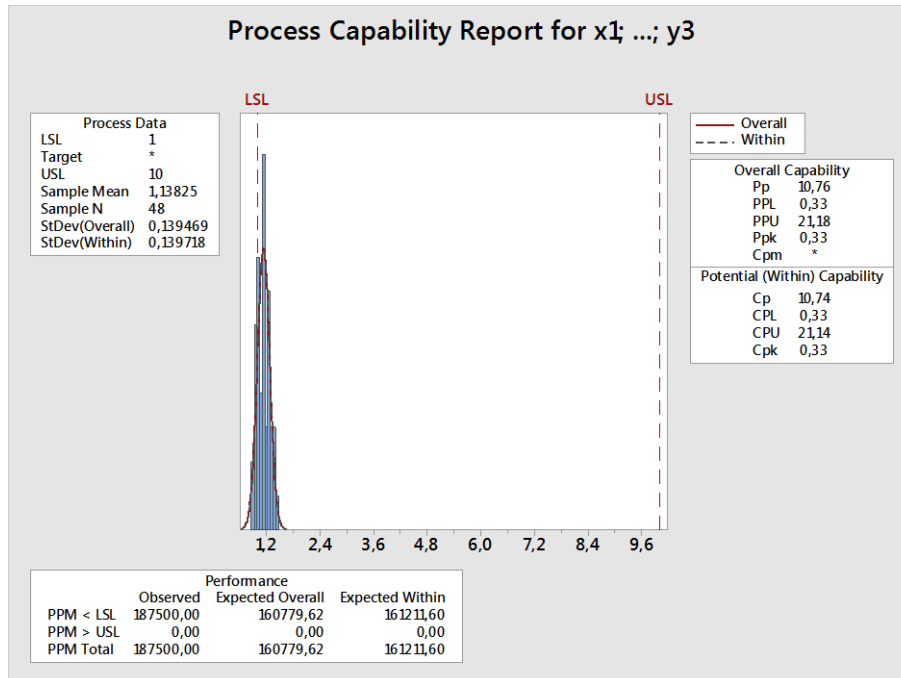


Figure 7.17 - Minitab® process capability report for roughness profile evaluation of HA/MCD blasted samples over time, with a LSL and a USL of 1 μm and 10 μm , respectively.

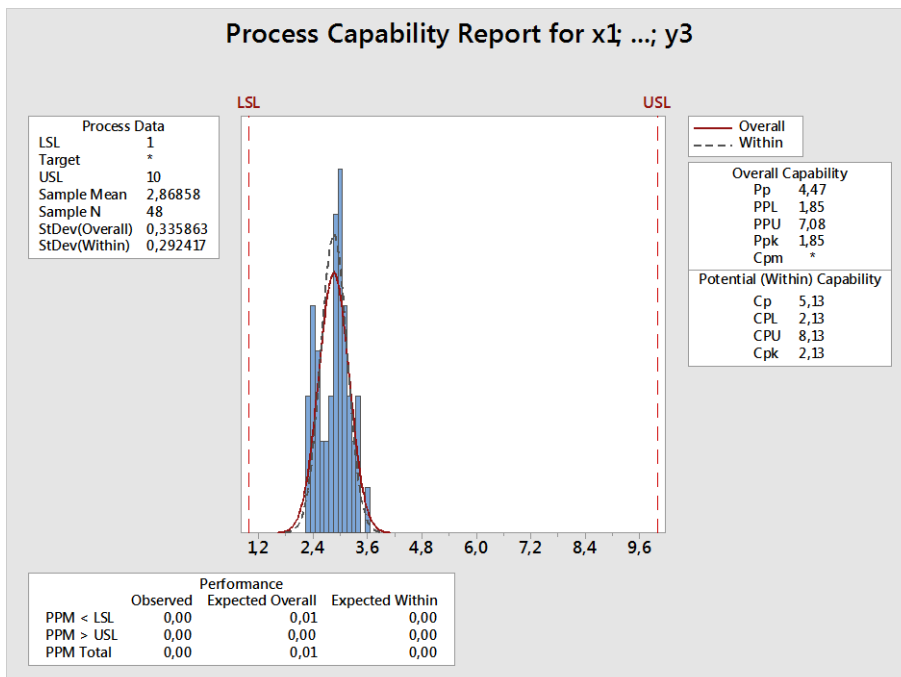


Figure 7.18 - Minitab® process capability report for roughness profile evaluation of HA/MCD blasted samples over time, with a LSL and a USL of 1 μm and 10 μm , respectively.

C_p is a process capability index calculated taking into account LSL, USL and standard deviation of the evaluated feature of samples. C_{pk} is another process capability index that requires LSL, USL, standard deviation and average value of the measured feature to be calculated. Both are used to evaluate process capability and the limit value from bad performance process to a good performance one is 1 for both. A value of 1.33 can be considered a reference value for which a process has a high degree of assurance of producing a conforming product.

Process capability evaluation of CoBlast using HA/MCD resulted in a $C_p = 10,74$ and a $C_{pk} = 0.33$. The large value found for C_p can be attributed to the small standard deviation of samples compared with range LSL-USL specified. This is the same as saying that the client allowed the manufacturer to produce a product with a broader range of roughness, but the controlled process is stable for a smaller one. Even so, this index fails in detecting were this smaller range is positioned in between the specification limits. Since some of the samples used to characterise and evaluate the process had roughness measurements of less than $1 \mu\text{m}$ (i.e. less than the specified LSL) it was expectable that the C_{pk} value would not be as good as desirable. The obtained C_{pk} of 0.33 reflects the proximity of the produced samples roughness profile average to the lower specification limit of $1 \mu\text{m}$ and, furthermore, it reflects the probability of a non-conform product arise from this process in terms of roughness profile specifications.

Process capability evaluation of CoBlast using HA/ Al_2O_3 resulted in a $C_p = 5.13$ and a $C_{pk} = 2.13$. CoBlast process was considered capable by both indexes, with values of more than 1.33. Since surfaces blasted with HA/ Al_2O_3 had a mean roughness value of $2.869 \mu\text{m}$ with a within standard deviation of $0.336 \mu\text{m}$, it was expectable that a both indexes would retrieve such good values taken into account the specification limits of LSL = $1 \mu\text{m}$ and USL = $10 \mu\text{m}$.

As a conclusion, the specification limits used in this evaluation can be different from the future values that the client will require, and this can alter the results of this performance evaluation. But more important than this, this evaluation showed that both HA/MCD and HA/ Al_2O_3 CoBlast processing are under statistical control. This means that both processes are stable by now and that adjusting them to the specification limits required hereafter should not be laborious. Perchance, if the client requires exactly the studied LSL of $1 \mu\text{m}$ for roughness, HA/MCD processing can be worked to meet this requirements by rising slightly the blasting pressure and revising the needed steps of the process validation here made.

7.3.1 Monitoring plan

A monitoring plan for CoBlast HA coated specimens of Ti-6Al-4V was made using concept of apparent density of bulk powders according to ISO 60 and ISO 697, roughness of surfaces following ISO 4287:1997 procedures and coatings thickness evaluation using an Elcometer 355 equipment.

Powders blending monitoring plan consists on sampling the HA/Abrasive mixture using the cup of 50 ml used on powders blending OQ, to sample bottom, middle and top of the produced bulk. Sampling involves collecting the amount of powder necessary to overflow the volume of the receiving cup and levelling it with a spatula such that it is completely full. Care must be taken not to compress or shake the powder. If the total weight of each of the three

cups plus collected bulk system is between the range of $\xi \pm 3\sigma$ (i.e. control limits) considering the measurements taken, there is no need for process re-validation.

Each time a new hopper is filled, three small coupons of Ti-6Al-4V must be coated using the same principle of action: sampling the effect of the bottom, middle and top bulk of the powder feeder hopper. Resultant coatings roughness shall be measured using a calibrated profilometer, if possible the one used to perform this study of validation, control charts shall be created. If this sampling still indicates that the process is in a state of control, no need for revising or process re-validation is needed.

Samples that were inspected for coating thickness using optical microscopy in OQ procedures were analysed previously using an Elcometer equipment calibrated for 0–12.6 μm coating's thickness detection. Elcometer 355 has great accuracy with a detection precision of $\pm 1\%$ or $1\mu\text{m}$. It acts by the principle of electromagnetic induction for non-magnetic coatings on magnetic substrates, and by eddy current principle for non-conductive coatings on non-ferrous metals substrates. Ninety-nine measurements performed on HA/MCD samples using this equipment retrieved a thickness value of $6.77 \pm 1.02 \mu\text{m}$. Analysing the data collected using the optical microscope, regardless of the nozzle height, HA/MCD coatings had a thickness of $6.06 \pm 1.37 \mu\text{m}$. Further studies shall be made using a control situation where a surface was only blasted with an abrasive particle, since the zero point used to calibrate the Elcometer at this point was smooth Ti-6Al-4V surface. The influence of the blasting effect (e.g. as seen before capable of creating jagged features on the substrate) shall be studied in order to certify in which conditions Elcometer can and cannot be used to evaluate CoBlast thickness. Yet, relating this preliminary results with the principle of action of the equipment, when calibrated within an acceptable range, Elcometer is probably a suitable equipment to monitor CoBlast coatings thickness. Thickness measurements shall be performed at least using the same principle of action described previously: sampling the effect of the bottom, middle and top bulk of the powder feeder hopper. A control chart shall be created. If it is under statistical control, there is no need for process revising or re-validation.

7.4 Internal procedures

An internal company designation for these sets of equipment was created so that they could take place in Ceramed's production equipment list. COB.01 is now Ceramed's internal designation for the set of equipment used to perform coBlasting of surfaces. COB.01.00 stands internally for Advanced Lathe LA-3250, COB.01.01 stands for Sulzer Metco Powder Feeder Single 10-C and PLA.06.01 stands for Sablex Universal Vacuum Cleaner. BLD.01 is the internal designation of the equipment used for powders blending. V-Blender is designated BLD.01.00, and Retsch Vibratory Feeder is BLD.01.01. These were named according to the internal company procedures. Productive equipment sheets were created as a result.

Furthermore, maintenance checklists and work instruction sheets (Appendix C) were created so that CoBlast processing can start once all conditions are met and Ceramed's management team desires.

7.5. Economic Evaluation

Launching a new product or service involves many steps. The first is to develop an economic analysis to determine whether there will be a profit or loss before starting production. If there is a projected profit based on the best available information, then a business plan should be developed.

It is important to know if there is a need or desire for the new product and if there is any existing alternative products already on the market. It is also good to determine the price range consumers will pay for the product and how this compares to the average cost to produce the product.

First, a cost analysis should be developed. The information needed to determine whether or not the product will make a profit over several years is based on average annual production costs and returns, also known as economic feasibility study. To estimate income potential, each new product should have a technical feasibility examination completed to ensure it can be produced in a form and at a cost acceptable to the consumer. On the other hand, any cost analysis will be only as good as the information used to estimate average costs per unit.

In this study, actual fixed and variable costs and expected production (Table 7.15) were used to estimate the cost per unit of a pedicle screw HA coating using HA/MCD or HA/Al₂O₃ to blast the surface. Once the market price and average cost per unit was calculated, these were used to estimate a cash flow analysis. This information will be useful to determine the feasibility of the initial investment by Ceramed and the amount of money needed for a successful over-the-years business continuation.

Table 7.15 - Economic factors taken into consideration in the economical evaluation made.

Fixed Costs	Variable Costs
<u>Depreciable</u>	<u>Labour Wages</u>
Equipment	Hourly rate per worker
<u>Non depreciable</u>	<u>Labour Non-wages</u>
Rent (per square meter)	Materials
	Equipment Repairs
Production	Utilities (e.g. electricity)
Units per year	

This study was made with Ceramed's real production costs such as equipment investment, raw materials cost practised by the suppliers, current energy costs per kWh of the company, packaging costs, and others. In order to preserve Ceramed's industrial privacy this data was not disclosed here and only major considerations and conclusions of this economical appraisal will be mentioned.

Initial investment was considered amortized after ten years. Part of the production line already in place at Ceramed would be used on CoBlast HA coating production (e.g. pre-clean pieces, quality control, post-clean pieces, packaging and expedition step). One worker and one auxiliary worker would be necessary to operate CoBlast and blending equipment, respectively. The equipment installed requires both electrical and pneumatic energy, which were both considered in the analysis. Furthermore, raw materials costs were taken into consideration, being the imported MCD the most expensive one.

Calculated cost per unit of a CoBlast HA coating of a pedicle screw was compared with a plasma sprayed HA coating of the same piece at Ceramed. Results show that for the production parameters in place, the initial cost per unit of a HA/Al₂O₃ blasted pedicle screw would be about 2 to 3 times cheaper than a plasma-sprayed one, and HA/MCD blasted pedicle screw would cost almost the same as a HA plasma-sprayed pedicle screw coating.

The economic potential of CoBlast processing against Plasma-spray lies on the energy necessary to put the process in place. Plasma-spray requires high amounts of energy to electrical heat industrial gases and to extract the inner chamber wastes and heat, while CoBlast works under room temperature and requires a conventional vacuum cleaner only.

Regarding the similarity of costs between HA/MCD blasted pedicle and HA plasma-sprayed pedicle screws, the major conclusions are that although the costs of MCD are high, several production steps and energy are spared with CoBlast, and the reason why final costs of both products are similar lies on the high mass flow rate currently used on CoBlast processing.

Mass flow rate optimization shall be made to search the minimum value for which coating coverage and features are not destructively affected. Furthermore wasted powder particles saving and recycling shall be considered.

References

2009. Warning Letters - Hammill Manufacturing Company 1/06/09.
- Ceramed 2015a. Available from <http://www.ceramed.pt/>.
- Ceramed | Partnerships 2015b. Available from <http://www.ceramed.pt/parcerias>.
- Enbio | About the Company 2015c. Available from <http://enbio.eu/enbio>.
- Enbio | Coblast Clean metal coating process: solvent free, low energy 2015d. Available from <http://www.enbio.eu/coblast>.
- Enbio | Industries 2015e. Available from <http://www.enbio.eu/industries>.
- Enbio | Redefining performance, function, value of metals | News 2015f. Available from <http://enbio.eu/news>.
- Albrektsson, T, and C Johansson. 2001. "Osteoinduction, osteoconduction and osseointegration." *European Spine Journal* no. 10 (2):S96-S101.
- Barry, JN, and Denis P Dowling. 2012. "Comparison between the SBF response of hydroxyapatite coatings deposited using both a plasma-spray and a novel co-incident micro-blasting technique." *Key Engineering Materials* no. 493:483-488.
- Barry, JN, Barry Twomey, A Cowley, Liam O'Neill, Patrick J McNally, and Denis P Dowling. 2013. "Evaluation and comparison of hydroxyapatite coatings deposited using both thermal and non-thermal techniques." *Surface and Coatings Technology* no. 226:82-91.
- Bilezikian, John P, Lawrence G Raisz, and T John Martin. 2008. *Principles of Bone Biology: Two-Volume Set*: Academic Press.
- Birka, Mark P, Timothy F O'brien, and Judson H Whiteside. 2012. Gas/plasma spray coating. Google Patents.
- Boccaccini, AR, S Keim, R Ma, Y Li, and I Zhitomirsky. 2010. "Electrophoretic deposition of biomaterials." *Journal of The Royal Society Interface* no. 7 (Suppl 5):S581-S613.
- Bodo, Maria, Cinzia Lilli, Catia Bellucci, Paolo Carinci, Mario Calvitti, Furio Pezzetti, Giordano Stabellini, Silvia Bellocchio, Chiara Balducci, and Francesco Carinci. 2002. "Basic fibroblast growth factor autocrine loop controls human osteosarcoma phenotyping and differentiation." *Molecular medicine* no. 8 (7):393.
- Borsari, Veronica, Gianluca Giavaresi, Milena Fini, Paola Torricelli, Armando Salito, Roberto Chiesa, Loris Chiusoli, Andreas Volpert, Lia Rimondini, and Roberto Giardino. 2005. "Physical characterization of different-roughness titanium surfaces, with and without hydroxyapatite coating, and their effect on human osteoblast-like cells." *Journal of Biomedical Materials Research Part B: Applied Biomaterials* no. 75 (2):359-368.
- Brone, Dean, Albert Alexander, and FJ Muzzio. 1998. "Quantitative characterization of mixing of dry powders in V-blenders." *AIChE journal* no. 44 (2):271-278.
- Busscher, Henk J, Henny C van der Mei, Guruprakash Subbiahdoss, Paul C Jutte, Jan JAM van den Dungen, Sebastian AJ Zaat, Marcus J Schultz, and David W Grainger. 2012. "Biomaterial-associated infection: locating the finish line in the race for the surface." *Science translational medicine* no. 4 (153):153rv10-153rv10.
- Byrne, Greg D, Liam O'Neill, Barry Twomey, and Denis P Dowling. 2013. "Comparison between shot peening and abrasive blasting processes as deposition methods for hydroxyapatite coatings onto a titanium alloy." *Surface and Coatings Technology* no. 216:224-231.

- Capello, William N, James A D'Antonio, William L Jaffe, Rudolph G Geesink, Michael T Manley, and Judy R Feinberg. 2006. "Hydroxyapatite-coated femoral components: 15-year minimum followup." *Clinical orthopaedics and related research* no. 453:75-80.
- Davis, J.R., and A.S.M.I.T.S.S.T. Committee. 2004. *Handbook of Thermal Spray Technology*: ASM International.
- Dobkin, D., and M.K. Zuraw. 2003. *Principles of Chemical Vapor Deposition*: Springer.
- DOD, US, and Deputy under secretary for defense for science and technology (DUSD(S&T)). 2003. Technology readiness assessment (TRA) deskbook.
- Dorozhkin, Sergey V. 2007. "Calcium orthophosphates." *Journal of materials science* no. 42 (4):1061-1095.
- Dorozhkin, Sergey V. 2009. "Calcium orthophosphates in nature, biology and medicine." *Materials* no. 2 (2):399-498.
- Dorozhkin, Sergey V. 2011. "Calcium orthophosphates: occurrence, properties, biomineralization, pathological calcification and biomimetic applications." *Biomatter* no. 1 (2):121-164.
- Dorozhkin, Sergey V. 2012. "Calcium orthophosphate coatings, films and layers." *Prog Biomater* no. 1:1-40.
- Dorozhkin, Sergey V. 2013. "A detailed history of calcium orthophosphates from 1770s till 1950." *Materials Science and Engineering: C* no. 33 (6):3085-3110.
- Dunne, Conor F, Barry Twomey, Ciara Kelly, Jeremy C Simpson, and Kenneth T Stanton. 2015. "Hydroxyapatite and fluorapatite coatings on dental screws: effects of blast coating process and biological response." *Journal of Materials Science: Materials in Medicine* no. 26 (1):1-14.
- Dunne, Conor F, Barry Twomey, Liam O'Neill, and Kenneth T Stanton. 2013. "Co-blasting of titanium surfaces with an abrasive and hydroxyapatite to produce bioactive coatings: Substrate and coating characterisation." *Journal of biomaterials applications*:0885328213480534.
- Dunne, Conor F, Barry Twomey, and Kenneth T Stanton. 2015. "Effect of a blast coating process on the macro-and microstructure of Grade 5 titanium foam." *Materials Letters* no. 147:75-78.
- ECDC, European Centre of Disease prevention and Control. 2007. Surveillance of healthcare-associated infections in Europe. http://www.ecdc.europa.eu/en/publications/Publications/120215_SUR_HAI_2007.pdf
- Fauchais, P. 2004. "Understanding plasma spraying." *Journal of Physics D: Applied Physics* no. 37 (9):R86.
- FDA, U.S. Food and Drug Administration. 2011. Guidance for Industry: Process Validation: General Principles and Practices. <http://www.fda.gov/downloads/Drugs/Guidances/UCM070336.pdf>.
- Fleming, David, Liam O'Neill, Greg Byrne, Nicholas Barry, and Denis P Dowling. 2011. "Wear resistance enhancement of the titanium alloy Ti-6Al-4V via a novel co-incident microblasting process." *Surface and Coatings Technology* no. 205 (21):4941-4947.
- GHTF, Study Group 3. 2004. Quality Management Systems - Process Validation Guidance. In *GHTF/SG3/N99-10*, edited by The Global Harmonization Task Force.
- Gristina, Anthony G. 1987. "Biomaterial-centered infection: microbial adhesion versus tissue integration." *Science* no. 237 (4822):1588-1595.
- Hasegawa, Toru, Akihiko Inufusa, Yoshiyuki Imai, Yoshihiro Mikawa, Tae-Hong Lim, and Howard S An. 2005. "Hydroxyapatite-coating of pedicle screws improves resistance against pull-out force in the osteoporotic canine lumbar spine model: a pilot study." *The spine journal* no. 5 (3):239-243.
- Hong, Zhendong, Lan Luan, Se-Bum Paik, Bin Deng, Donald E Ellis, John B Ketterson, Alexandre Mello, Jean G Eon, Joice Terra, and Alexandre Rossi. 2007. "Crystalline hydroxyapatite thin films produced at room temperature—An opposing radio frequency magnetron sputtering approach." *Thin Solid Films* no. 515 (17):6773-6780.
- Ishikawa, Kunio, Youji Miyamoto, Masaru Nagayama, and Kenzo Asaoka. 1997. "Blast coating method: New method of coating titanium surface with hydroxyapatite at room temperature." *Journal of biomedical materials research* no. 38 (2):129-134.

- Kang, S.J.L. 2004. *Sintering: Densification, Grain Growth and Microstructure*: Elsevier Science.
- Keady, F, and BP Murphy. 2013. "Investigating the feasibility of using a grit blasting process to coat nitinol stents with hydroxyapatite." *Journal of Materials Science: Materials in Medicine* no. 24 (1):97-103.
- Klein, CPAT, P Patka, JGC Wolke, JMA de Blicck-Hogervorst, and K De Groot. 1994. "Long-term in vivo study of plasma-sprayed coatings on titanium alloys of tetracalcium phosphate, hydroxyapatite and α -tricalcium phosphate." *Biomaterials* no. 15 (2):146-150.
- Kotz, S., and N.L. Johnson. 1993. *Process Capability Indices*: Taylor & Francis.
- Kurella, Anil, and Narendra B Dahotre. 2005. "Review paper: surface modification for bioimplants: the role of laser surface engineering." *Journal of biomaterials applications* no. 20 (1):5-50.
- Landi, E, A Tampieri, G Celotti, and S Sprio. 2000. "Densification behaviour and mechanisms of synthetic hydroxyapatites." *Journal of the European Ceramic Society* no. 20 (14):2377-2387.
- Mankins, John C. 2009. "Technology readiness assessments: A retrospective." *Acta Astronautica* no. 65 (9):1216-1223.
- Maruyama, Toru, and Katsushi Takeshita. 2008. "Surgical treatment of scoliosis: a review of techniques currently applied." *Scoliosis* no. 3 (6):1-6.
- Mattox, D.M. 2010. *Handbook of Physical Vapor Deposition (PVD) Processing*: Elsevier Science.
- O'donoghue, J.G., and D. Haverty. 2008. Method of doping surfaces. Google Patents.
- O'Hare, Peter, Brian J Meenan, George A Burke, Greg Byrne, Denis Dowling, and John A Hunt. 2010. "Biological responses to hydroxyapatite surfaces deposited via a co-incident microblasting technique." *Biomaterials* no. 31 (3):515-522.
- O'Neill, L, C O'Sullivan, P O'Hare, L Sexton, F Keady, and J O'Donoghue. 2009. "Deposition of substituted apatites onto titanium surfaces using a novel blasting process." *Surface and Coatings Technology* no. 204 (4):484-488.
- O'Sullivan, C, P O'Hare, ND O'Leary, AM Crean, K Ryan, ADW Dobson, and L O'Neill. 2010. "Deposition of substituted apatites with anticolonizing properties onto titanium surfaces using a novel blasting process." *Journal of Biomedical Materials Research Part B: Applied Biomaterials* no. 95 (1):141-149.
- O'Sullivan, Caroline, Peter O'Hare, Greg Byrne, Liam O'Neill, Katie B Ryan, and Abina M Crean. 2011. "A modified surface on titanium deposited by a blasting process." *Coatings* no. 1 (1):53-71.
- Ogiso, Makoto, Yasuo Yamashita, and Toshio Matsumoto. 1998. "Microstructural changes in bone of HA-coated implants." *Journal of biomedical materials research* no. 39 (1):23-31.
- Pandey, R. K., S. N. Sahu, and Suresh Chandra. 1996. *Handbook of Semiconductor Electrodeposition*: Taylor & Francis.
- Pawlowski, L. 2008. *The Science and Engineering of Thermal Spray Coatings*: Wiley.
- Radin, SR, and P Ducheyne. 1992. "Plasma spraying induced changes of calcium phosphate ceramic characteristics and the effect on in vitro stability." *Journal of materials science: Materials in medicine* no. 3 (1):33-42.
- Rousseau, Richard M. 2001. "Detection limit and estimate of uncertainty of analytical XRF results." *The Rigaku Journal* no. 18 (2):33-47.
- Singhai, Sanjay K., V. S. Chopra, Mona Nagar, Nilesh Jain, and Piyush Trivedi. 2010. Scale Up factor determination of V Blender: An over view.
- Sun, Limin, Christopher C Berndt, Karlis A Gross, and Ahmet Kucuk. 2001. "Material fundamentals and clinical performance of plasma-sprayed hydroxyapatite coatings: a review." *Journal of biomedical materials research* no. 58 (5):570-592.
- Taguchi, Genichi, and Don Clausing. 1990. "Robust quality." *Harvard Business Review* no. 68 (1):65-75.
- Tan, Fei, Mariam Naciri, and Mohamed Al-Rubeai. 2011. "Osteoconductivity and growth factor production by MG63 osteoblastic cells on bioglass-coated orthopedic implants." *Biotechnology and bioengineering* no. 108 (2):454-464.

- Tan, Fei, Mariam Naciri, Denis Dowling, and Mohamed Al-Rubeai. 2012. "In vitro and in vivo bioactivity of CoBlast hydroxyapatite coating and the effect of impaction on its osteoconductivity." *Biotechnology advances* no. 30 (1):352-362.
- Thomas, Meurig, Trevor Lindley, Dave Rugg, and Martin Jackson. 2012. "The effect of shot peening on the microstructure and properties of a near-alpha titanium alloy following high temperature exposure." *Acta Materialia* no. 60 (13):5040-5048.
- Upasani, Vidyadhar V, Christine L Farnsworth, Tucker Tomlinson, Reid C Chambers, Shunji Tsutsui, Michael A Slivka, Andrew T Mahar, and Peter O Newton. 2009. "Pedicle screw surface coatings improve fixation in nonfusion spinal constructs." *Spine* no. 34 (4):335-343.
- Veselov, Vladimir, Helen Roytman, and Lori Alquier. 2012. "Medical Device Regulations for Process Validation: Review of FDA, GHTF, and GAMP Requirements." *Journal of Validation Technology* no. 18 (2).
- Wang, Lijun, and George H Nancollas. 2008. "Calcium orthophosphates: crystallization and dissolution." *Chemical reviews* no. 108 (11):4628-4669.
- Wasa, K. 2012. *Handbook of Sputter Deposition Technology: Fundamentals and Applications for Functional Thin Films, Nano-materials and MEMS*: William Andrew.
- WHO, World Health organisation. 2012. Healthcare-associated infections. http://www.who.int/gpsc/country_work/gpsc_ccisc_fact_sheet_en.pdf.
- Wright, J.D., and N.A.J.M. Sommerdijk. 2000. *Sol-Gel Materials: Chemistry and Applications*: Taylor & Francis.
- Xu, H., and H. Guo. 2011. *Thermal Barrier Coatings*: Elsevier Science.
- Yang, Sen, HC Man, Wen Xing, and Xuebin Zheng. 2009. "Adhesion strength of plasma-sprayed hydroxyapatite coatings on laser gas-nitrided pure titanium." *Surface and Coatings Technology* no. 203 (20):3116-3122.
- Zeng, Haitong, and William R Lacefield. 2000. "XPS, EDX and FTIR analysis of pulsed laser deposited calcium phosphate bioceramic coatings: the effects of various process parameters." *Biomaterials* no. 21 (1):23-30.
- Zhang, Bill GX, Damian E Myers, Gordon G Wallace, Milan Brandt, and Peter FM Choong. 2014. "Bioactive Coatings for Orthopaedic Implants—Recent Trends in Development of Implant Coatings." *International journal of molecular sciences* no. 15 (7):11878-11921.

Standards and regulations

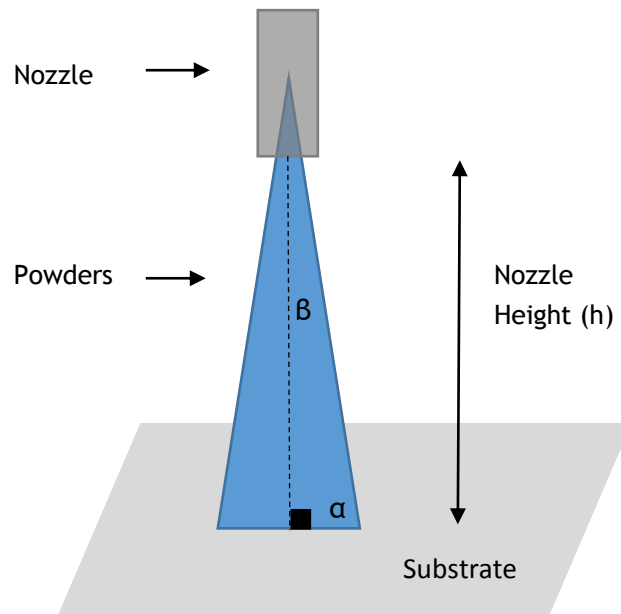
- FDA 21 CFR 820.3, Quality System Regulation: General Provisions - Definitions
- FDA 21 CFR 820.70, Quality System Regulation: Production and Process Controls - Production and process controls
- FDA 21 CFR 820.75, Quality System Regulation: Production and Process Controls - Process Validation
- ISO 9001:2008, Quality Managements Systems - Requirements
- ISO 13485:2012, Medical devices - Quality management Systems - Requirements for regulatory purposes. (7.5.2, Validation of processes for production and service provision.)
- ISO 13779-1:2008, Implants for surgery - Hydroxyapatite - Part 1: Ceramic hydroxyapatite
- ISO 13779-2:2008, Implants for surgery - Hydroxyapatite - Part 2: Coatings of hydroxyapatite
- ISO 13779-3:2008, Implants for surgery - Hydroxyapatite - Part 3: Chemical analysis and characterization of crystallinity and phase purity
- ISO 13779-4:2002, Implants for surgery - Hydroxyapatite - Part 4: Determination of coating adhesion strength
- ISO 4287:1997, Geometrical Product Specifications (GPS) - Surface texture: Profile method - Terms, definitions and surface texture parameters

- ISO 4288:1996, Geometrical Product Specifications (GPS) – Surface texture: Profile method – Rules and procedures for the assessment of surface texture
- ASTM F1147-05(2011), Standard Test Method for Tension Testing of Calcium Phosphate and Metallic Coatings
- ASTM F1185-03(2014), Standard Specification for Composition of Hydroxyapatite for Surgical Implants
- ASTM F603-12, Standard Specification for High-Purity Dense Aluminum Oxide for Medical Application
- ISO 60, Plastics -- Determination of apparent density of material that can be poured from a specified funnel
- ISO 697, Surface active agents – Washing powders – Determination of apparent density – Method by measuring the mass of a given volume
- ASTM F136-02a, Standard Specification for Wrought Titanium-6 Aluminum-4 Vanadium ELI (Extra Low Interstitial) Alloy for Surgical Implant Applications (UNS R56401)
- ASTM F67-06, Standard Specification for Unalloyed Titanium, for Surgical Implant Applications (UNS R50250, UNS R50400, UNS R50550, UNS R50700)
- ASTM B348-06a, Standard Specification for Titanium and Titanium Alloy Bars and Billets

Appendix A

Calculations

Raster Offset determination for each nozzle height



Nozzle exit diameter (d_1)	2.66 mm	} Known start parameters
Base diameter (d_2)	3.3 mm	
h	50 mm	

$$\alpha = \tan^{-1} \frac{h}{d_2/2} = 88.11^\circ, \quad h = 50 \text{ mm}$$

$$\beta = 90^\circ - \alpha = 1.89^\circ$$

$$h = \frac{d_1}{2} \times \sin \beta$$

$$d_2 = \sqrt{\frac{d_1^2}{2} - h^2}$$

Total half triangle measures can be now calculated (total height (H) is the height until reaching the De Laval nozzle constriction).

$$H = h + \frac{d_2}{\sin \beta} = 90,3 \text{ mm}$$

$$\beta = \tan^{-1} \frac{d_2/2}{H}$$

$$R = 2 \times (H - 50 + h) \times \tan \beta$$

$$R = 3,3 \text{ mm} \quad , \quad h = 50 \text{ mm}$$

$$R = 2,9 \text{ mm} \quad , \quad h = 40 \text{ mm}$$

$$R = 2,6 \text{ mm} \quad , \quad h = 50 \text{ mm}$$

Appendix B

Equipment IQ checklists

CoBlast equipment IQ checklists

The following checklists were created to guide IQ procedures of CoBlast equipment installed.

System identification checklist

Purpose: List all system specifications and check them.

Equipment		Yes	No
Comco LA3250 Advanced Lathe			
Model	LA3250 - 29		
Serial No.	---		
Pressure min-max.	620 - 965 kPa (6.2 - 9.6 bar)		
Electrical connection	115 VAC, 50/60 Hz		
Transformer	220-240 VAC		
Power Input	400 W		
Air Input	198 l/min		
Software Version	Comco User Interface V 12.2		
	Comco Galil Service V 10.2		
	Comco Serial Service V 2.0		
	Comco Axis Control Utility V 7.0		
	Comco Bus Control Utility V 1.3		
Sulzer Metco Powder Feeder Single 10-C			
Model	Single 10-C		
Serial No.	---		
Pressure min-max.	0 - 400 kPa (0 - 4 bar)		
RPM min-max.	0 - 10 rpm		
Flow rate	0 - 10 l/min		
Electrical connection	230 VAC, 50 Hz		
Power Input	250 W		
Sablex Universal Vacuum Cleaner			
Model	Sablex Universal		
Serial No.	---		
Flow rate	600 m ³ /h		
Electrical connection	220 VAC, 50/60 Hz		
Power Input	550 W		

Declaration:

Systems are identified and specifications verified.	Yes	No
---	-----	----

Remarks:	
----------	--

Components identification checklist

Purpose: Identify and verify the availability of the equipment components.

Equipment	Available?	
	Yes	No
Comco LA3250 Advanced Lathe		
Air drier AD5300		
Mandril part tooling size 1		
Mandril part tooling size 1 (2)		
Mandril part tooling size 2		
Platform part tooling		
Sulzer Metco Powder Feeder Single 10-C		
Powder hopper of 1100 cm ³		

Declaration:

The components are identified and available.	Yes	No
Remarks:		

Consumables identification checklist

Purpose: Identify and verify the availability of the consumable components.

Equipment	Available?	
	Yes	No
Comco LA3250 Advanced Lathe		
Inside chamber halogen lamp		
Air filter		
Sulzer Metco Powder Feeder Single 10-C		
Spreader		
Suction unit		
Universal Vacuum Cleaner		
Air filter		

Declaration:

The consumables are identified and available.	Yes	No
---	-----	----

Remarks:	
----------	--

Documentation checklist

Purpose: To ensure that the necessary documentation for production with this equipment is correct and complete.

Equipment	Available?	
	Yes	No
Comco LA3250 Advanced Lathe		
Operating instructions		
Declaration of conformity by the manufacturer		
Sulzer Metco Powder Feeder Single 10-C		
Operating instructions		
Declaration of conformity by the manufacturer		
Universal Vacuum Cleaner		
Operating instructions		
Declaration of conformity by the manufacturer		

Declaration:

System documentation required is correct and available.	Yes	No
Remarks:		

System damages checklist

Purpose: To report any type of system damage.

Equipment	Damaged?	
	Yes	No
Comco LA3250 Advanced Lathe		
Is there any component or consumable damaged in this item?		
Sulzer Metco Powder Feeder Single 10-C		
Is there any component or consumable damaged in this item?		
Universal Vacuum Cleaner		
Is there any component or consumable damaged in this item?		

Declaration:

The equipment, components and consumables are free of visible damage?		Yes	No
Remarks:			

System installation checklist

Purpose: To determine if the system is placed properly with correct wiring and utilities available.

Equipment	Specification fulfilled?	
	Yes	No
Comco LA3250 Advanced Lathe		
Is the equipment properly connected to company's air system without any visible defect?		
Is the electrical connection made using a 220-240V transformer?		
Is the pressure regulator working properly from 0 to 1000 kPa?		
Sulzer Metco Powder Feeder Single 10-C		
Is the equipment properly connected to company's air system without any visible defect?		
Is the single phase electrical connection correctly made?		
Is the powder connection made between the powder exit and Comco LA 3250 Advanced Lathe single nozzle entry?		
Is the pressure regulator working properly from 0 to 400 kPa?		
Universal Vacuum Cleaner		
Is the three phase electrical connection correctly made?		
Is the air connection with the Comco LA 3250 Advanced Lathe collar made, and using an appropriate duct?		

Declaration:

Installation of CoBlast equipment is complete and correct		Yes	No
Remarks:			

User Interface Menu Settings Checklist

Purpose: To ensure the user interface comes with the specified settings.

Equipment	Setting fulfilled?	
	Yes	No
Comco LA3250 Advanced Lathe		
Does the software language is English?		
Does the user interface exhibits a time countdown when a coating program is at work?		
Does the STOP button stops the program and returns the axis to home position?		
Does the START button re-starts the coating program?		

Declaration:

All user interface important features are implemented properly.	Yes	No
Remarks:		

Blending equipment IQ checklists

The following checklists were created to guide IQ procedures of Blending equipment installed.

System identification checklist

Purpose: List all system specifications and check them.

Equipment	Yes		No	
	V-Blender			
Model	90 ° V-blender			
Serial No.	---			
Speed	20 RPM			
Electrical connection	230 VAC, 50/60 Hz			
Power Input	90 W			
Retsch Vibratory Feeder				
Model	DR 15/40			
Serial No.	---			
Frequency	50 - 60 Hz			

Declaration:

Systems are identified and specifications verified.		Yes	No
Remarks:			

Components identification checklist

Purpose: Identify and verify the availability of the equipment components.

Equipment	Available?	
	Yes	No
Retsch Vibratory Feeder		
Chute		
Hopper		

Declaration:

The components are identified and available.		Yes	No
Remarks:			

Documentation checklist

Purpose: To ensure that the necessary documentation for production with this equipment is correct and complete.

Equipment	Available?	
	Yes	No
V-Blender		
Operating instructions		
Retsch Vibratory Feeder		
Operating instructions		
Declaration of conformity by the manufacturer		

Declaration:

System documentation required is correct and available.	Yes	No
Remarks:		

System damages checklist

Purpose: To report any type of system damage.

Equipment	Damaged?	
	Yes	No
V-Blender		
Is there any visible damage in this item?		
Retsch Vibratory Feeder		
Is there any component damaged in this item?		

Declaration:

The equipment and components are free of visible damage?	Yes	No
Remarks:		

System installation checklist

Purpose: To determine if the system is placed properly with correct wiring and utilities available.

Equipment	Specification fulfilled?	
	Yes	No
V-Blender		
Is the system placed on a horizontal and planar surface?		
Is the horizontal axis drilled in the correct central position?		
Is the three phase electrical connection correctly made?		
Does the blender cover insulates it efficiently?		
Retsch Vibratory Feeder		
Is the system placed on a horizontal and planar surface?		
Is the single phase electrical connection correctly made?		
Does the power button and switchers work properly?		

Declaration:

Installation of Blending equipment is complete and correct.	Yes	No
Remarks:		

Result of IQ checklist

Overall result IQ check list

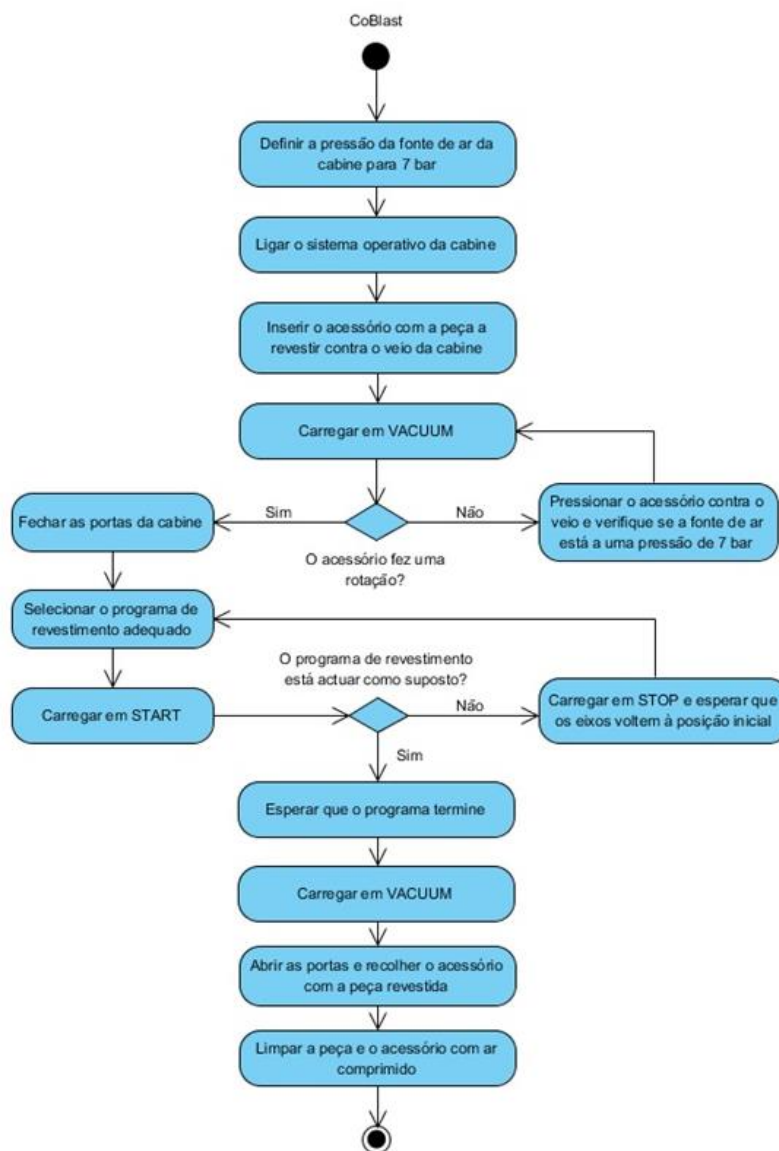
Purpose: List all the parameters evaluated in IQ. Confirm that all were executed and conclude about its success.

IQ result	Check carried out successfully?	
	Yes	No
System identification checklist		
Components identification checklist		
Documentation of conformity checklist		
Consumables identification checklist		
System damages checklist		
System installation checklist		
User interface checklist		

Appendix C

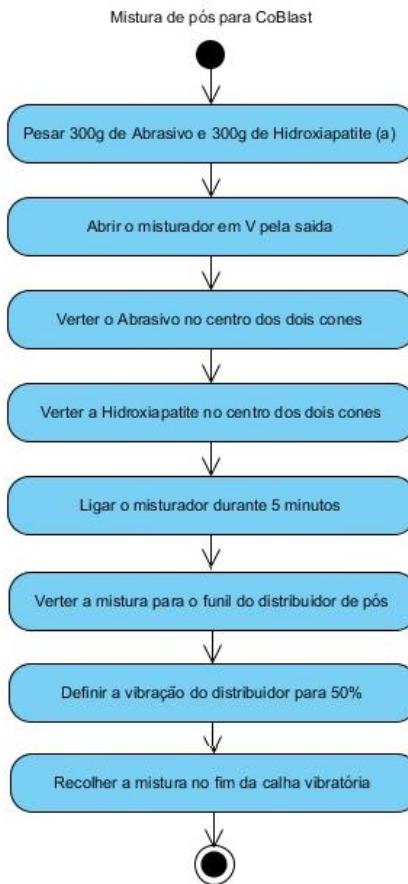
Production Internal documentation

Work instructions



ELABORADO: _____ APROVADO: _____ DATA: ____/____/____

	INSTRUÇÃO DE TRABALHO MISTURA DE PÓS PARA COBLAST
---	---



(a) A hidroxiapatite utilizada deve ter um tamanho de partícula entre 20 – 60 μm e o abrasivo deve ser < 180 μm .

ELABORADO: _____ APROVADO: _____ DATA: ____/____/____

Appendix D

Raw material Certificates of Compliance

Ti-6Al-4V compliance certificate

CERTIFICATE OF CONFORMITY



Certificate NO.TC 07/03010

Applicant: Baoji Tidu Nonferrous Metals Co., Ltd

Applicant Address: Gaoxin Development East Zoon, Baoji City, Shanxi, China

Manufacturer: Baoji Tidu Nonferrous Metals Co., Ltd

Manufacturing Site: Gaoxin Development East Zoon, Baoji City, Shanxi, China

Product Name: Titanium Stick

Model No. : TC4 GR2
TA1 GR1
TA1,TA2,GR1,GR2,GR4,GR5

THE TEST REPORT

Technical Construction File: TR07032002 TR07032003 TR07032004

Referenced NO./Rev:

Codes/Standards Applied: ASTM F 136-02a; ASTM F 67-06; ASTM B 348-06a

Date Of Issuance: March. 23, 2007

Remarks:

This Certificate Is Only Valid For The Equipment And Configuration Described, And In Conjunction With The Test Data Detailed Above.

Conclusion of Assessment:

We Hereby Confirm That The Technical Construction File And Manufacturing, Inspection And Testing Processes For Above Mentioned Equipment Comply With The Essential Safety Requirements Of EU MD Directive 98/37/EC Applied Codes And Standards.

Chief Assessor:

A handwritten signature in black ink, appearing to be a stylized 'W' or similar character, written over a light grey background.

United Kingdom Product Safety Test Center
241-243 Baker Street, London, NW1 6XE
info@scteu.org



HA compliance certificates

altakitın
Health Engineering

Altakitın, S.A.
Rua João Francisco do Casal, Arm 4
Zona Industrial da Taboeira
3800-266 Aveiro - Portugal

Analysis Report Nº Prod 2015004A
ISO 13779-1:2008 compliance determination
pg. 1 / 1

Product: *Hydroxyapatite*
Batch Ref.: **2015004**
Production date: **Mar/2015**

XRD Nuno Costa
Laboratório de Análises / Dept. Química / Faculdade de Ciências e Tecnologia
MiniFlex 2 diffractometer with MiniFlex 2 goniometer

ICP-AES Carla Rodrigues
Laboratório de Análises / Dept. Química / Faculdade de Ciências e Tecnologia
ICP-AES Horiba Jobin-Yvon model Ultima

PSD Ana Ribeiro
Laboratório Técnico / Depto. Eng^a. de Materiais e Cerâmica / Universidade de Aveiro
Coulter LS Particle Size Analyzer

Test	Result	ISO 13779-1:2008 Specifications
Ca : P ratio	1,667 ± 0,001	1,65 ≤ Ca:P ≤ 1,82
Trace Elements	As: not detected	As < 3,0 ppm
	Cd: not detected	Cd < 5,0 ppm
	Hg: not detected	Hg < 5,0 ppm
	Pb: 5,18 ± 0,13 ppm	Pb < 30,0 ppm
	THM: < 8,0 ppm	THM < 50,0 ppm
Crystalline Phase Composition	HAp: 100,0% ± 0,2%	HAp ≥ 50%
	β-TCP: not detected	β-TCP ≤ 5%
	α-TCP: not detected	α-TCP ≤ 5%
	TTCP: not detected	TTCP ≤ 5%
	CaO: not detected	CaO ≤ 5%
Crystalline Phase Composition	β-TCP: not detected	β-TCP ≤ 5%
	α-TCP: not detected	α-TCP ≤ 5%
	TTCP: not detected	TTCP ≤ 5%
	CaO: not detected	CaO ≤ 5%
Crystallinity Ratio	102,4% ± 0,3%	At least 95% crystalline
Particle Size Distribution	d (0,1): 25,8 μm	---
	d (0,5): 39,3 μm	---
	d (0,9): 52,4 μm	---
Density	-	---

Notes:

The samples were crushed in a glass mortar and sieved ($\phi < 38 \mu\text{m}$) prior to analysis.

The Crystalline Phase Composition results were obtained by MAUD XRD software v.2.33.

ICP Detection limits: As: 100 ppb Cd: 10 ppb Hg: 4ppb Mg: 5 ppb Pb: 100 ppb

Total Heavy Metal (THM) is calculated by the sum of the average results of the following elements: Ag, As, Bi, Cd, Cu, Hg, Mo, Pb, Sb and Sn.



Aveiro, 2015 / 05 / 06



Altakitin, S.A.
Rua João Francisco do Casal, Arm 4
Zona Industrial da Taboeira
3800-266 Aveiro – Portugal

Analysis Report Nº Prod 2015004
ISO 13779-1:2008 compliance determination
pg. 1 / 1

Product: *forCOAT*
Batch Ref.: 2015004
Production date: Mar/2015

XRD Nuno Costa
Laboratório de Análises / Dept. Química / Faculdade de Ciências e Tecnologia
MiniFlex 2 diffractometer with MiniFlex 2 goniometer

ICP-AES Carla Rodrigues
Laboratório de Análises / Dept. Química / Faculdade de Ciências e Tecnologia
ICP-AES Horiba Jobin-Yvon model Ultima

PSD Ana Ribeiro
Laboratório Técnico / Depto. Eng^a. de Materiais e Cerâmica / Universidade de Aveiro
Coulter LS Particle Size Analyzer

Test	Result	ISO 13779-1:2008 Specifications
Ca : P ratio	1,667 ± 0,001	1,65 ≤ Ca:P ≤ 1,82
Trace Elements	As: not detected	As < 3,0 ppm
	Cd: not detected	Cd < 5,0 ppm
	Hg: not detected	Hg < 5,0 ppm
	Pb: 5,18 ± 0,13 ppm	Pb < 30,0 ppm
	THM: < 8,0 ppm	THM < 50,0 ppm
Crystalline Phase Composition	HAp: 100,0% ± 0,2%	HAp ≥ 50%
	β-TCP: not detected	β-TCP ≤ 5%
	α-TCP: not detected	α-TCP ≤ 5%
	TTCP: not detected	TTCP ≤ 5%
	CaO: not detected	CaO ≤ 5%
Crystallinity Ratio	102,4% ± 0,3%	At least 95% crystalline
Particle Size Distribution	d (0,1): 64,3 μm	---
	d (0,5): 97,8 μm	---
	d (0,9): 156,4 μm	---
Density	1,037 ± 0,016 g/mL	---

Notes:

The samples were crushed in a glass mortar and sieved ($\phi < 38 \mu\text{m}$) prior to analysis.

The Crystalline Phase Composition results were obtained by MAUD XRD software v.2.33.

ICP Detection limits: As: 100 ppb Cd: 10 ppb Hg: 4ppb Mg: 5 ppb Pb: 100 ppb

Total Heavy Metal (THM) is calculated by the sum of the average results of the following elements: Ag, As, Bi, Cd, Cu, Hg, Mo, Pb, Sb and Sn.

2015/04/24
SJM.-

altakitin

Aveiro, 2015 / 04 / 23

Luis Pinto

Al₂O₃ compliance certificate

CERAMED

Estrada do Paço do Lumiar, 22
Campus do Lumiar, Edifício Q R/C
1649-038 Lisboa

CERTIFICADO DE ANÁLISE

Designação:	CORINDO BRANCO WFA-EK F120														
Descrição:	Óxido de alumínio branco														
Dimensões:	FEPA F120														
Lote:	0555														
Quantidade:	25 kg														
Peso específico:	3,9 – 4,1 g/cm ³														
Data:	2015-03-06														
Análise química (valores médios):	<table> <tr> <td>Al₂O₃</td> <td>99,730%</td> </tr> <tr> <td>Na₂O</td> <td>0,140%</td> </tr> <tr> <td>Fe₂O₃</td> <td>0,030%</td> </tr> <tr> <td>SiO₂</td> <td>0,010%</td> </tr> <tr> <td>CaO</td> <td>0,020%</td> </tr> <tr> <td>MgO</td> <td>0,010%</td> </tr> <tr> <td>TiO₂</td> <td>0,020%</td> </tr> </table>	Al ₂ O ₃	99,730%	Na ₂ O	0,140%	Fe ₂ O ₃	0,030%	SiO ₂	0,010%	CaO	0,020%	MgO	0,010%	TiO ₂	0,020%
Al ₂ O ₃	99,730%														
Na ₂ O	0,140%														
Fe ₂ O ₃	0,030%														
SiO ₂	0,010%														
CaO	0,020%														
MgO	0,010%														
TiO ₂	0,020%														

Especificação do crivo de acordo com FEPA – F 120			
	Crivo (µm)	Restante no crivo	Análises
Crivo 1	180	0 %	0,00%
Crivo 2	125	Max.20 %	15,00%
Crivo 3	106	Min.40 %	46,00%
Crivo 4	90	3+4 min.65 %	74,00%
Crivo 5	63	-. %	10,00%
Restante	0	Máx.3 %	1,00%

Nota: Os dados apresentados refletem o documento original do fabricante.

BLASQEM, Lda.

Data: 14-04-2015

**** Documento enviado por meios informáticos, assinatura não requerida. ****

BLASQEM, Lda.
ZI MAIA - Sector IV
Rua Albino José Domingues, 74 - 2 AY, 4470-034 MAIA
T 229 444 050 | F 229 444 055 | E info@blasqem.pt

NIPC: 510607411 | Capital Social: 50.000,00 Euros

www.blasqem.pt

MCD 180 compliance certificate

himed	CERTIFICATION	Cert#:
		10655
HITEMCO MEDICAL 160 Sweet Hollow Rd. Old Bethpage, NY 11804 PH: 516-752-7682 FX: 516-752-7951		

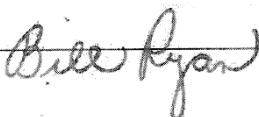
Hitemco Job/Lot#: 9168
 Customer: ENBIO

 Customer PO#: 231
 Part#: Mcd Apatitic Abrasive Powder
 Part Name: -180 um
 Other ID: UOM: kg
 Part Quantity: 10 Order Quantity: 10
 Process or Material:
 Attachments:

MATERIAL APPEARANCE-White color with green tint, irregular shape with sharp edges. GRIT BLAST TEST:
 COMPLIES WITH HM-2002. MICROHARDNESS (100 gr. LOAD) 550HV (GREATER THAN 510 HV) - (REFERENCE
 VALUE ONLY-not normally measured) TRACE ELEMENTS: As: <3.0 ppm Cd: <5.0 ppm Hg: < 5.0 ppm Pb:
 <30 ppm TOTAL HEAVY METALS (as lead) LESS THAN: 50 PPM TRACE ELEMENTS CONCENTRATION
 CONFORMS TO ASTM F1185-03. PHASE COMPOSITION (by XRD) - results below:

Item	Result	Complies With
HA%	>65	HM-2006
b-TCP,a-TCP,TTCP phases %	<35	HM-2006
TOTAL CaP phases %	<5	HM-2006
MCD LOT NUMBER:	110410-4291	N/A
>180 microns	<5%	HM-2006
<180 microns	>95%	HM-2006

By: BILL RYAN



Date: 3-7-11

Appendix E

CNC codes

SUB STEP A

[Filename]
name=SUB_STEPA

[Parameters]
units=mm

[ProgramData]

N10 G01 Y3.0 F13

N20 G01 X29.0

(Blank space, height = 40 mm)

N30 G01 Y-28.0 F13

(1 pass)

N40 G01 X2.9

N50 G01 Y25.0 F13

(3 pass)

N60 G01 X2.9

N70 G01 Y-25.0 F13

(4 pass)

N80 G01 X2.9

N90 G01 Y25.0 F13

(5 pass)

N100 G01 X2.9

N110 G01 Y-25.0 F13

(6 pass)

N120 G01 X2.9

N130 G01 Y25.0 F13

(7 pass)

N140 G01 X2.9

N150 G01 Y-25.0 F13

(8 pass)

N160 G01 X2.9

N170 G01 Y25.0 F13

(9 pass)

N180 G01 X2.9

N190 G01 Y-25.0 F13

(10 pass)

N200 G01 X2.9

N210 G01 Y25.0 F13

(11 pass)

N220 G01 X2.9

N230	G01 Y-25.0 F13	(12 pass)
N240	G01 X2.9	
N250	G01 Y25.0 F13	(13 pass)
N260	G01 X2.9	
N270	G01 Y-25.0 F13	(14 pass)
N280	G01 X2.9	
N290	G01 Y28.0 F13	(15 pass)
N300	G01 X2.9	
N365	G04 P.3	
N370	G01 X5.0 Z10.0	(Blank space and drop down to 30mm)
N380	G01 Y-28 F13	
N390	G01 X2.6	(1 pass)
N400	G01 Y25.0 F13	
N410	G01 X2.6	(2 pass)
N400	G01 Y-25.0 F13	
N420	G01 X2.6	(3 pass)
N430	G01 Y28.0 F13	
N440	G01 X2.6	(4 pass)
N490	G04 P.3	
N500	G01 X17.65 Z-10.0	(Blank space and drop to 40 mm)
N520	G01 Y-28.0 F13	
N530	G01 X2.9	(1 pass)
N540	G01 Y25.0 F13	
N550	G01 X2.9	(2 pass)
N560	G01 Y-25.0 F13	
N570	G01 X0.1	(3 pass)
N370	M30	(end of program)

SUB STEP B

[Filename]

name=SUB_STEPB

[Parameters]

units=mm

[ProgramData]

N10 G01 X3.3 F13.0

N15 G01 Z10

(Nozzle drop to 30 mm)

N20 G01 Y-28.0

N25	G01 X-3.3 F13	
N30	G01 Y9.0 F13	(1 pass)
N40	G01 X-2.6	
N50	G01 Y-9.0 F13	(2 pass)
N60	G01 X-2.6	
N70	G01 Y9.0 F13	(3 pass)
N80	G01 X-2.6	
N90	G01 Y-9.0 F13	(4 pass)
N100	G01 X11.1	
N110	G01 Y28.0 F13	
N115	G04 P0.5	
N116	G01 Z-10	(Nozzle way up to 40 mm)
N120	G01 X-3.3	
N130	G01 Y-8.0 F13	(1 pass)
N140	G01 X-2.9	
N150	G01 Y8.0 F13	(2 pass)
N160	G01 X-2.9	
N170	G01 Y-8.0 F13	(3 pass)
N180	G01 X-2.9	
N190	G01 Y11.0 F13	(4 pass)
N200	G01 X-8.0	
N201	G04 P0.5	
N202	G01 Z-10	(Nozzle way up to 50 mm)
N210	G01 Y-11.0 F13	(1 pass)
N220	G01 X-3.3	
N230	G01 Y8.0 F13	(2 pass)
N240	G01 X-3.3	
N250	G01 Y-25.0 F13	(3 pass)
N260	G01 X-3.3	
N270	G01 Y25.0 F13	(1 pass)
N280	G01 X-3.3	
N290	G01 Y-25.0 F13	(2 pass)
N300	G01 X-3.3	
N310	G01 Y28.0 F13	(3 pass)
N340	G01 X-8.0	
N341	G04 P0.5	

N342	G01 Z20	(Nozzle drop to 30 mm)
N350	G01 Y-28.0 F13	(1 pass)
N360	G01 X-2.6	
N370	G01 Y25.0 F13	(2 pass)
N380	G01 X-2.6	
N390	G01 Y-25.0 F13	(3 pass)
N400	G01 X-2.6	
N410	G01 Y25.0 F13	(4 pass)
N420	G01 X-2.6	
N430	G01 Y-25.0 F13	(5 pass)
N440	G01 X-2.6	
N450	G01 Y25.0 F13	(6 pass)
N460	G01 X-2.6	
N470	G01 Y-25.0 F13	(7 pass)
N480	G01 X-2.6	
N490	G01 Y25 F13	(8 pass)
N500	G01 X-2.6	
N510	G01 Y-25.0 F13	(9 pass)
N520	G01 X-2.6	
N530	G01 Y25.0 F13	(10 pass)
N540	G01 X-2.6	
N550	G01 Y-25.0 F13	(11 pass)
N560	G01 X-2.6	
N570	G01 Y25.0 F13	(12 pass)
N580	G01 X-2.6	
N590	G01 Y-28.0 F13	(13 pass)
N600	G01 X-15.0	
N601	G04 P0.5	
N602	G01 Z-10	(Nozzle way up to 40 mm)
N610	G01 Y28.0 F13	(1 pass)
N620	G01 X-2.9	
N630	G01 Y-25.0 F13	(2 pass)
N640	G01 X-2.9	
N650	G01 Y25.0 F13	(3 pass)
N660	G01 X-2.9	
N670	G01 Y-25.0	(4 pass)
N370	M30	(end of program)

SUB STEP C

[Filename]

name=SUB_STEP C

[Parameters]

units=mm

[ProgramData]

N10 G01 X-3.3 F13.0

N15 G01 Z10 (Nozzle drop to 30 mm)

N20 G01 Y-28.0

N25 G01 X3.3 F13

N30 G01 Y9.0 F13 (1 pass)

N40 G01 X2.6

N50 G01 Y-9.0 F13 (2 pass)

N60 G01 X2.6

N70 G01 Y9.0 F13 (3 pass)

N80 G01 X2.6

N90 G01 Y-9.0 F13 (4 pass)

N100 G01 X-11.1

N110 G01 Y28.0 F13

N115 G04 P0.5

N116 G01 Z-10 (Nozzle way up to 40 mm)

N120 G01 X3.3

N130 G01 Y-8.0 F13 (1 pass)

N140 G01 X2.9

N150 G01 Y8.0 F13 (2 pass)

N160 G01 X2.9

N170 G01 Y-8.0 F13 (3 pass)

N180 G01 X2.9

N190 G01 Y11.0 F13 (4 pass)

N200 G01 X8.0

N201 G04 P0.5

N202 G01 Z-10 (Nozzle way up to 50 mm)

N210 G01 Y-11.0 F13 (1 pass)

N220 G01 X3.3

N230 G01 Y8.0 F13 (2 pass)

N240	G01 X3.3	
N250	G01 Y-25.0 F13	(3 pass)
N260	G01 X3.3	
N270	G01 Y25.0 F13	(1 pass)
N280	G01 X3.3	
N290	G01 Y-25.0 F13	(2 pass)
N300	G01 X3.3	
N310	G01 Y25.0 F13	(3 pass)
N320	G01 X3.3	
N330	G01 Y-25.0 F13	(4 pass)
N340	G01 X3.3	
N350	G01 Y25.0 F13	(5 pass)
N360	G01 X3.3	
N370	G01 Y-25.0 F13	(6 pass)
N380	G01 X3.3	
N390	G01 Y25.0 F13	(7 pass)
N400	G01 X3.3	
N410	G01 Y-25.0 F13	(8 pass)
N420	G01 X3.3	
N430	G01 Y25.0 F13	(9 pass)
N440	G01 X3.3	
N450	G01 Y-28.3 F13	(10 pass)
N460	G01 X8.0	
N470	G04 P0.5	
N480	G01 Z10	(Nozzle drop to 40mm)
N270	G01 Y28.3 F13	(1 pass)
N280	G01 X2.9	
N290	G01 Y-25.0 F13	(2 pass)
N300	G01 X2.9	
N310	G01 Y25.0 F13	(3 pass)
N320	G01 X2.9	
N330	G01 Y-25.0 F13	(4 pass)
N340	G01 X2.9	
N350	G01 Y25.0 F13	(5 pass)
N360	G01 X2.9	
N370	G01 Y-25.0 F13	(6 pass)
N380	G01 X2.9	
N390	G01 Y25.0 F13	(7 pass)
N400	G01 X2.9	
N410	G01 Y-30.0 F13	(8 pass)
N370	M30	(end of program)

ADHESION

[Filename]

name=Adhesion40

[Requirements]

PartTooling=COUPON_TRAY

[Parameters]

units=mm

[ProgramData]

N10	F.125	(set the feedrate)
N20	G91	
N25	G01 y52.0 F33.0	(use relative coordinates)
N27	G01 x9 z-25.0 F33.0	(nozzle def to 40 mm above sample)
N30	G04 P.9	(hold position)
N40	G91	
N50	G01 X105.0 F13	(1 pass)
N60	G01 Y-3.3	
N70	G01 X-105.0 F13	(2 pass)
N80	G01 Y-3.3	
N90	G01 X105.0 F13	(3 pass)
N100	G01 Y-3.3	
N110	G01 X-105.0 F13	(4 pass)
N120	G01 Y-3.3	
N130	G01 X105.0 F13	(5 pass)
N140	G01 Y-3.3	
N150	G01 X-105.0 F13	(6 pass)
N160	G01 Y-3.3	
N170	G01 X105.0 F13	(7 pass)
N180	G01 Y-3.3	
N190	G01 X-105.0 F13	(8 pass)
N200	G01 Y-3.3	
N210	G01 X105.0 F13	(9 pass)
N220	G01 Y-3.3	
N230	G01 X-35.0 F13	(10 pass)
N240	G01 Y-3.3	
N250	G01 X35.0 F13	(11 pass)
N260	G01 Y-3.3	
N270	G01 X-35.0 F13	(12 pass)
N280	G01 Y-3.3	
N290	G01 X35.0 F13	(13 pass)
N300	G01 Y-3.3	
N310	G01 X-35.0 F13	(14 pass)

N320	G01 Y-3.3	
N330	G01 X35.0 F13	(15 pass)
N340	G01 Y-3.3	
N350	G01 X-35.0 F13	(16 pass)
N360	G01 Y-3.3	
N370	G01 X35.0 F13	(17 pass)
N380	G01 Y-3.3	
N390	G01 X-35.0 F13	(18 pass)
N400	G01 Y-3.3	
N405	G01 X35.0 F13	(19 pass)
N410	G01 Y-3.3	
N480	G04 P1	
N490	G28	(finish homing, slowly)
N500	M30	(end of program)

SCREW

[Filename]
name=Screw

[Requirements]
PartTooling=PIN_TOOLING

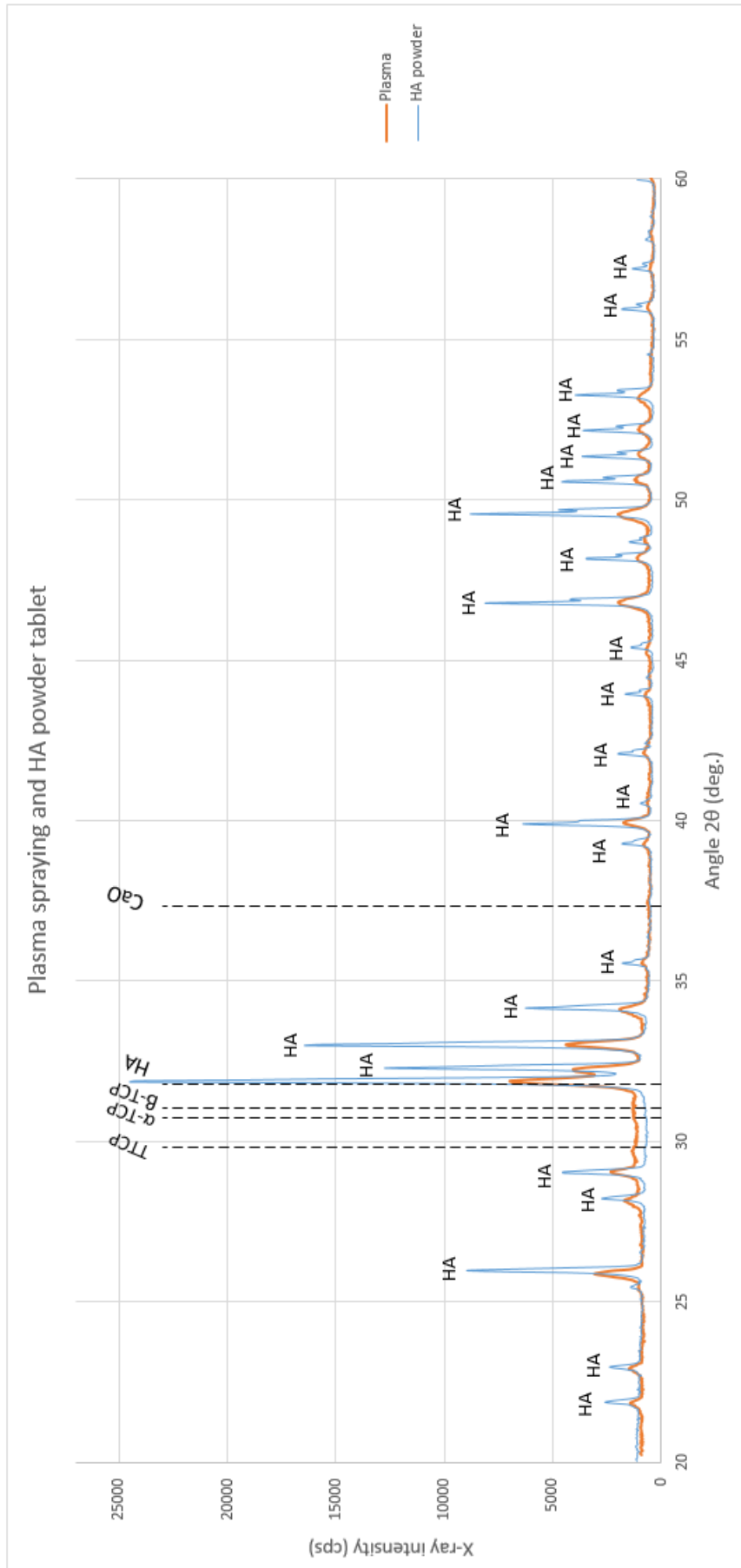
[Parameters]
units=mm

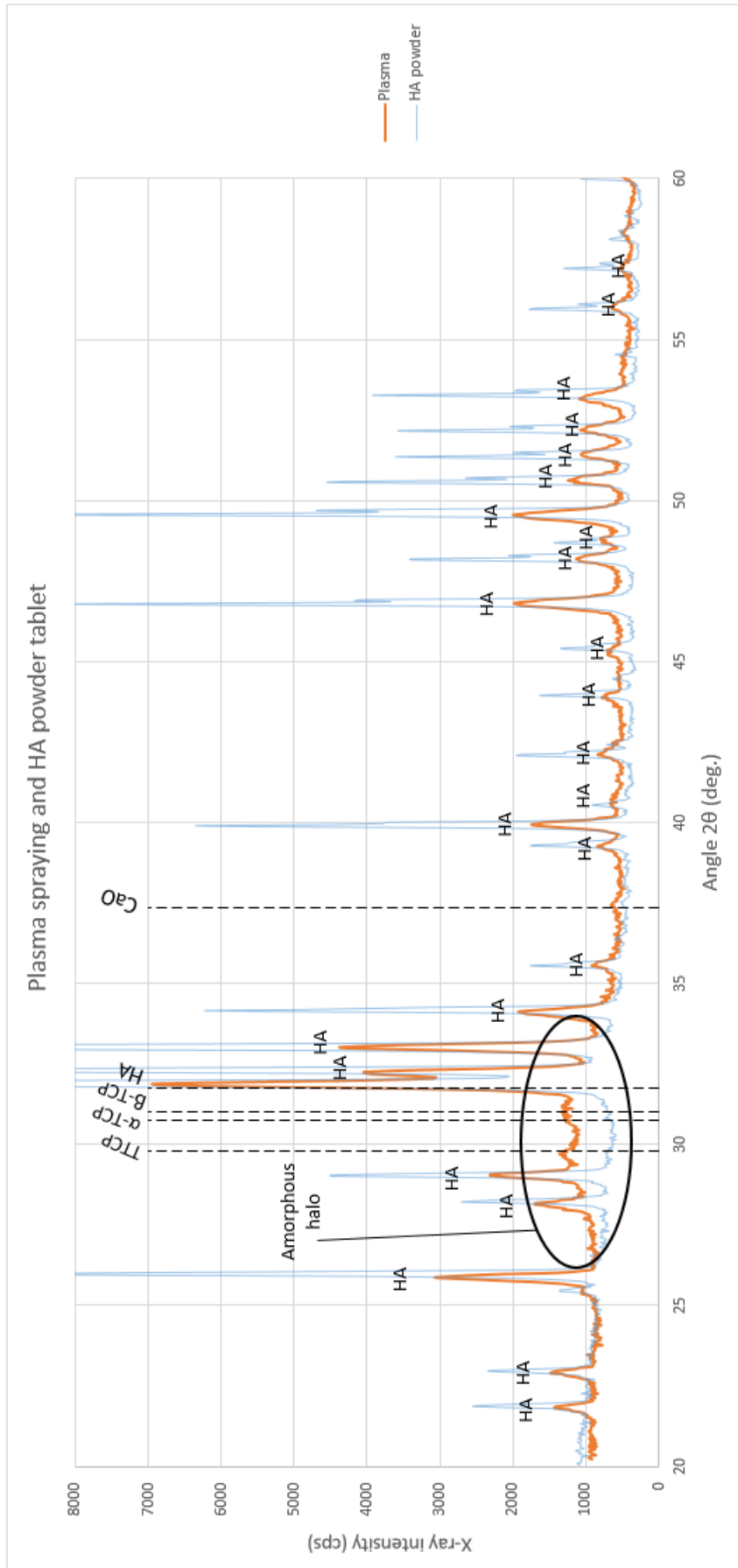
[ProgramData]

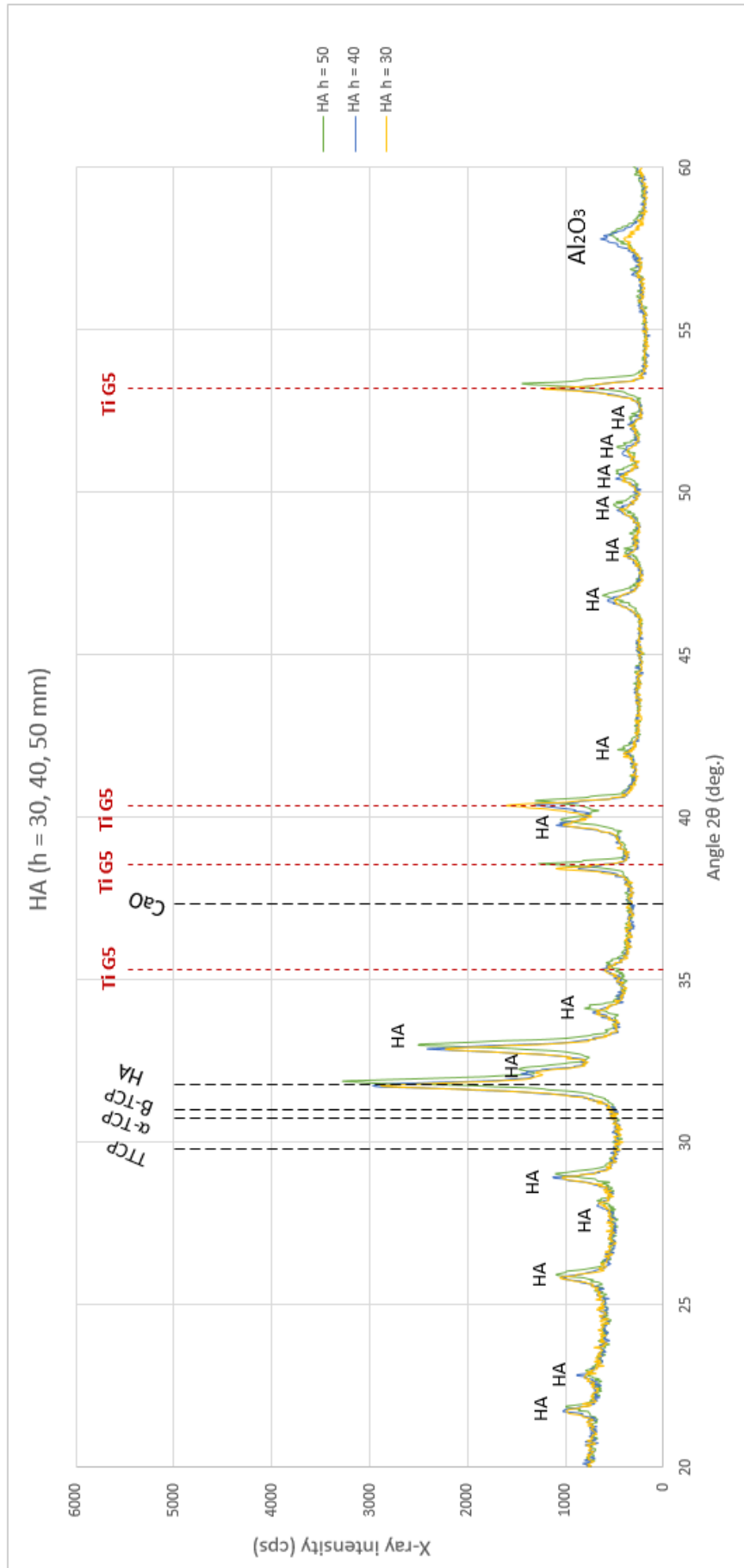
N10 G91	(use relative coordinates)
N20 G01 X150.0 Y18 Z10 F50	(move to purge position)
N50 G04 P1	(hold position)
N90 S20	(set spindle rotational speed)
N100 M04	(start spindle counter clockwise)
N110 G04 P2.5	(wait for spindle to spin up before blasting)
N120 G01 Y-10 F60.0	(move to start position)
N125 G04 P0	
N130 G01 X-50.0 F2.0	(blast the spindle part)
N135 G04 P0	
N140 G01 Y0 F60.0	(move off spindle)
N147 G04 P0	
N150 M05	(stop the spindle)
N150 G90	(absolute coordinates)
N160 G01 X0 Y20 Z0 F75.0	(head towards home)
N170 G28	(finish homing, slowly)
N180 M30	(end of program)

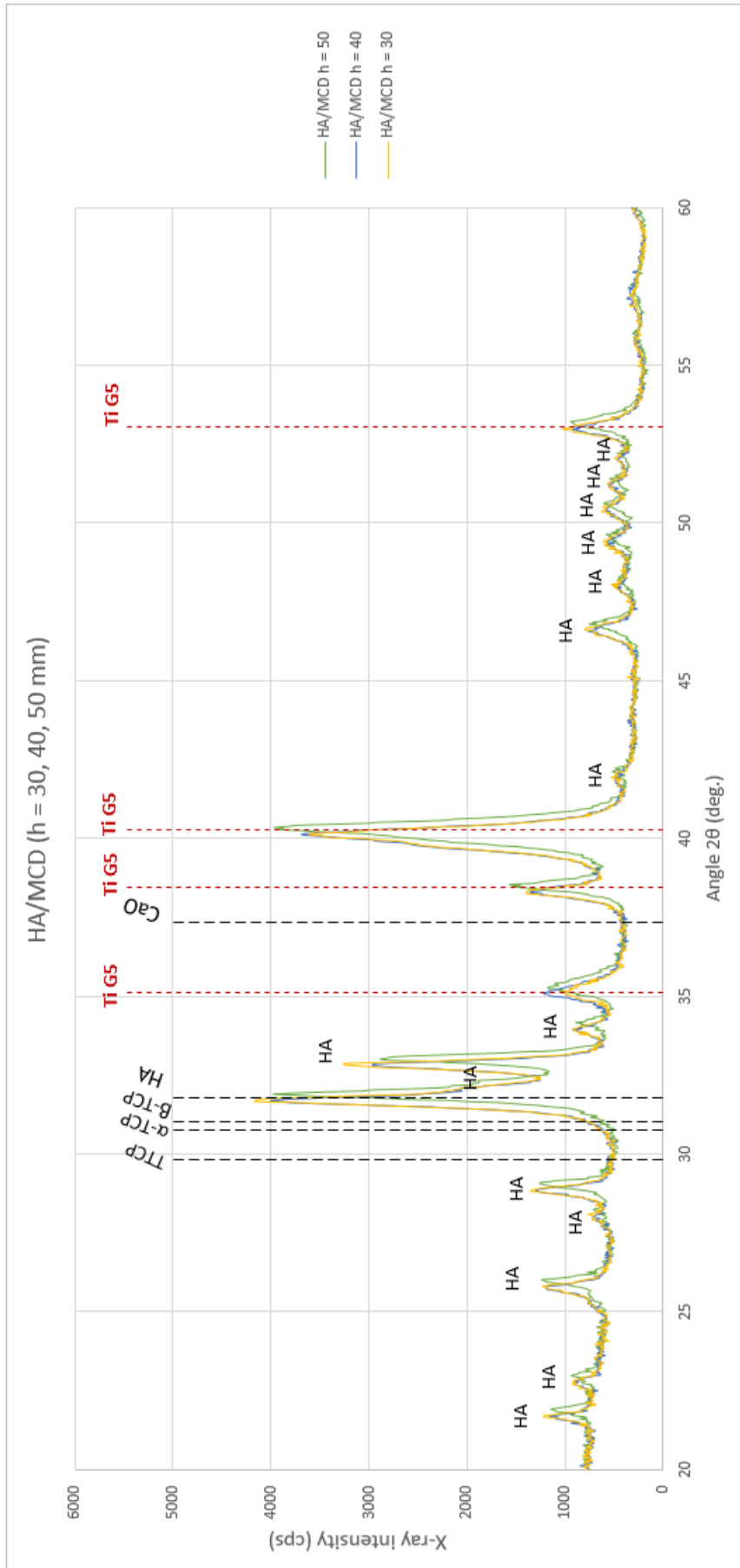
Appendix F

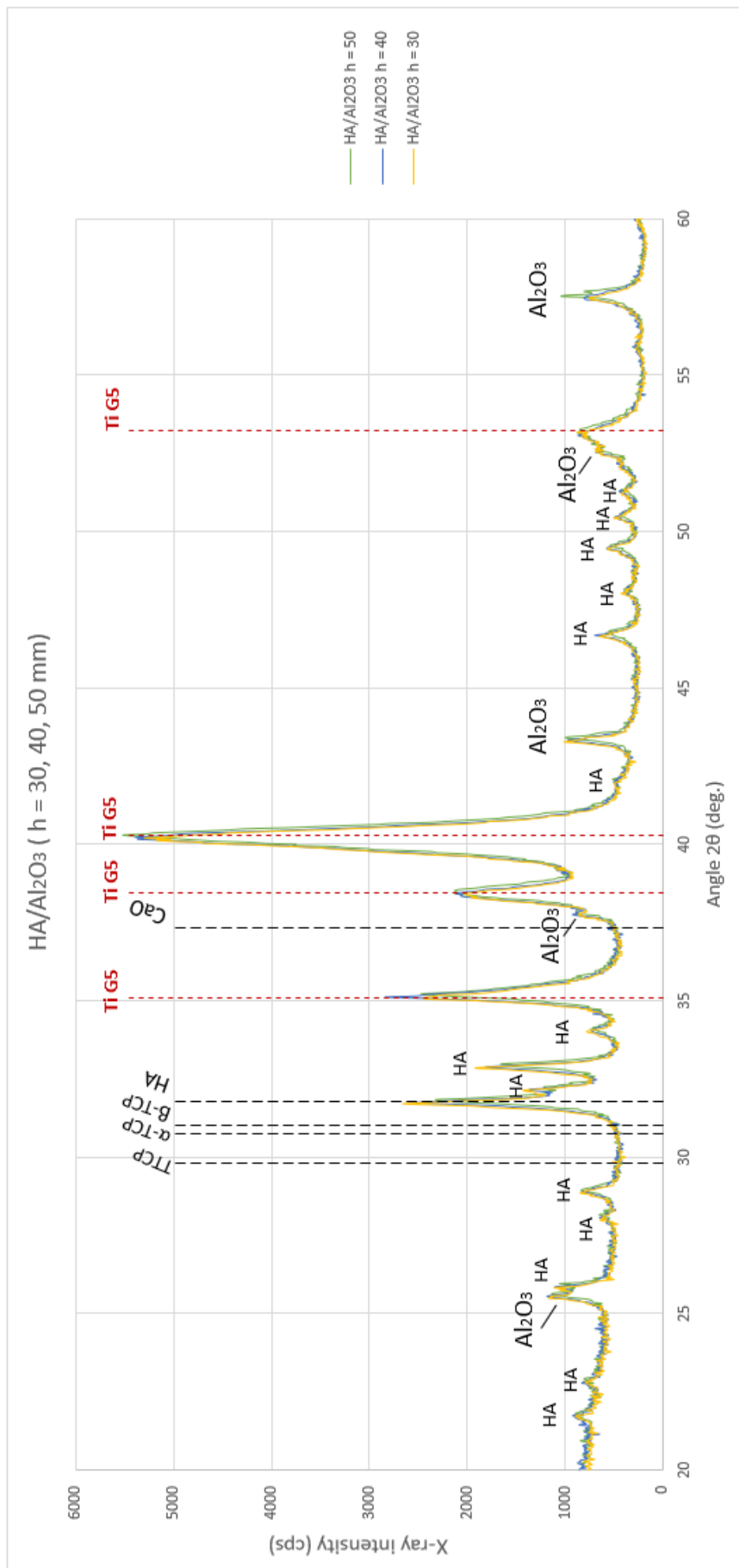
X-ray diffraction plots

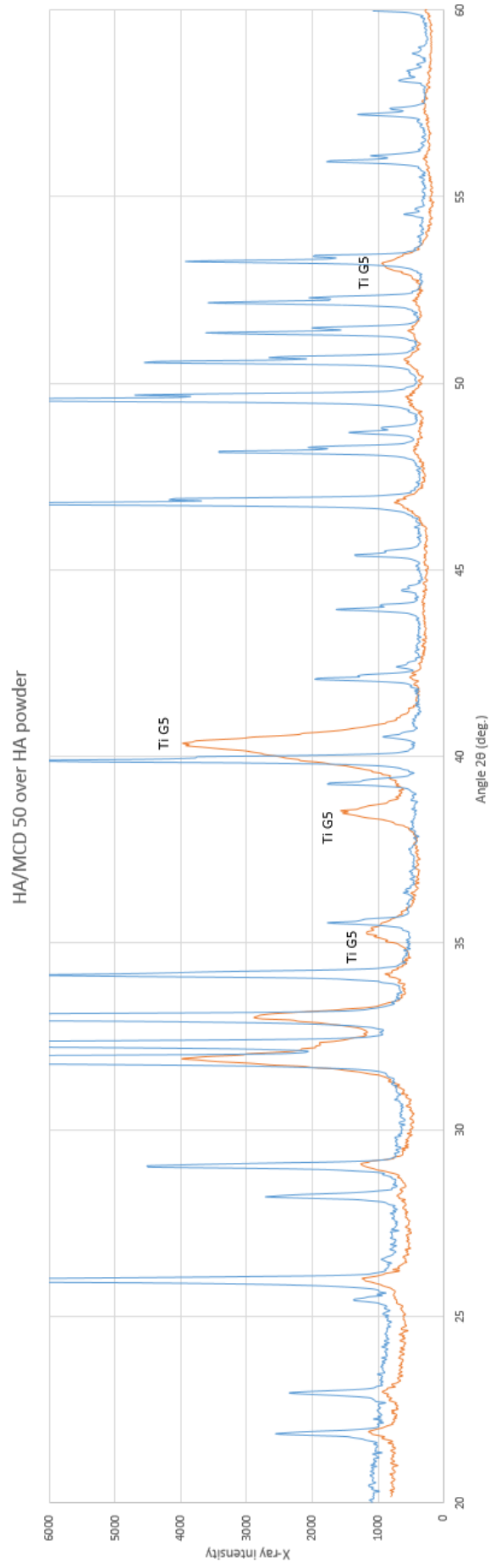












HA/MCD 40 over HA powder

